2017

Spatio-temporal Modeling of Louisiana Land Subsidence Using High-resolution Geo-spatial Data

Hanyu Xiang
Louisiana State University and Agricultural and Mechanical College

SPATIO-TEMPORAL MODELING OF LOUISIANA LAND SUBSIDENCE USING HIGH-RESOLUTION GEO-SPATIAL DATA

A Dissertation

Submitted to the Graduate Faculty of the
Louisiana State University and
Agricultural and Mechanical College
in partial fulfillment of the
requirements for the degree of
Doctor of Philosophy

in

The Department of Geography and Anthropology

by
Hanyu Xiang
B.S., Wuhan University of Technology, 2005
M.E., Peking University, 2009
August 2017

Acknowledgments

For this dissertation, I thank my advisor, Dr. Lei Wang, who provided valuable guidance for my research and residence in the United States for these years. I have learned much from him. I also thank the committee members, including Dr. Nina Lam, Dr. Xuelian Meng, and Dr. Okeil, who helped improve the dissertation. Next, I thank Yaping Xu, who helped my research greatly. Finally, I must thank my family, who represented a strength in the support of my study in the United States.

Table of Contents

Abstract

Land subsidence, defined as a land sinking or a gradual inward caving of land, presents a common disturbance observed in many areas of the world. In Louisiana, this specific problem posed a serious threat to the populace living there. Considered by denizens to be an adverse impact of land use, the extant Louisiana subsidence causes serious problems that tend to worsen, such as excessive wetland formation or land loss. Unless researchers find appropriate treatments to address this increasingly serious problem, the present issues will be exacerbated.

To visualize the spatio-temporal subsidence patterns, this study used data collected by high-precision GPS stations and processed high-accuracy land elevation data in coastal Louisiana by means of a GIS-based spatio-temporal data model. I used the Kriged Kalman Filter (KKF) to map the spatial temporal field of land elevation change in southern Louisiana from 2011 to 2013, which showed a clear subsidence area after 2012. The coincidence of the Bayou Corne Sinkhole enabled a validation of the GPS data and the spatio-temporal data model.

In addition, the spatial pattern for subsidence was predicted by Regression-Kriging and based on observed GPS data in tandem with the data on contributing subsidence factors. The prediction results using Regression-Kriging had high and acceptable accuracy.

I applied the geographically weighted regression (GWR) model to show the spatial heterogeneity of contributing factors to subsidence in the study site. The statistical results showed that spatial heterogeneity for the data of contributing factors

would be useful to recognize the agglomeration of communities in the study area. The regionalization work of these contributing factors could also be helpful to form location-based subsidence mitigation policies.

This research contributes to the knowledge of GIS data modeling by incorporating a spatio-temporal interpolation—the Kriged Kalman filter (KKF)—into mapping and monitoring the land elevation change. This technique overcomes the problems of traditional spatial interpolation methods that disregard the time dependency of the geospatial data. The second contribution of this research is to predict the spatial pattern of subsidence using the information in regard to the subsidence factors at GPS stations. A cross-scale subsidence prediction, drawn solely on point based data from GPS stations, was made possible by Regression-Kriging. The third contribution of this research is that the spatial statistical models used for data analysis enable location-based policy-making. In other words, the local government can embrace smart policies that are specifically effective for certain regions to prevent further land loss or subsidence.

Chapter 1 Introduction

1.1. Background

The term “subsidence” refers to the downward movement of the earth’s surface with respect to a reference point (Dokka 2006; Kent and Dokka 2012), which may be produced by both geophysical and anthropogenic factors (Kent and Dokka 2012). The subsidence may cause many adverse effects on affected living space, such as excessive wetland formation or land loss, depending on whether appropriate treatments are applied to the extant irregular subsidence (Kent and Dokka 2012).

Multiple regions around the world suffer from serious subsidence problems, yet for different reasons (Hung et al. 2011). For instance, Italy’s Venice, renowned as a historical city, displays a subsidence phenomenon. The city’s local problems include issues such as the stability of buildings, waterways, and coastal erosion, thus constituting major problems that consistently contribute to subsidence phenomena yearly (Bitelli et al. 2000). Other classic areas that show emerging dramatic subsidence are inclusive of the United States’ lower Mississippi Valley and northern Gulf coast, with multiple contributing factors, such as groundwater withdrawal and the extraction of oil by pumping (Abdollahzadeh et al. 2013; Shinkle and Dokka 2004). The experiential subsidence in this area, deemed a “slow disaster,” threatens critical habitats in large and small cities, farms, and economic infrastructures in several states and threatens a harbinger of eventual inundation by the Gulf of Mexico (Shinkle and Dokka 2004).

The State of Louisiana, located in the lower Mississippi Valley and the northern Gulf Coast area as well, reflects a gradual, evident subsidence, especially in the coastal parishes, thus causing a huge area of wetland to form. To account for this serious problem, the following figure shows the vertical displacement of height for a Louisiana ground point (point name: 1 LSU) throughout 2012, based on the research methods of Shinkle and Dokka in 2004 (Dokka 2006; Shinkle and Dokka 2004).

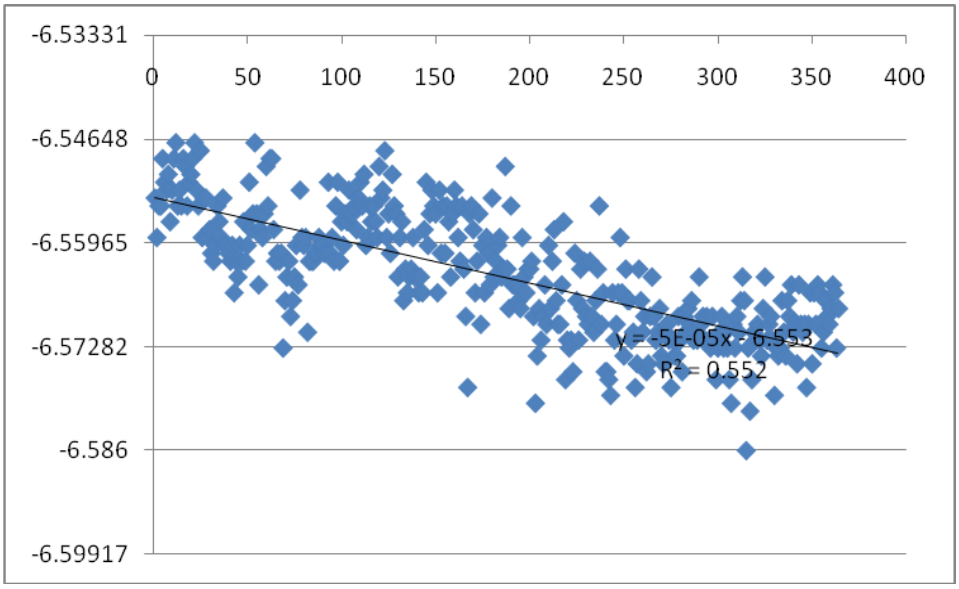

Figure 1. Height changes for one site (1LSU) in Louisiana in 2012, units: day (Horizontal axis), meter (Vertical axis)

Figure 1 uses the trendline slope (0.00005) to calculate an annual subsidence rate, which equals 18.3 mm or 0.05 mm per day. We must not lose sight of this rate, calculating a serious subsidence problem in the area, as the future cumulative subsidence found over a long period, such as 50 to 100 years, will be significant, should this subsidence rate remain stable. The effects of such a subsidence disaster would be felt by the entire country at that time, as the looming inundation would

gradually destroy America's largest coastal wetland and continue on to ravage its energy production heartland (Shinkle and Dokka 2004).

Hence, facing the gravity of the Louisiana situation regarding this serious subsidence problem, relevant researchers should increasingly focus on subsidence studies of high importance, such as subsidence prediction. Governments should assume immediate and powerful actions to control the high speed of adverse subsidence. This research may, in fact, substantially serve as a potential and feasible attempt to monitor, predict, and treat subsidence in Louisiana.

1.2. Literature review

The subsidence study may be done as an interdisciplinary project, applying the various methods of geotechnical engineering, geology, geophysics, geography, or the geographic information system (GIS). In potential research, the recent geographic subsidence study is focused mainly on backgrounds. The literature review results indicate that relevant papers on subsidence may be classified into two subsets for research topics: 1) how to make a highly accurate subsidence observation and prediction, and 2) how to collect relevant contributing factors by means of modeling during a dramatic subsidence.

Subsidence observation and prediction

Recently, three common kinds of techniques have been widely used in the process of subsidence observation: leveling, GPS observation, and Interferometric Synthetic Aperture Radar (InSAR) (Lu, C. et al. 2012).

In the early 1950s, engineers and researchers initiated subsidence surveys by means of leveling, usually quantifying the vertical displacement at relevant benchmarks for land subsidence (Shinkle and Dokka 2004). By means of geodesy methods, the survey accuracy in leveling has the potential to be high at a millimeter level, while the temporal resolution is technically limited (Lu, C et al. 2012); conventional survey cycles usually exceed 10 years. However, since the GPS technique emerged and expanded widely, the GPS survey has become yet another available method to quantify land subsidence by applying millimeter-level point heights and relatively higher temporal resolution, whereas the survey point density tends to be relatively low (Lu, C. et al. 2012). As an innovation of the new 21st century, the InSAR technique provides an alternative to leveling and GPS observations, due to the high spatial density (Lu, C. et al. 2012)/ In the entire InSAR survey imaging process, the differences in phases of microwaves from repeat-pass InSAR satellites are used to calculate the displacements of ground downward movements as land subsidence (Extracted from: http://treuropa.com/technique/insar-evolution/); in turn, this imaging process will definitely produce multiple categories of unwanted errors, especially atmosphere effect, topographic distortion, and de-correlation noise (Extracted from: http://treuropa.com/technique/insar-evolution/).

A new, advanced InSAR technique, such as differential InSAR (DInSAR), may emerge that presents a differential method with the corresponding digital elevation model (DEM). Nevertheless, the present technique has the capability to reduce or

eliminate multiple topographic distortions, although errors, such as atmospheric effects, may remain unprocessed. Thus, each one of three techniques—leveling, GPS, and InSAR—has relatively evident advantages and flaws. The integration or combination of such techniques remains a common research trend, necessary for developing an accurate land subsidence survey.

Notably, many researchers initially completed the integration of leveling and GPS observations at the inception stage of a techniques-integration study. A paper released in 2007 shows that a comparison of historical leveling and recent GPS data reveals the subsidence rates on the Thessaloniki Plain of Greece for the past 50+ years (Psimoulis et al. 2007). Around 2000, a data information system capable of connecting the leveling network with GPS data was operated to monitor the ground subsidence in the Southern Po Valley (Bitelli et al. 2000). Additionally, the NOAA data report by Shinkle and Dokka in 2004 reveals that the GPS observation data in the Continuously Operating Reference Station (CORS) had assisted the integrated leveling benchmark data from many epochs, by calculating and interpolating the steady state of subsidence rates in the lower Mississippi Valley and Northern Gulf Coast; based on these calculated subsidence rates, the increasing land loss areas in the Lower Mississippi River Basin from 2011 to 2050 were evaluated by Zou et al. in 2016 (Shinkle and Dokka 2004; Kent and Dokka 2012; Zou et al. 2016).

Hence, this method on leveling and GPS combination produces more accurate subsidence data and thereby extends the subsidence observation periods from the past to the future (Shinkle and Dokka 2004; Kent and Dokka 2012). Nevertheless, it may

prove unfeasible to solve the low point-density problem easily, especially in cases where observation points are distributed on less of an average or less randomly in the study area.

Recently, many papers on subsidence have indicated that the most acknowledged and popular subsidence survey method involves an integration technique between InSAR/DInSAR) and GPS. In the entire integration process, DInSAR should be used rather than ordinary InSAR, as the DInSAR data display much less topographic error when applied with the corresponding DEM (Extracted from: http://treuropa.com/technique/insar-evolution/). Moreover, many areas of land subsidence (such as Appin Township, located southwest of Sydney, Australia) were globally surveyed by means of this popular integration technique (Linlin Ge et al. 2003). In Appin Township, GPS data over the same study site were used to geo-reference the DInSAR results. Further, the differential tropospheric delay (atmosphere effect) was estimated by the GPS data for interpolation into an image to correct the atmosphere disturbance in the InSAR results (Linlin Ge et al. 2003; Ge 2000) (Extracted from: http://treuropa.com/technique/insar-evolution/).

Thus, DInSAR may be regarded as a popular technique to monitor land subsidence when combined with GPS. However, this technique may be subject to uncertainties induced by errors in atmosphere, satellite orbits, and terrain effects. According to research, the land coverage showing various surface properties over different seasons will cause spatial de-correlation in DInSAR, as well as degraded measurement accuracy (Hung et al. 2011; Hung et al. 2010). Permanent scatterer

interferometry (PSI) was proven to reduce the deficiency in DInSAR (Hooper et al. 2004; Hung et al. 2011). PSI, a relatively recent development from conventional InSAR, relies on a study of pixels, which remains coherent over a sequence of interferograms, thus providing consistent and stable radar reflections (Burgmann et al. 2000). In one subsidence case over the Choushui River Alluvial Fan in Taiwan, PSI reduced errors affected conventional DInSAR techniques. As a result, PSI was used for data fusion work, coupled with high-precision and low point-density leveling data, thus producing a smoothed correction to the PSI results (Hung et al. 2011; Lu, C. et al. 2012). Such fusion work allows the surveyed result to be more representative of overall deformation characteristics than the sole use of the PSI field, or leveling (Hung et al. 2011). In addition, the fusion work provides a superior, classic study on the integration of PSI (InSAR) and leveling. In this fusion process, a simple "draping" method was applied to merge the PSI result with that of the leveling (Hung et al. 2011; Forsberg and Skourup 2005). Future studies on data fusion will include either an improved method that uses wavelet functions or a spectral combination to represent various kinds of subsidence data (Hung et al. 2011; Addison 2002).

In addition, with the exception of leveling, other subsidence survey techniques, such as GPS and InSAR, were used in recent research cases, such as Analog weather charts (AWC), which was applied to the high-precision Grid point value of Meso-Scale Model(GPV-MSM) and combined with water vapor data (Zheng et al. 2014). In this instance, the spatial distribution of the atmospheric delay by water vapor was quantified using AWC by permitting the atmosphere effect of DInSAR data

to be reduced, thus rendering GPV-MSM data effective for DInSAR analysis (Zheng et al. 2014; Lu, C. et al. 2012).

Although the integration of such techniques tends to result in high accuracy in subsidence surveys, recent media announcements indicate that NASA is in the process of developing a new, airborne interferometer system named UAVSAR, which will provide much higher spatial resolutions and accuracy for future subsidence surveys in the future (Blom et al. 2009).

Furthermore, with the exception of common techniques and their integration, some methods from geo-statistics models may also be used to process subsidence data for higher prediction accuracy, such as the Kriged Kalman Filter (Mardia et al. 1998). The Kriged Kalman filter (KKF), regarded as a combination or integration of Kalman filter and Kriging interpolation, may be used to process and predict spatio-temporal data, such as long-term point data on subsidence (Kalman 1960; Mardia et al. 1998; Shang et al. 2011; Olea 1999). The long-term GPS subsidence data may be especially applied to KKF due to characteristics of high temporal resolution, as well as low point density, and based on the GPS points' input, raster data may be produced; large areas of subsidence data near these scatter GPS points may then be interpolated and predicted accurately for a long-term period (Shang et al. 2011; Lu, C. et al. 2012). Thus, KKF may provide a possible and accurate method for surveying and predicting long-term subsidence data (Shang et al. 2011).

Modeling of contributing factors to subsidence

The factors for subsidence may be classified as both geophysical and anthropogenic (Kent and Dokka 2012). A recent study on subsidence in southern coastal Louisiana indicates that sediment compaction, low-angle faulting, and the regional subsidence associated with mass loading may display the major factors controlling subsidence in the delta, coupled with a finding that the coastal regions outside the delta tend to undergo slower subsidence, probably related to factors such as fluid withdrawal encompassing ground water, petroleum, and natural gas extraction (Abdollahzadeh et al. 2013).In other words, the natural process of subsidence in many active areas can be mainly attributed to the following factors: a) sediment compaction, b) faulting, c) anthropogenic mass loading, d) groundwater withdrawal, e) oil pumping, and f) natural gas extraction (Abdollahzadeh et al. 2013; Kent and Dokka 2012). Thus, the methodology on how to use an appropriate model to establish relationships between subsidence and factors and how to quantify such factors will be prevailing topics for subsidence researchers from a variety of academic backgrounds.

Geophysical factors that contribute to subsidence (Kent and Dokka 2012) indicate that faulting emanating from a series of dramatic crust movements is popularly considered a vital study topic on subsidence, especially for geological and geophysical researchers (Abdollahzadeh et al. 2013; Dolezalova et al. 2009; Brodie et al. 2007). A strong example in this context comes from an evaluation project regarding a mining subsidence in Karvina, located in the Czech Republic, which used GPS data as well (Dolezalova et al. 2009). In the Karvina project, the subsidence

depression acquired from two years of GPS survey data revealed that the complicated tectonic situation importantly influenced the behavior of surface subsidence (Dolezalova et al. 2009). Tectonic faults evidently shaped the subsidence depression in an irregular form; yet importantly, on sites without a tectonic fault, the subsidence depression experienced a smooth and regular development. Consequently, this research instance strongly corroborates a close correlation between the shape of a subsidence, as well as the characteristics of a fault on the same site (Dolezalova et al. 2009).

As a commonly anthropogenic factor relating to subsidence (Kent and Dokka 2012), groundwater withdrawal (Kent and Dokka 2012; Abdollahzadeh et al. 2013) remains a common indicator to researchers from many backgrounds, notably because groundwater can be the most direct factor leading to subsidence (Shang et al 2011; Abdollahzadeh et al. 2013). A classic hydrology and GIS case involves a spatial and temporal prediction system for groundwater flow and subsidence in the Japanese coastal plain (Zhou et al. 2003). In this case, by means of hydrology and GIS knowledge, the required data were converted to GIS data in the database, while the surface water cycle was simulated to obtain the spatial and temporal groundwater infiltration quantity (Zhou et al. 2003). A 3D groundwater flow model based on hydrology then was established a) to simulate the groundwater flow, and b) to calculate or predict the corresponding subsidence in different water pumping scenarios (Zhou et al. 2003). Another recent GIS instance involving water withdrawal (Abdollahzadeh et al. 2013) shows the spatial and temporal characteristics of a

subsidence induced by groundwater over-exploitation in Beijing (Chen et al. 2011; Abdollahzadeh et al. 2013). Using data collected by GPS and InSAR, a model on the dynamic variation from hydro-dynamics was established to analyze the subsidence response to groundwater withdrawal (Chen et al. 2011).

In addition to such models that form hydrology, many geo-statistics models can be even more available for quantifying the factors related to subsidence, such as geographically weighted regression (GWR) (Fotheringham et al. 2002). The most recent GWR case on subsidence was released by a research group from Taiwan, which involved the groundwater factor for modeling (Shang et al 2011).

In the GWR case from Taiwan, the study site was selected in the Choshuichi Alluvial Fan, using ground subsidence data collected by GPS observation. The data were inclusive of groundwater levels from three underground aquifers, obtained from the Water Resources Agency (Shang et al. 2011). By means of interpolation, the spatial distribution of subsidence in the study site and the groundwater levels at each GPS station may be estimated for GWR (Shang et al. 2011; Shepard and Donald 1968).

In the GWR modeling process, the changes in groundwater levels from three aquifers were selected as predictors, applying subsidence as the dependent variable (Shang et al 2011). GWR is more advantageous than other geo-statistics models in this instance, as the other models used for subsidence research usually involve a "global" approach, thus lacking spatial heterogeneity of the data. On the other hand, GWR definitively displays a spatial variation of predictors, as well as spatially varied

coefficients of predictors (Shang et al. 2011; Fotheringham et al. 2002). Thus, by the GWR model, all four of the spatially varied coefficients may be calculated; as a result, by using these coefficients, land subsidence in the study site may be predicted (Shang et al 2011). As a result, an important comparison between the prediction result from GWR and the one from ordinary least squares (OLS) was made, showing that GWR can better approach the real subsidence distribution by means of a higher accuracy and an adjusted R-square (Shang et al 2011; Hayashi and Fumio 2000). Although this GWR case for subsidence may be classic, it still has many drawbacks, including the lack of long-term or seasonal GPS data for showing a more detailed correlation between groundwater levels and subsidence (Shang et al. 2011). Further, multiple kinds of important factors, with the exclusion of groundwater levels, may be collected to access GWR for more accurate modeling results. These drawbacks are expected to improve through future research (Shang et al. 2011; Fotheringham et al. 2002; Abdollahzadeh et al. 2013).

Many of the subsidence cases discussed refer to a natural process of subsidence; however, in some small site areas, subsidence may be produced by loadings from certain human activities, such as mining. For such cases, especially for a mining subsidence, the factors related to subsidence should largely differ, such as a) depth and distance from drift, b) DEM and slope gradient, c) groundwater permeability, d) geology, and e) land use (Kim et al. 2006; Kim et al. 2009; Oh and Lee 2010; Oh et al. 2011).

Hyun-Joo Oh's researchers from Korea initiated a series of studies on mining subsidence by collecting relevant contributing factors and using many classic models from general statistics (Kim et al. 2006; Kim et al. 2009; Oh and Lee 2010; Oh et al. 2011). The case study sites, located in abandoned coal mines, modeled a) frequency ratios, b) logistic regression, c) weights of evidence, and d) artificial neural networks; these were tested successively. The testing sought possible relationships between subsidence and contributing factors by calculating factor ratings/weights to map subsidence hazards; this was accomplished by means of overlaying the ratings or weights. The results for most of the tested models showed predicted accuracies of over 90% (Kim et al. 2006; Kim et al. 2009; Oh and Lee 2010; Oh et al. 2011; Freedman 2009). This series of studies on mining subsidence evidenced a maximum progress, yet also revealed evident drawbacks. The tested models involved the global approach on subsidence prediction, as the spatial heterogeneity of factors was not yet considered (Shang et al 2011; Kim et al 2006; Kim et al 2009; Oh and Lee 2010; Oh et al 2011). Moreover, the dependent variable of subsidence was regarded initially as a dichotomous or categorical one (presence/absence). In fact, subsidence is a numerical variable; therefore, the modeling process by a dichotomous variable as a subsidence may tend to cause a coarser prediction with much less detailed information (Kim et al. 2006; Kim et al. 2009; Oh and Lee 2010; Oh et al. 2011; Freedman 2009).

1.3. Research questions

According to the drawbacks of recent techniques and methods on subsidence, as discussed in the literature review chapter, KKF and GWR will be selected as the two

main methods of this research to process the Louisiana subsidence data. Therefore, research questions are proposed as follows:

In this research, GPS subsidence data in the coastal area of Louisiana were collected and processed by KKF, rather than benchmark subsidence data collected to interpolate in the former research (Zou et al. 2016; Kent and Dokka 2012). Then, further work will serve to validate the KKF raster results.

1. Do the results processed by KKF validly reflect the real spatio-temporal distribution of subsidence patterns in the study site?

In the modeling process, multiple factors that may cause subsidence were collected, and the GWR model and the Regression-Kriging model were selected to process these kinds of data (Pebesma 2006).

2. Do the GWR results reflect the spatial heterogeneity of Louisiana subsidence?

3. Can the Regression-Kriging results accurately predict the spatial pattern of Louisiana subsidence?

1.4. Research significance

The KKF method may be used to process GPS subsidence data for the long term in Louisiana to overcome the flaw of low point density, thereby accurately interpolating a large area of subsidence; KKF, as a combination of the Kalman filter and Kriging interpolation, has features of both (Mardia et al. 1998; Lu, C. et al. 2012). Therefore, it may be considered more advantageous to interpolate and predict subsidence accurately, due to the optimal prediction with time for the Kalman filter (Mardia et al. 1998; Kalman 1960; Zhang 2008). Results by KKF may show the

spatio-temporal subsidence pattern which is varied each year, rather than the spatial pattern of subsidence which is not varied each year in the former benchmark subsidence research, because GPS subsidence data can be collected every year while benchmark subsidence data can only be collected every many years (Zou et al. 2016; Kent and Dokka 2012; Mardia et al. 1998). In addition, multiple kinds of subsidence factors may be modeled and analyzed using GIS to map the spatial heterogeneity for each kind of subsidence factor. Mapping the regression coefficients should serve as the theoretical foundation for government and administrative agencies to make location-based decisions for mitigating subsidence in Louisiana. Additionally, the spatial pattern of Louisiana subsidence can be modeled by Regression-Kriging based on observations from GPS stations in the study site and multiple contributing factors to subsidence (Pebesma 2006; Hengl et al. 2004). Thus, spatial prediction for Louisiana subsidence may be made accurately from contributing factors by Regression-Kriging; to date, such spatial points-to-area prediction based on OLS regression has not yet been accomplished in existing subsidence research.

Chapter 2 Research Methods

2.1. Research workflow

Based on the above proposed research questions, added to the research methods by Mardia et al. in 1998 and Fotheringham et al. in 2002, and strengthened by the characteristics of collected data, permit the methods used in this research to be summarized into a research workflow as follows (Mardia et al. 1998; Fotheringham et al. 2002):

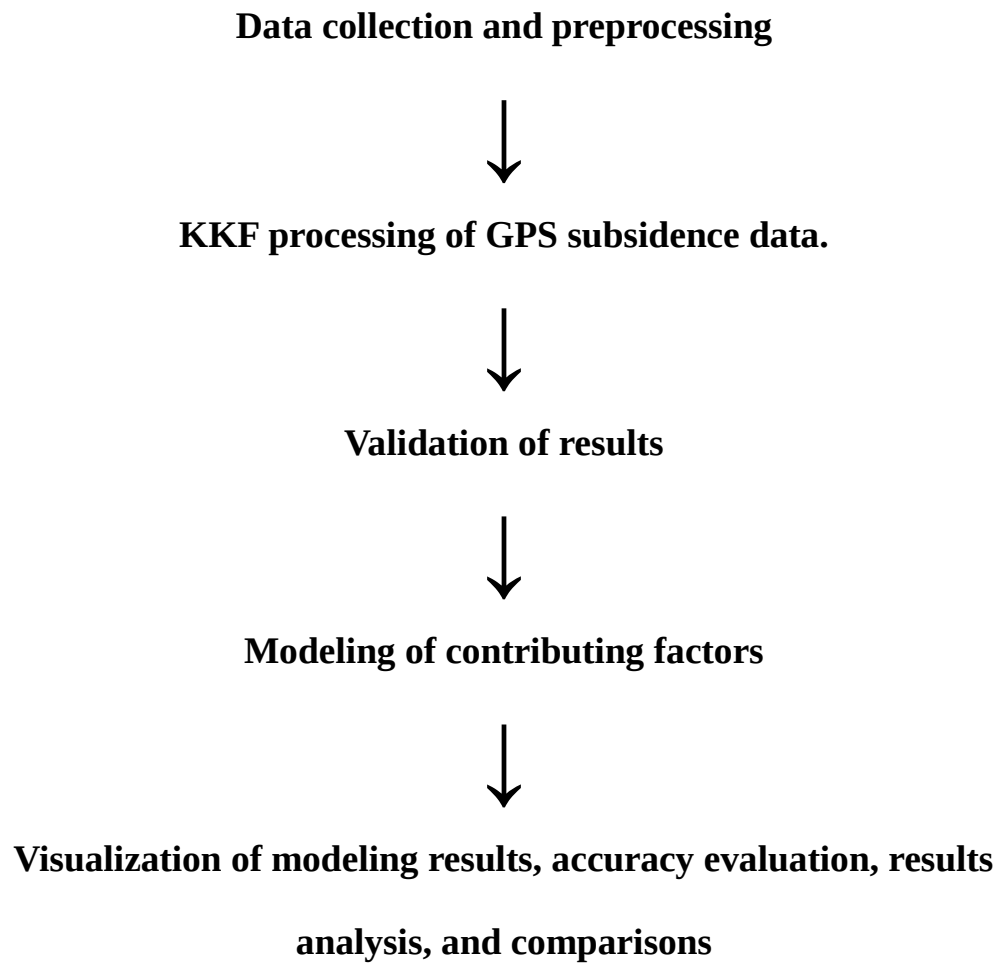

Figure 2. Research workflow

2.2. Data collection

The entire study site has been confined within the geographic boundaries of the State of Louisiana, USA. The data collection work was comprised of the following two parts: GPS data collection and data collection for contributing factors.

2.2.1. GPS data collection

For the GPS data collection on subsidence, an ftp server from National Geodetic Survey (NGS) websites is available online to download all sites of GPS data required since 1994 for this research. The corresponding link is shown as follows:

ftp://www.ngs.noaa.gov/cors/rinex/

From this link and NGS websites, findings indicate that 18 GPS observation sites representing an entire CORS system were installed in Louisiana. The distribution map of all GPS sites in the study area may be shown as follows:

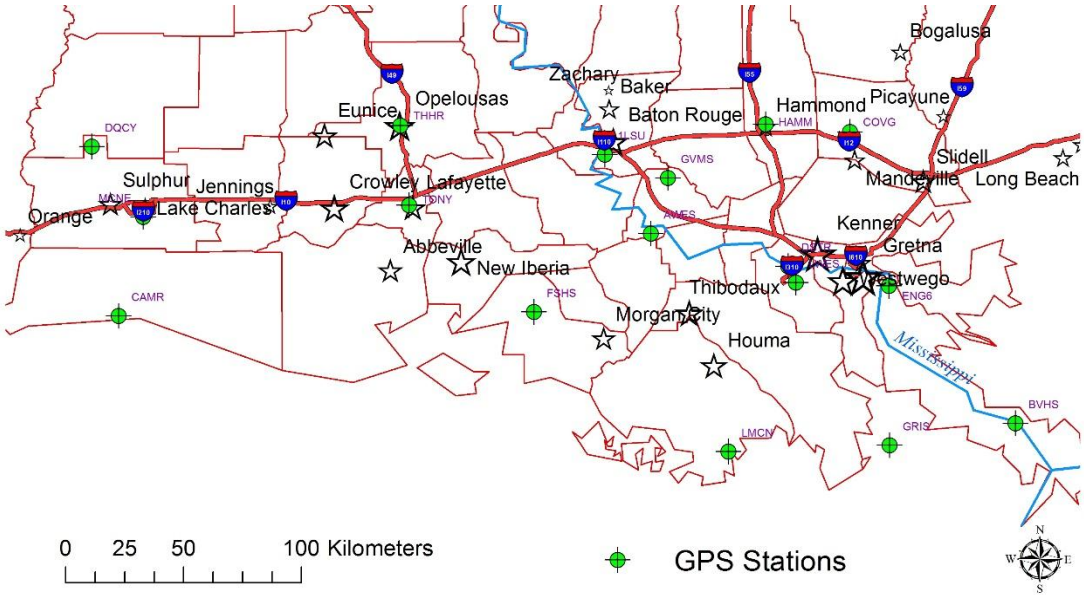

Figure 3. Distribution map for all GPS stations, green points: GPS stations

The 18 stations of GPS data for the last five years to the present were downloaded by this NGS link. The original format for this dataset is kept as a compressed Rinex and is unavailable for direct use on a subsidence survey. As a result, this original set of downloaded data must be preprocessed by geodetic software, such as GIPSY by NASA Jet Propulsion Laboratory (JPL), to be converted to a format with longitude, latitude, and height of sites. Changes in height were used for quantifying the subsidence for GPS sites; by using this GIPSY software by NASA JPL, the height accuracy for all GPS sites may be controlled within 2mm.

2.2.2. Data collection for contributing factors

According to previous research on subsidence factors in Louisiana, multiple data, such as a) groundwater, b) oil, c) natural gas, d) sediment, and e) faulting, were selected for collection (Abdollahzadeh et al. 2013).

For groundwater collection, the data on groundwater levels for observation wells in Louisiana may be collected and recorded online from the USGS website (Extracted from: http://groundwaterwatch.usgs.gov/). Additionally, for data collection, the Louisiana Department of Natural Resources provides a website to collect desired data in GIS format, such as oil, gas, and sediment (Abdollahzadeh et al. 2013). This website is as follows: http://sonris.com. Further, the distribution map of the data for oil and gas in Louisiana parish units are shown on the following map; maps for other data, such as sediment, were obtained as well.

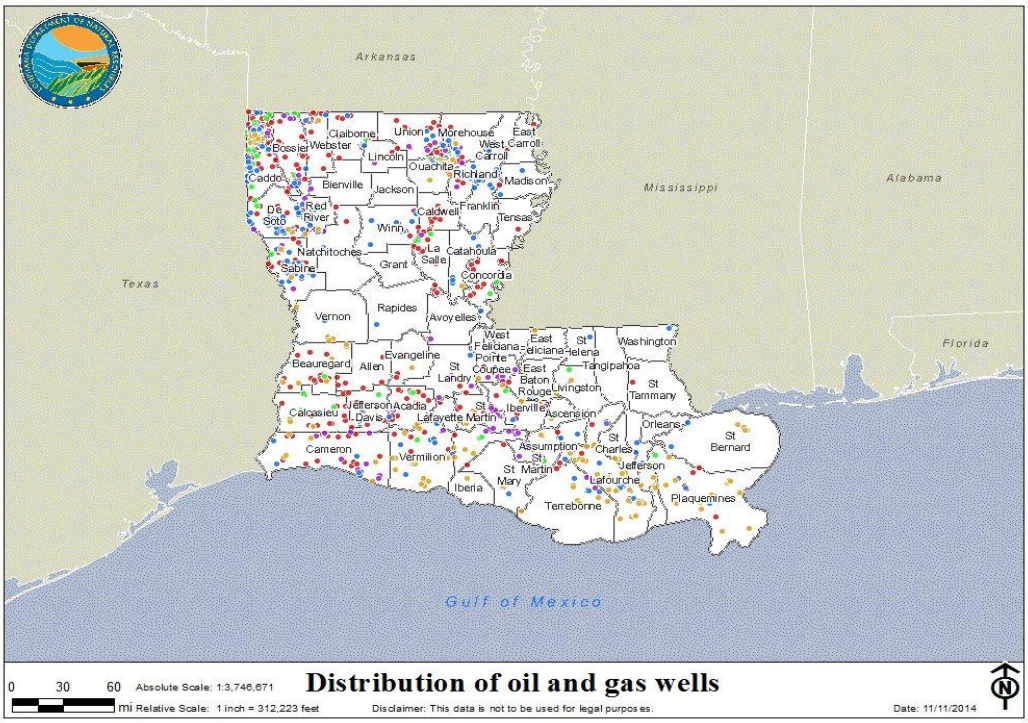

Figure 4. Distribution of oil and gas wells in Louisiana (Extracted from:http://sonris-www.dnr.state.la.us/gis/agsweb/IE/JSViewer/index.html?TemplateID=181)

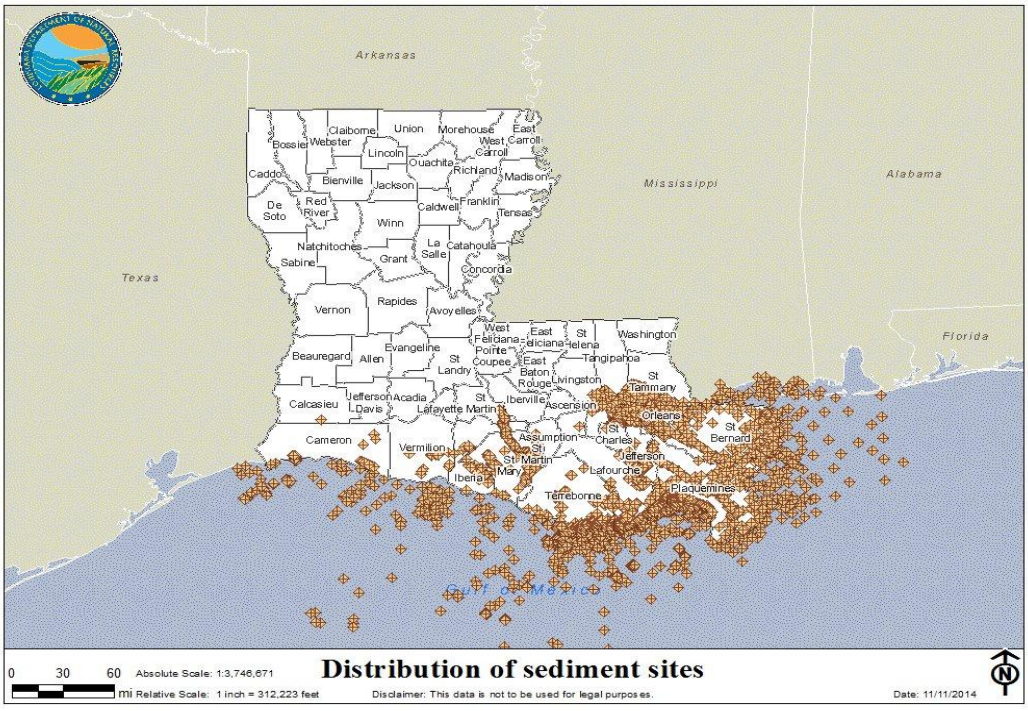

Figure 5. Distribution of sediment measurement sites in Louisiana (Extracted from:http://sonris-www.dnr.state.la.us/gis/agsweb/IE/JSViewer/index.html?TemplateID=181)

For the data collection on anthropogenic mass loading, the data after image classification from the National Land Cover Database (NLCD) website were used to collect the data of buildings cover in Louisiana, thus allowing researchers to extract useful classified information on the mass loading of buildings in the study site (Abdollahzadeh et al. 2013; Kent and Dokka 2012).

2.3. Main methods

As discussed in the research workflow above, the main methods used in this research had three parts as follows:

2.3.1. Kriged Kalman Filter

The Kalman filter, proposed by Kalman in 1960, may provide a feasible process for dynamically changing data in a time series by calculating each state of the optimal estimation for the data (Kalman 1960; Zhang 2008; Mardia et al. 1998). As a recursive process to make estimations in general state models, the Kalman filter minimizes the converged errors the data contains (Kalman 1960; Mardia et al. 1998; Zhang 2008).

Conversely, the Kriging interpolation method from geo-statistics may be used for estimating a large area of spatial data from some spatially correlated scatter points nearby, thus providing a possible means to predict data in a spatial domain (Mardia et al. 1998; Zhang 2008; Olea 1999).

Based on the respective characteristics for two such methods above, a combination of the Kalman filter and Kriging interpolation may be possible for data prediction in a spatio-temporal domain. KKF has proven to be an applicable model to

process spatio-temporal data (Mardia et al. 1998; Kalma 1960; Zhang 2008; Olea 1999).

The fundamental model of KKF:

First, consider the state space model from the Kalman filter as follows (Mardia et al. 1998; Kalman 1960; Zhang 2008):

$$x(t) = h^T \alpha(t) + \varepsilon(t)$$

$$\alpha(t) = P\alpha(t-1) + K\eta(t)$$

The upper equation is the observation equation, and the lower one is the system equation; moreover, $x(t)$ is the observation variable at state t, h is the parameter p-vector, $\alpha(t)$ is the state p-vector, $\varepsilon(t)$ is the scalar observation error, $P : p \times p$ is the transition matrix, $K : p \times d$ *is* the innovation coefficient matrix, and $\eta(t)$ is the innovation (or system error or state noise) d-vector (Mardia et al. 1998; Kalman 1960).

Then, in a spatio-temporal domain, the observation variable $x(t)$ should be extended to $x(s, t)$ for spatio-temporal data (Mardia et al. 1998).

In addition, $x(s, t)$ can be decomposed and expressed as follows (Mardia et al. 1998):

$$x(s, t) = u(s, t) + \varepsilon(s, t)$$

$$u(s, t) = h_1(s)\alpha_1(t) + h_2(s)\alpha_2(t) + \ldots + h_p(s)\alpha_p(t) = h(s)^T \alpha(t)$$

Thus, the observation equation of KKF can be shown as follows (Mardia et al. 1998; Kalman 1960):

$$x(s, t) = h_1(s)\ \alpha_1(t) + h_2(s)\alpha_2(t) + \ldots + h_p(s)\alpha_p(t) + \varepsilon(s, t) =$$

$$h(s)^T\ \alpha(t) + \varepsilon(s, t)$$

The system equation of KKF can also be same as that of the classic Kalman filter as follows (Mardia et al. 1960; Kalman 1960):

$$\alpha(t) = P\alpha(t - 1) + K\eta(t)$$

Moreover, in the observation equation of KKF, the error term $\varepsilon(s, t)$ should be spatially correlated (Mardia et al. 1998) and shown as follows (Mardia et al. 1998):

$$cov(\varepsilon(s, t),\ \varepsilon(s', t')) = 0 \text{ for } t \neq t' \text{ all } s, s'$$

Applying these two key equations above, the KKF observation equation and the KKF system equation may be regarded as the general format of the KKF model (Mardia et al. 1998). As applications to process spatio-temporal data, the principle fields should be calculated by the Kriging predictor, in tandem with the transition matrix and other parameters also specified by the expectation–maximization (EM) algorithm (Mardia et al. 1998; Dempster et al. 1977; Olea 1999).

2.3.2. GWR modeling

GWR is proposed to solve problems on spatial heterogeneity in geo-statistics, using a linear multiple regression model with varied coefficients in different geographic areas (Fotheringham et al. 2002; Shang et al. 2011). By calculating varied coefficients as respective weights for predictors, GWR can also be an effective tool to

show relationships between the dependent variable and predictors, by showing which factor contributes most to the dependent variable in a special geographic area (Fotheringham et al. 2002; Shang et al. 2011).

The fundamental model of GWR:

As a linear multiple regression model, GWR may be shown as follows (Shang et al. 2011; Fotheringham et al. 2002):

$$y(g) = \beta_0(g) + \beta_1(g)\ x_1 + \beta_2(g)x_2 + \ldots + \beta_n(g)\ x_n + \varepsilon$$

The varied coefficients β may be calculated in the following way (Fotheringham et al. 2002; Shang et al. 2011):

$$\beta = (X^T W(g) X)^{-1} (X^T W(g) Y)$$

W(g) is the Gaussian weight function (Fotheringham et al. 2002; Shang et al. 2011) (Extracted from: http://www.cs.cmu.edu/~schneide/tut5/node12.html).

GWR modeling on subsidence

Multiple kinds of collected data displaying useful attribute information contribute to the subsidence in Louisiana, such as groundwater, oil, natural gas, sediment, faulting, and anthropogenic mass loading. These data should be totally quantified to numeric data as important inputs to predictors in the GWR model, such as the groundwater level of each aquifer in a certain site (Fotheringham et al. 2002; Shang et al. 2011; Abdollahzadeh et al. 2013). After GWR modeling, the varied coefficients as GWR results should be identified in a census tract unit (Fotheringham et al. 2002; Shang et al. 2011).

The calculating process of GWR may be made by ArcGIS software, and the results on varied coefficients may be visualized as raster files (Fotheringham et al. 2002; Shang et al. 2011).

To analyze the results, GWR results may be compared with OLS results with respect to prediction accuracy on subsidence to show the advantage of GWR (Fotheringham et al. 2002; Shang et al. 2011; Hayashi and Fumio 2000). Thus, after the GWR modeling process, researchers could identify the possible distribution of major factors on fast subsidence rates for each census tract in the Louisiana study site, which in turn could be used for making special and correct treatments on subsidence in certain areas (Shang et al. 2011).

2.3.3 Regression-Kriging

The GWR model may be used to show the spatial heterogeneity of factors, which contributes to subsidence in Louisiana (Fotheringham et al. 2002; Shang et al. 2011). Unlike GWR, the regression-kriging model may be used based on OLS regression and kriging interpolation of the regression residuals to predict the spatial pattern of Louisiana subsidence (Pebesma 2006; Hengl et al. 2004).

OLS regression model

In modeling any dataset with no clear spatial autocorrelation or spatial dependency with the samples, the OLS model is used to show the relationship between the dependent variable and the independent variables (Wang 2006; Wang et al. 2014; Hayashi and Fumio 2000; Knegt et al. 2010).

The fundamental model is as follows:

$$\mathbf{y = X\beta + \varepsilon}$$

y is the dependent variable vector, and X is the independent variables vector, β is the regression coefficients vector, and ε is the errors vector (Hayashi and Fumio 2000; Wang 2006; Wang et al. 2014). Based on OLS regression, the dependent variable y at one spatial position s can be predicted in the fundamental Regression-Kriging model as follows (Hengl et al. 2004):

$$y(s) = m(s) + e(s)$$

m(s) is the drift term by OLS regression, and e(s) are the interpolated value of OLS regression residuals by Kriging (Hengl et al. 2004).

Thus, the dependent variable y(s) can also be calculated as follows:

$$y(s) = X\beta + \sum_{i=1}^{n} w_i(s) * e(s_i)$$

β is the vector for the regression coefficient by OLS, and $w_i(s)$ are the kriging weights (Wang 2006; Hengl et al. 2004).

In this dissertation, the subsidence rates observed from GPS stations in the study site will be collected as the independent variable y, and likewise, the contributing factors to subsidence will be collected and quantified as the dependent variable X. Then, by OLS, the regression coefficient vector β and the residuals may be generated.

Based on these generated residuals, the interpolated raster may be made by Kriging, and the spatial pattern of the subsidence rate may be predicted by summing the OLS drift, together with the interpolated value from this raster (Hengl et al. 2004).

Chapter 3 Spatio-temporal Pattern Visualizations of Subsidence

3.1. The general equations for KKF and the main processing steps

As the research workflow shows, the KKF processing for GPS subsidence data may be operated after the data collection. The research methods chapter also displays the fundamental model of KKF as follows:

$$x(s, t) = h_1(s)\ \alpha_1(t) + h_2(s)\alpha_2(t) + \ldots + h_p(s)\alpha_p(t) + \varepsilon(s, t)$$

$$= h(s)^T \alpha(t) + \varepsilon(s, t)$$

$$\alpha(t) = P\alpha(t - 1) + K\eta(t)$$

The upper equation above is the observation equation for KKF, and the lower equation is the state equation (Kalman 1960; Mardia et al. 1998), where *x(s, t)* is the observation variable for spatio-temporal data, *h* is the parameter *p*-vector, $\alpha(t)$ is the state *p*-vector, $\varepsilon(t)$ is the scalar observation error, *P : p*×*p* is the transition matrix, *K : p x d is* the innovation coefficient matrix, and $\eta(t)$ is the innovation (or system error or state noise) *d*-vector (Mardia et al. 1998; Kalman 1960).

In the application of KKF processing, the study should specify all essential and intermediate parameters, such as the GPS subsidence data processing (Mardia et al. 1998). Mardia et al.'s findings showed the specification method for the KKF model parameters. This method can help to determine which essential variables or parameters should be summarized. These essential parameters are the covariance matrix, the bending energy matrix B, the principal fields, the parameter matrix *h*, and the transition matrix *P* (Mardia et al. 1998; Kalman 1960).

Additionally, based on these specified parameters, the main steps for KKF processing can be summarized as follows (Mardia et al. 1998; Kalman 1960):

Step 1: Based on the characteristics of the collected data, construct a variogram and fit a model to the variogram (Mardia et al. 1998; Olea and Ricardo 1991).

Step 2: Use the variogram model to generate the covariance matrix for this set of data (Mardia et al. 1998; Olea and Ricardo 1991).

Step 3: Use the covariance matrix to calculate the bending energy matrix B (Mardia et al. 1998).

Step 4: Use the B matrix from the last step to generate the principal fields (Mardia et al. 1998).

Step 5: Use the principal fields from the last step to calculate the parameter matrix *h* from the Kalman filter (Mardia et al. 1998).

Step 6: Use the Kalman filter and EM algorithm to generate the transition matrix *P*, as well as the spatio-temporal field $\alpha(s, t)$ (Mardia et al. 1998; Dempster et al. 1977; Shumway and Stoffer 1982; Olea 1999).

Step 7: Use the spatio-temporal field $\alpha(s, t)$ from the last step to make an interpolation in a time series (Mardia et al. 1998; Dempster et al. 1977; Shumway and Stoffer 1982; Olea 1999).

Step 8: Use the interpolation result to make a raster, showing the distribution of subsidence rates of the study site (Mardia et al. 1998).

Before processing the collected data by GPS observation, this set of original data should be preprocessed by geodetic software, such as NASA's GIPSY. The final data format by preprocessing will show the longitude, latitude, and height for the GPS station, thus allowing the study to use the change in heights to calculate the

subsidence rate. In this research, the preprocessing work by GIPSY (version 6.2) was done by Mr. Zhengsong Chen from the Hubei Earthquake Administration in China.

The GPS subsidence data may be processed by KKF to show the distribution of subsidence rates in the study site. Thus, the following discussion will focus on how to generate the variogram model for subsidence research and will additionally show the final processing results by KKF (Mardia et al. 1998; Olea and Ricardo 1991).

3.2. Variogram

The semi-variogram (or variogram) modeling is essential for KKF processing (Mardia et al. 1998; Olea and Ricardo 1991; Olea 1999). The calculation formula for the semi-variogram (or variogram) is as follows:

$$\gamma(h) = \frac{1}{2N}\sum((Z(x) - Z(x+h))^2$$

The variable *h* is the distance between each pair of points in the study site, while *N* is the total number of point pairs (Olea and Ricardo 1991).

GPS data were collected from 18 coastal stations in Louisiana, using a particular set of data to calculate the average subsidence rate each year from 2011 to 2013. The distribution map of coastal stations in the study site is shown in Figure 6.

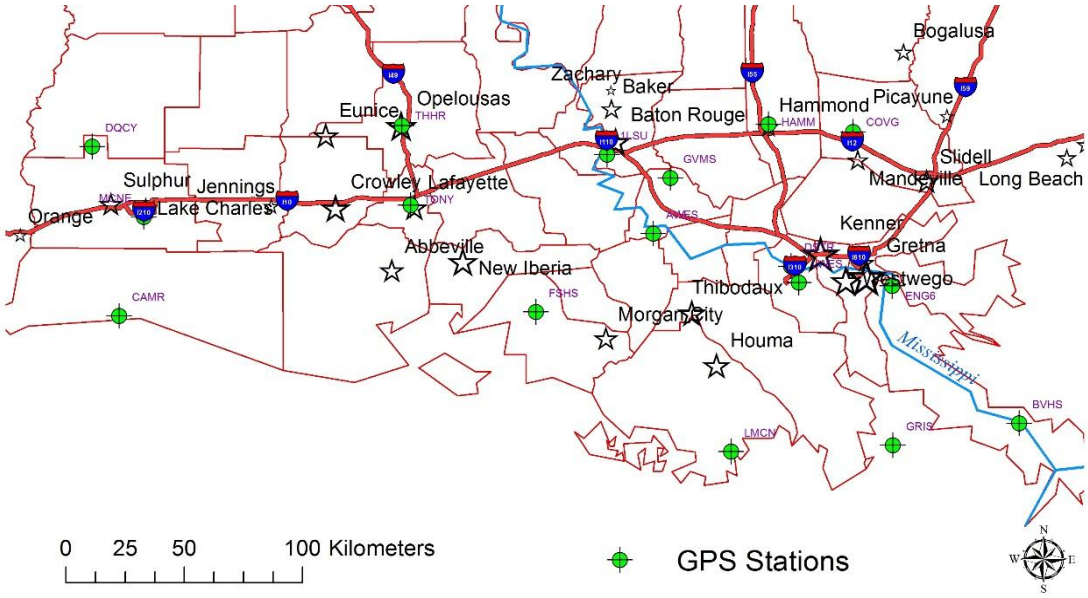

Figure 6. Distribution of 18 GPS stations in the study site, green points: GPS stations

Next, with the whole set of original data preprocessed through GIPSY, the calculation of the average yearly subsidence rate for each GPS station in the study site can be initiated. The preprocessing results found by GIPSY show the daily height value in one year for each GPS station, permitting the use of the total height values for one GPS station in one year; these data generate a straight line by OLS, and the slope for this straight line was used to calculate the yearly subsidence rate for the GPS station (Shinkle and Dokka 2004; Hayashi and Fumio 2000). Thus, we can summarize the calculation formula for the subsidence rate as follows:

Each year's subsidence rate = the slope * one year

(Shinkle and Dokka 2004; Hayashi and Fumio 2000)

Based on this calculation formula and the research methods by Shinkle and Dokka in 2004 as well as Hayashi and Fumio in 2000, I calculated each year's subsidence rate from 2011 to 2013 for all the GPS stations as follows (Shinkle and Dokka 2004; Hayashi and Fumio 2000):

Table 1. Each year's subsidence rate (2011–2013) for all the GPS stations in the study site, marked by Rate 2011, Rate 2012, and Rate 2013 (Unit: m/year)

Site	Longitude	Latitude	Slope 2011	Slope 2012	Slope 2013	Rate 2011	Rate 2012	Rate 2013
LLSU	-91.1803	30.40742	0.000002	-0.00005	-0.00003	0.00073	-0.0183	-0.01095
AWES	-90.983	30.10027	0.000005	-0.00002	-0.00003	0.001825	-0.00732	-0.01095
BVHS	-89.4064	29.33681	-0.000007	-0.000004	-0.000002	-0.002555	-0.001464	-0.00073
CAMR	-93.3251	29.7985	0.00009	0.000008	-0.000004	0.03285	0.002928	-0.00146
COVG	-90.0955	30.47591	0.000002	0.0000007	0.000003	0.00073	0.0002562	0.001095
DQCT	-93.4453	30.45118	0.00012	0.00002	-0.00002	0.0438	0.00732	-0.0073
DSTR	-90.3822	29.96456	0.000001	-0.00001	-0.000005	0.000365	-0.00366	-0.001825
ENGS	-89.9417	29.87896	-0.000001	-0.000009	0.000009	-0.000365	-0.003294	0.003285
ENGS	-89.9421	29.87918	0.0000003	-0.000008	-0.00001	0.0001095	-0.002928	-0.00365
FSHS	-91.5022	29.80531	-0.000004	0.000001	-0.00001	-0.00146	0.000366	-0.00365
GBIS	-89.9573	29.26553	-0.00002	-0.00002	0.00002	-0.0073	-0.00732	0.0073
GVMS	-90.9036	30.31439	0.000003	-0.000006	-0.000002	0.001095	-0.002196	-0.00073
HAMM	-90.4676	30.51308	0.00017	0.000005	0.000002	0.06205	0.00183	0.00073
LMCN	-90.6613	29.25498	-0.00002	-0.00002	0.00004	-0.0073	-0.00732	0.0146
LWES	-90.3494	29.90037	-0.00002	0.000002	0.00001	-0.0073	0.000732	0.00365
MCNE	-93.2177	30.18057	0.0000003	0.000007	-0.00002	0.0001095	0.002562	-0.0073
THHR	-92.0806	30.52935	0.00011	0.000009	0.0000002	0.04015	0.003294	0.000073
TONY	-92.0451	30.22138	0.000006	0.00002	0.000009	0.00219	0.00732	0.003285

The calculations of subsidence rates for all the GPS stations are as shown in Figure 7, 8, 9.

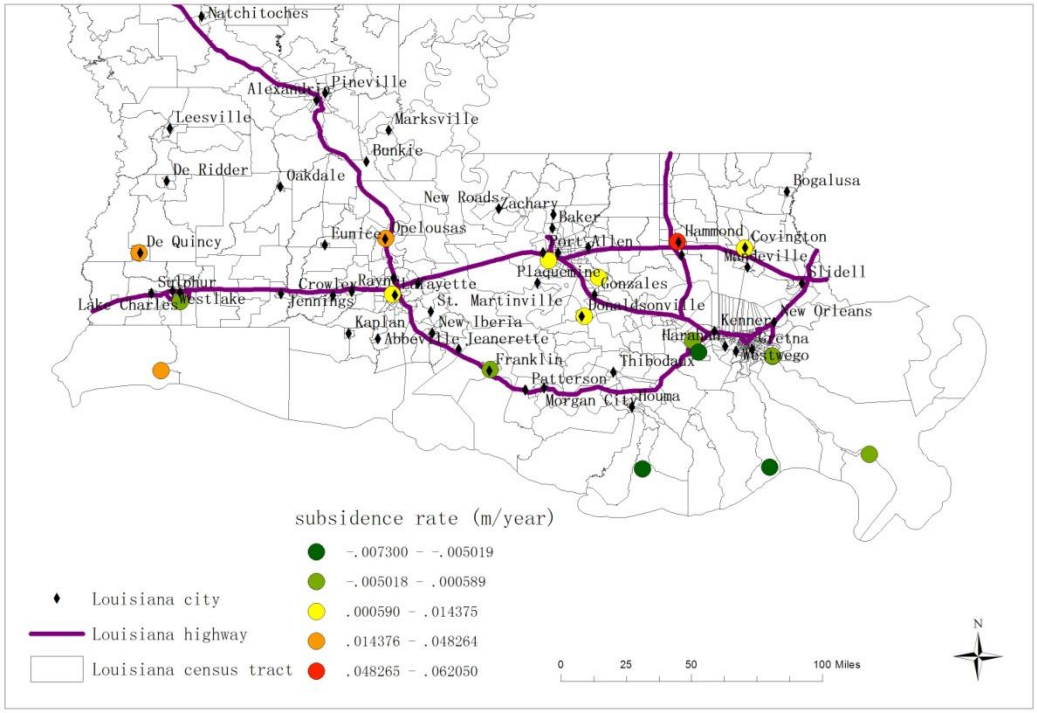

Figure 7. Subsidence rate for each GPS station in 2011 in the study site (Some map data were extracted from: http://atlas.lsu.edu)

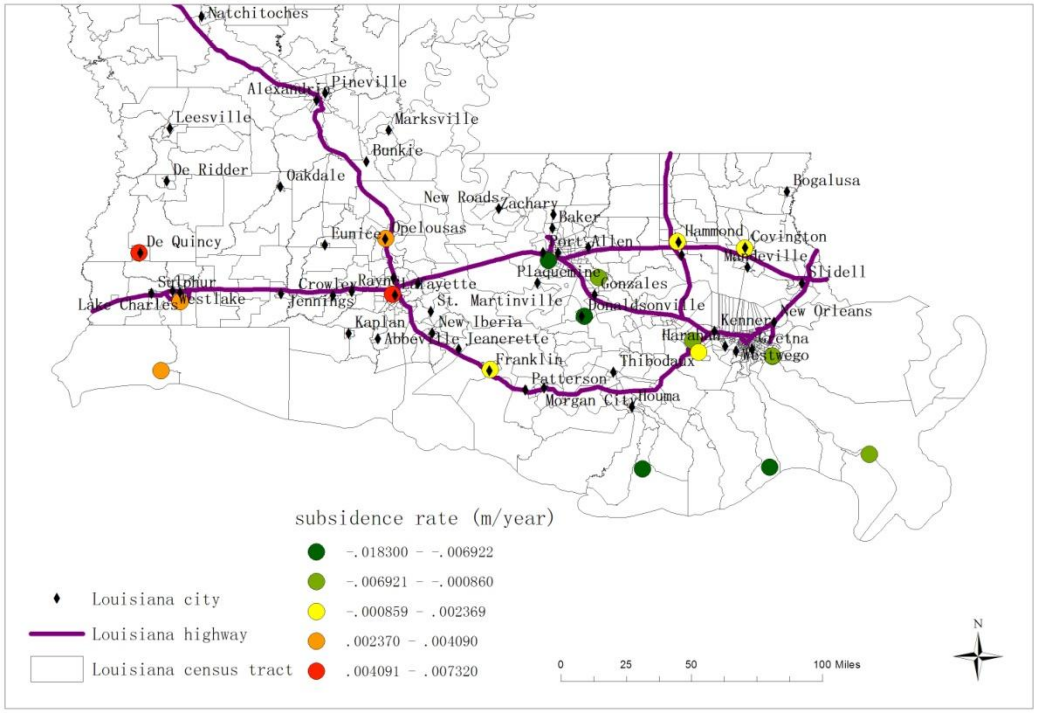

Figure 8. Subsidence rate for each GPS station in 2012 in the study site (Some map data were extracted from: http://atlas.lsu.edu)

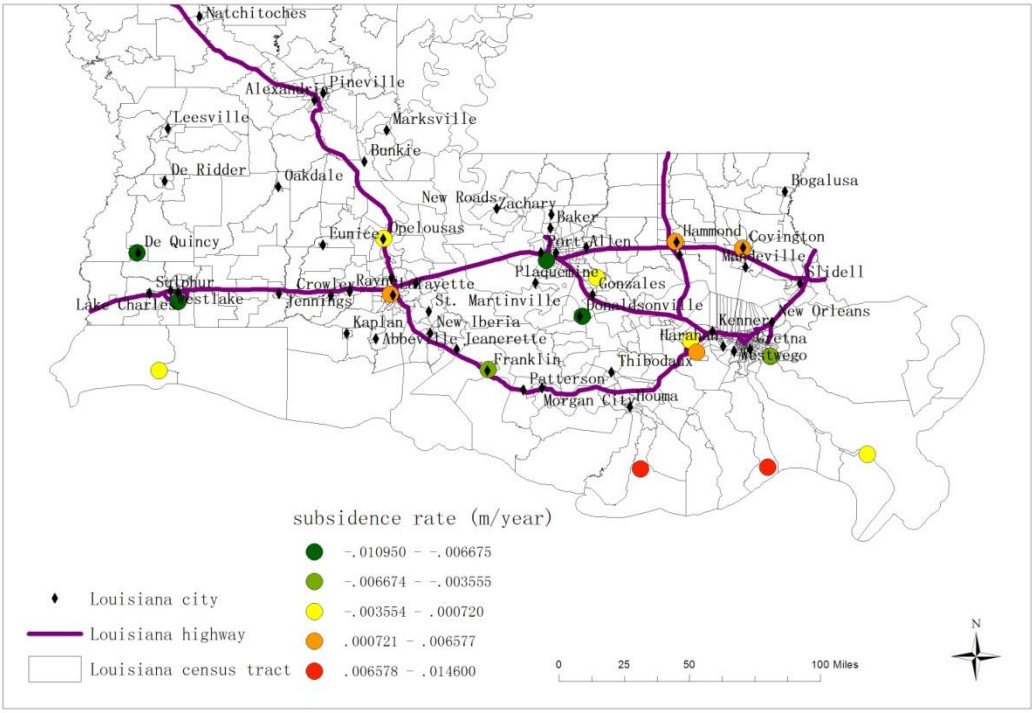

Figure 9. Subsidence rate for each GPS station in 2013 in the study site (Some map data were extracted from: http://atlas.lsu.edu)

Based on the calculation results for the subsidence rates, as well as the research methods by Mardia et al. in 1998 and Olea and Ricardo in 1991, a semi-variogram is generated as follows, using the semi-variogram formula above (Mardia et al. 1998; Olea and Ricardo 1991):

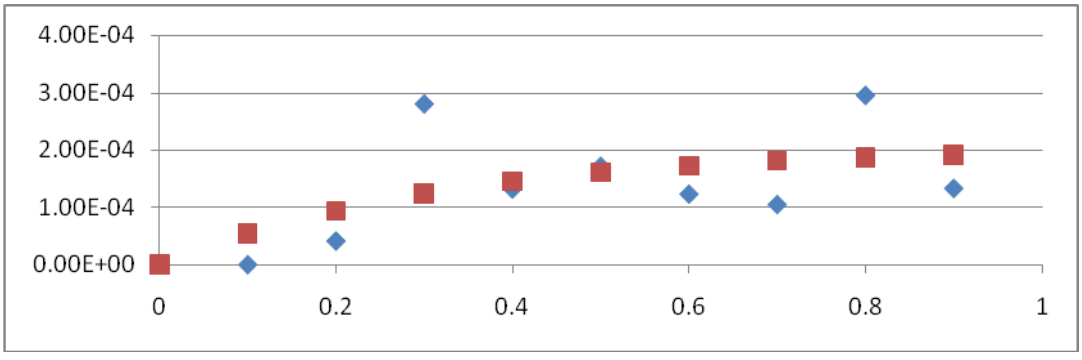

Figure 10. Semi-variogram for calculated subsidence rates in the study site, blue points: averaged γ values, red points: the fitted exponential model, the horizontal axis unit: degree

For the semi-variogram, this research fixed the bin size and number of bins in the horizontal axis *h*, to calculate the average γ value in each bin (blue points in the above figure) (Olea and Ricardo 1991; Mardia et al. 1998). Then, based on the points for these γ values, I used a model to fit these points (red points in the above figure) (Olea and Ricardo 1991; Mardia et al. 1998).

The bin size is fixed to 0.1, and the number of bins is fixed to 10. Then, we chose the exponential model to fit. The equation of the fitted model is as follows (Olea and Ricardo 1991; Mardia et al. 1998):

$$\gamma = 1.7316\text{E-}08 + 0.0002\ (1 - e^{-3.0798h}).$$

3.3. Final processing results and their consistency check

As Chapter 3.1 shows, the above KKF process, inclusive of the calculations and specifications for multiple variables and parameters drawn from collected spatio-temporal GPS data, may be coded into an executable program based on ArcGIS software. In this research, the computer program for KKF, coupled with ArcGIS software, was used to process subsidence rate data from GPS observations.

Using KKF, the distributions of the subsidence rates in 2011, 2012, and 2013 were generated. The question remains whether the KKF results are valid in this study. To assure that these KKF results are validated, further work should be conducted.

First, the model was validated using a cross-validation approach (Geisser and Seymour 1993). Each time a spatio-temporal field was calculated by leaving one GPS station out, the researcher compared the KKF modeled data with the GPS station data (Geisser and Seymour 1993), with the expectation that if the surface motion rate data

showed strong spatial and temporal continuity, certain GPS stations would be well replicated by the KKF model. The root mean square error (RMSE) was used to evaluate how the predicted surface motion rates compared to the observed surface motion rates (Geisser and Seymour 1993). Figure 8 shows the RMSEs of the GPS stations, based on research methods used by Geisser and Seymour in 1993 and Mardia et al. in 1998 (Geisser and Seymour 1993; Mardia et al. 1998). The GPS stations located inland displayed greater RMSE values (up to 40 mm/year), suggesting that those stations could not be replaced by model predictions. The reason might be that the inland area is more directly related to human activities, and therefore the land surface motion process could be very complex and thus difficult to predict from the surrounding GPS stations. Therefore, more GPS stations should be allocated toward the inland areas to capture the spatial continuity. Of course, considering the cost to build new GPS stations, the alternative to building more GPS stations is to use regression models to enhance the spatio-temporal prediction model.

The stations “LWES,” “BVHS,” and “LMCN” have quite a low RMSE (~5 mm/year). These stations are located where the major wetlands and swamps of Louisiana are preserved. The spatio-temporal model predicted the land surface motion rate well, even with some missing data.

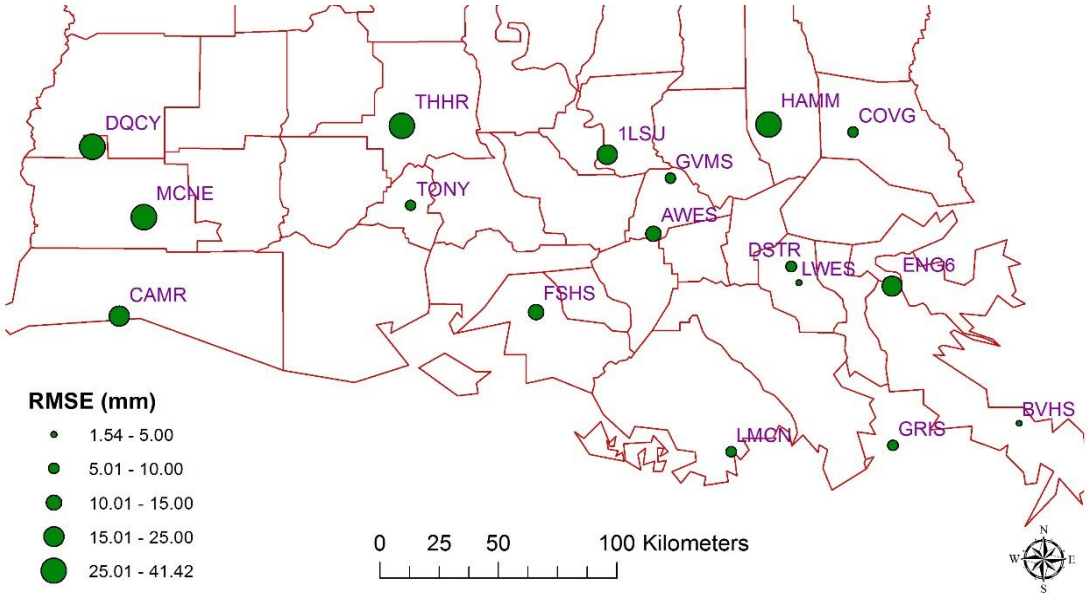

Figure 11. RMSE of the GPS stations from cross-validation

A sinkhole constitutes a threatening phenomenon, especially for people living in bayou areas all over the world. Indeed, in August of 2012, such a well-known phenomenon emerged near Bayou Corne in Louisiana and was termed the "Bayou Corne Sinkhole" (Cusanza 2013; Jones and Blom 2014). The collapse of one cavern in the salt dome under the bayou resulted in this sinkhole; the sinkhole size had increased from 1 hectare (Cusanza 2013; Jones and Blom 2014). The government issued emergent warnings to people living near Bayou Corne, and many were forced to evacuate (Cusanza 2013; Jones and Blom 2014).

For the Bayou Corne Sinkhole, a former study by experts revealed that rather than faulting, a sidewall collapse had formed the threatening sinkhole by creating a disturbed rock zone, thereby filling the cavern void (Jones and Blom 2014; Louisiana Department of Natural Resources 2013b). By radar interferometry, scientists found a pre-event and post-formation surface deformation near Bayou Corne, showing

significant vertical and horizontal ground movements (Jones and Blom 2014; Jones and Blom 2015).

This vertical downward surface movement detected by radar interferometry can be observed in the form of subsidence; therefore, subsidence may be used to signify sinkholes (Jones and Blom 2014; Jones and Blom 2015; Dokka 2006; Kent and Dokka 2012). Further, the precursory surface movement detected by radar interferometry in Bayou Corne indicated that the surrounding subsidence may have even accelerated prior to the sinkhole event (Jones and Blom 2014; Jones and Blom 2015). In fact, the accelerating subsidence near Bayou Corne was surveyed by many organizations, such as Fenstermaker and Itasca, when the sinkhole first emerged in 2012; these organizations still monitor the sinkhole (Jones and Blom 2014; Jones and Blom 2015; Fenstermaker 2014; Itasca 2013).

To check the consistency of the generated KKF results, the Bayou Corne Sinkhole location should be added to the distribution maps of subsidence rates from 2011 to 2013 as follows, based on the research methods used by Mardia et al. (1998), Kent and Dokka (2012), and Jones and Blom (2014 and in 2015):

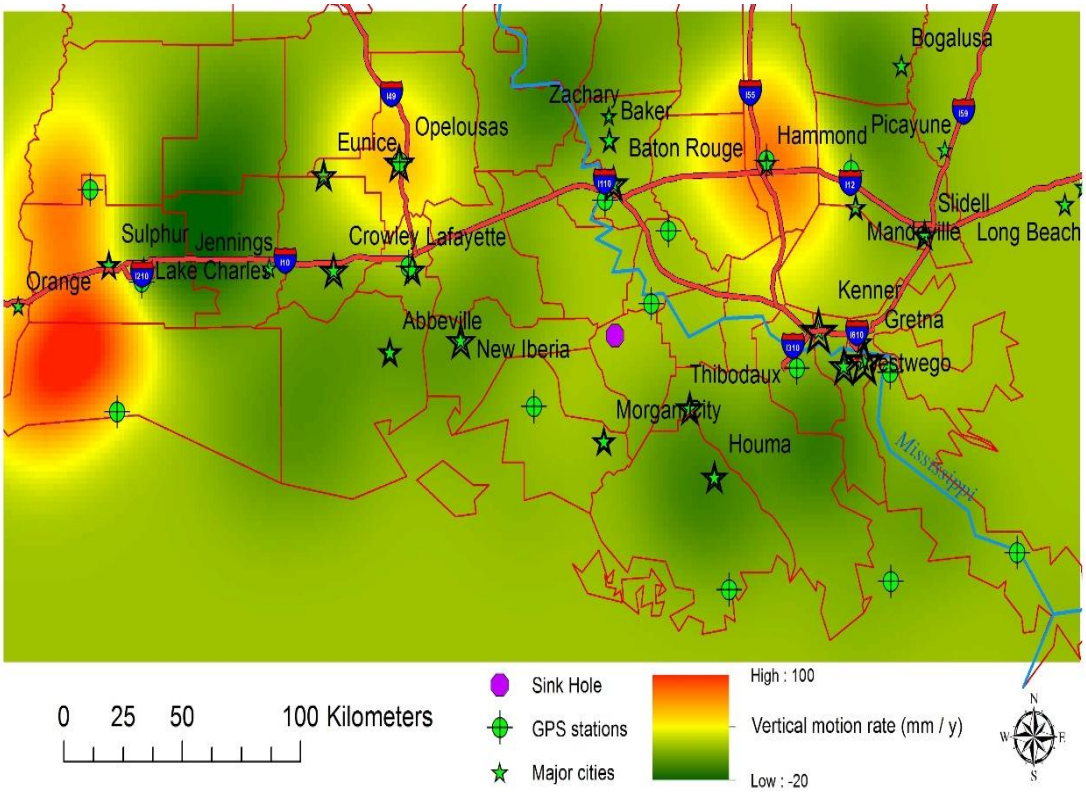

Figure 12. Distribution of subsidence rates (Unit: mm/year) in the study site in 2011 by KKF, green points: GPS stations, purple point: the Bayou Corne Sinkhole location

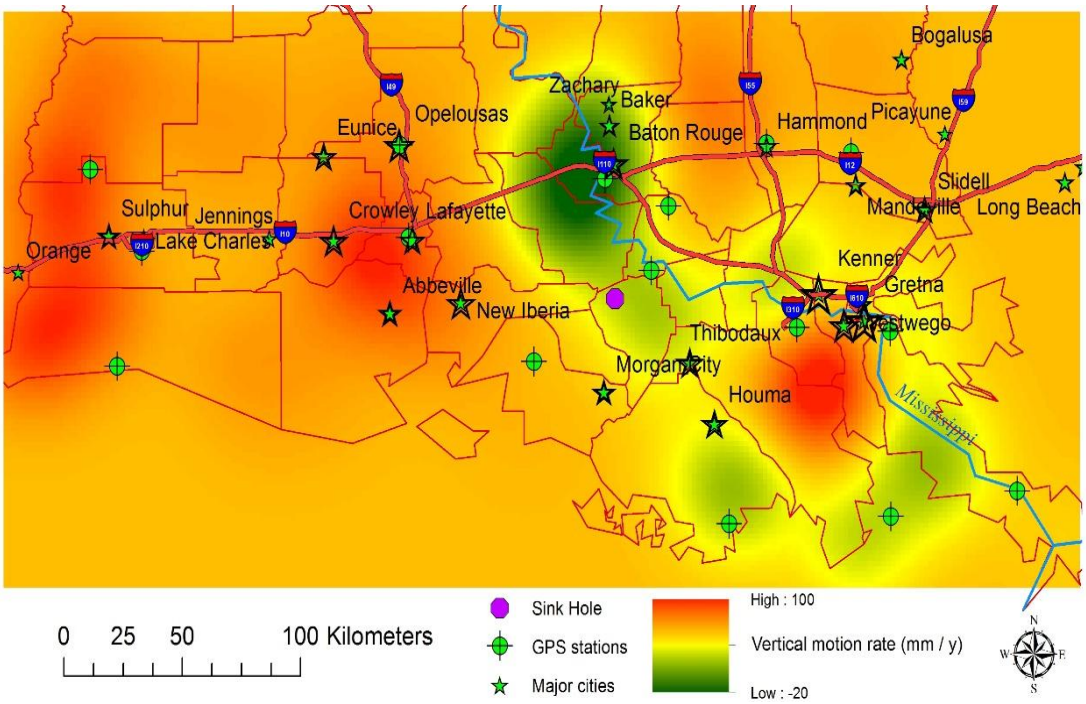

Figure 13. Distribution of subsidence rates (Unit: mm/year) in the study site in 2012 by KKF, green points: GPS stations, purple point: the Bayou Corne Sinkhole location

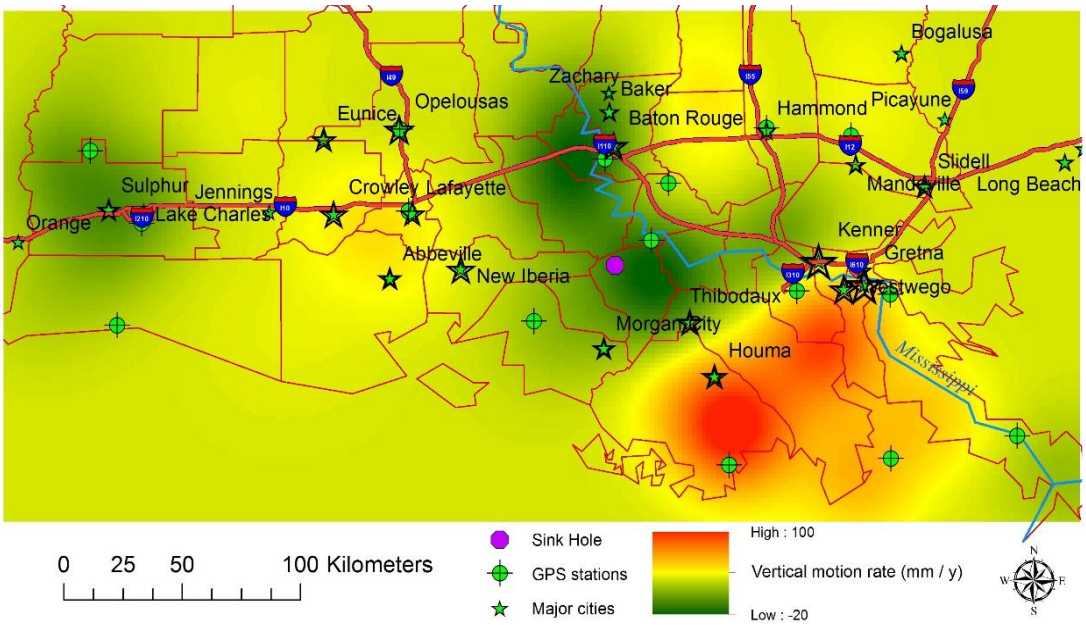

Figure 14. Distribution of subsidence rates (Unit: mm/year) in the study site in 2013 by KKF, green points: GPS stations, purple point: the Bayou Corne Sinkhole location

Figure 12 shows the spatial distribution of the subsidence rate in 2011, about one year prior to the Bayou Corne Sinkhole event. This distribution in 2011 appears to be uniform, with no significantly high subsidence area. No obvious subsidence was identified in this area during 2011. The vertical motion rates (Kent and Dokka 2012) around Bayou Corne were positive, ranging from 0 to 0.005 meters per year (5 mm/year). This data remained consistent with previous reports that the surface in this area had even made a slightly upward movement in 2011 (Jones and Blom 2014). Thus, from Figure 12, the study detected no significant precursory subsidence or vertical ground displacement around Bayou Corne Sinkhole in the 2011 period (Dokka 2006; Kent and Dokka 2012). In contrast to Figure 12, Figure 13 shows a much different and abnormal distribution of land vertical motion rates close to the sinkhole event (August 2012), with a significant accelerating subsidence to the north of Bayou Corne. The surface motion subsidence rate was approximately -15 mm/year

near Baton Rouge and north of Bayou Corne. Likewise, Figure 14 shows the spatial pattern of the surface motion in 2013 after the sinkhole event. In Figure 14, the negative motion (subsidence) was found around Baton Rouge and the Bayou Corne Sinkhole (Dokka 2006; Cusanza 2013). Interestingly, the center of the negative motion area coincides with the sinkhole (Cusanza 2013). However, the relatively large RMSEs of the GPS stations around the sinkhole (Figure 11) suggest that to better monitor such abrupt changes as sinkhole events, more GPS stations are required.

Thus, from Figures 12, 13, and 14, this study can confirm that the land area around Bayou Corne experienced an abrupt change, which may be caused by the sinkhole event in August 2012. The upward motion rate (5 mm/year) in 2011 was changed to a -14 mm/year downward motion in 2013 because of the sinkhole. Many research organizations also reported a negative land vertical motion caused by the Bayou Corne Sinkhole. For example, Itasca measured the land subsidence rate near Bayou Corne at approximately -0.4 inches/year (about -10 mm/year) (Itasca 2013). This study result is consistent with the previously reported land vertical motion around Bayou Corne. The consistency means that this subsidence area, showing a diameter of approximately 50 kilometers around Bayou Corne, may be correlated with or caused by a ground movement, such as a sinkhole (Louisiana Department of Natural Resources 2013b; Fenstermaker 2014; Jones and Blom 2014, 2015). In the consistency check of the KKF results in this dissertation, the Empirical Bayesian Kriging results may also be used to compare and show the differences for the same set of data (Extracted from:

http://www.esri.com/news/arcuser/1012/empirical-byesian-kriging.html) (Olea 1999). Based on the research method used by Kent and Dokka in 2012, the Empirical Bayesian Kriging results are as follows, shown with the Bayou Corne Sinkhole location (The interpolation method is extracted from: http://www.esri.com/news/arcuser/1012/empirical-byesian-kriging.html.) (Cusanza 2013; Kent and Dokka 2012):

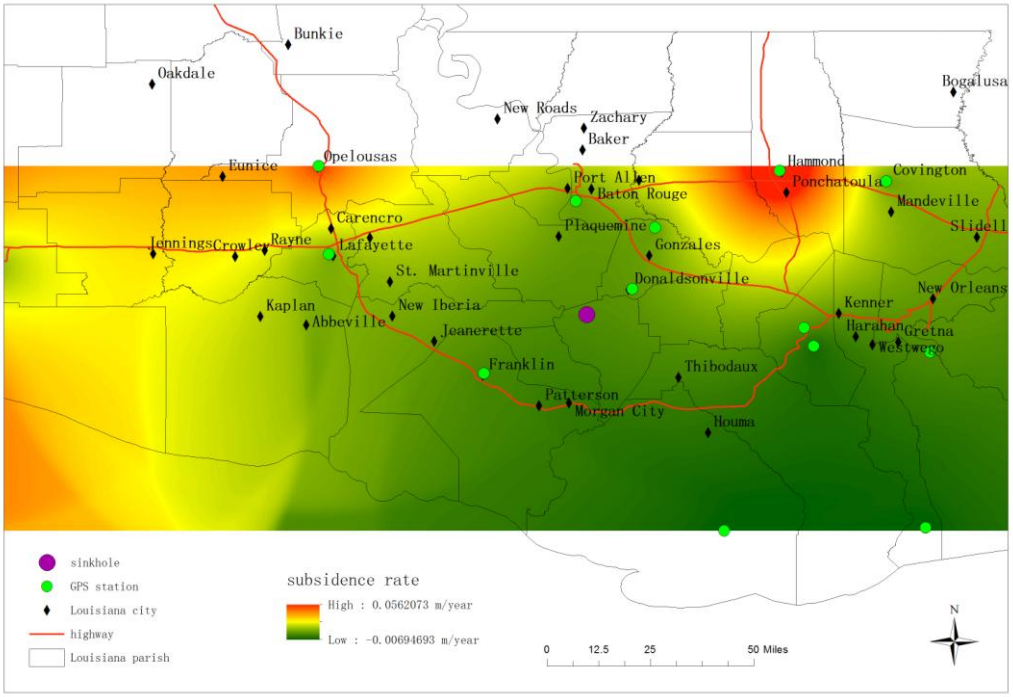

Figure 15. Distribution of subsidence rates (Unit: m/year) in 2011 using Empirical Bayesian Kriging, green points: GPS stations, purple point: the Bayou Corne Sinkhole location (Some map data were extracted from: http://atlas.lsu.edu)

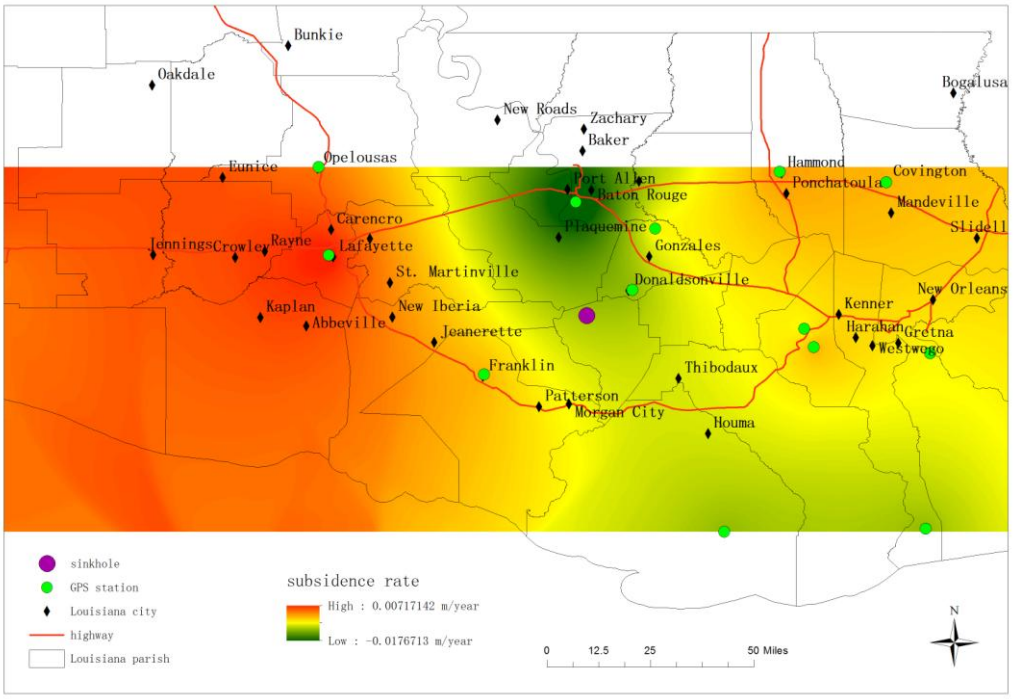

Figure 16. Distribution of subsidence rates (Unit: m/year) in 2012 using Empirical Bayesian Kriging, green points: GPS stations, purple point: the Bayou Corne Sinkhole location (Some map data were extracted from: http://atlas.lsu.edu)

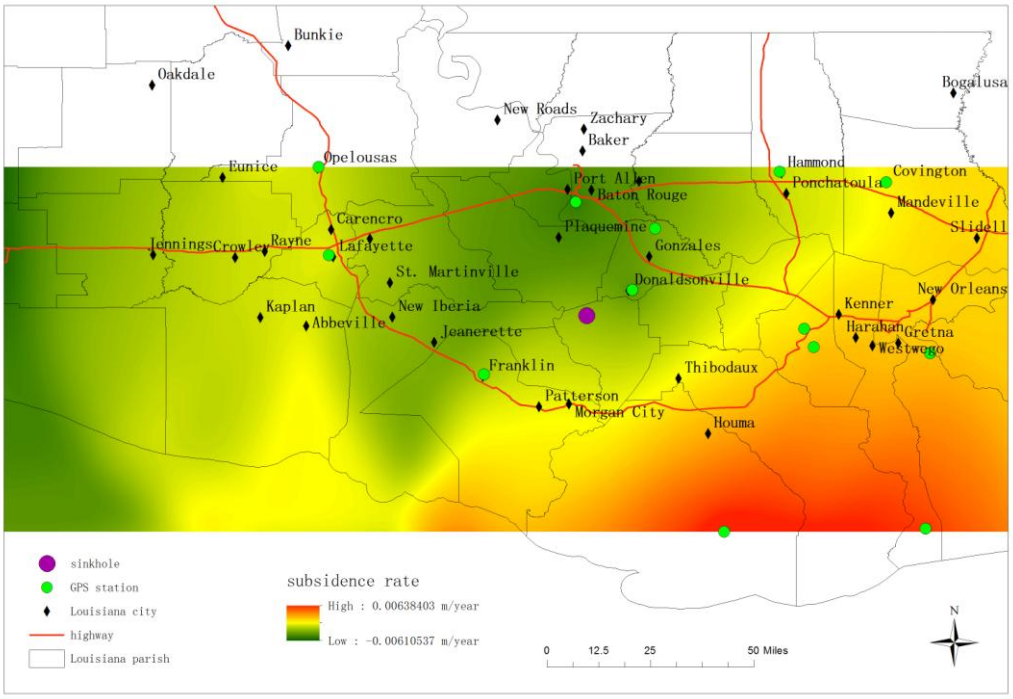

Figure 17. Distribution of subsidence rates (Unit: m/year) in 2013 using Empirical Bayesian Kriging, green points: GPS stations, purple point: the Bayou Corne Sinkhole location (Some map data were extracted from: http://atlas.lsu.edu)

Comparison between Figure 12 and Figure 15 shows that in 2011, the Empirical Bayesian Kriging results were similar those of KKF. It may be noted that while the distribution of subsidence rates in Figures 12 15 are similar, there are also clear differences. In Figure 12, the subsidence rates near Bayou Corne are positive, ranging from 0 to 0.005 m/year; yet in Figure 15, these values are near zero.

Comparisons between Figure 13 and Figure 16 show that in 2012, the KKF and Empirical Bayesian Kriging results are similar as well; again, there are clear and distinct differences. One difference is that in Figure 13, we see a subsidence area near Bayou Corne of approximately -0.01 m/year, yet in Figure 16, we find no such subsidence area near Bayou Corne.

Further comparisons between Figure 14and Figure 17 indicate that in 2013, the KKF and Empirical Bayesian Kriging results again are very different. The distribution of subsidence rates in Figure 14 shows a clear subsidence area near Bayou Corne of approximately -0.01m/year, while from contours in Figure 17, this distribution differs; the subsidence rates near Bayou Corne are clearly less, ranging from 0 to -0.005m/year.

From the above comparisons, it appears that the Empirical Bayesian Kriging rather than KKF results differ significantly due to significant interpolation error, which can not be checked consistently via Bayou Corne Sinkhole knowledge (Olea 1999; Cusanza 2013; Jones and Blom 2014; Jones and Blom 2015). Thus, because of a smaller interpolation error, KKF is advantageous over other models for processing subsidence data, permitting strong validation of the KKF results in this research (Olea 1999; Mardia et al. 1998; Kalman 1960).

3.4. Summary and discussion

In this chapter, the KKF model to process the GPS subsidence data was discussed. Based on research done by Mardia et al. in 1998, the steps on how to calculate the essential parameters in the KKF model were summarized (Mardia et al. 1998). Then, based on the subsidence data collected, the yearly subsidence rate for each coastal observation station was calculated. These final results indicate that from 2012 to 2013 in coastal Louisiana areas, one area in particular clearly exhibited high subsidence rates at approximately 10 mm each year and kept nearly the same rate (New Orleans area) in the coast of Louisiana. Additionally, the disaster knowledge of

the Bayou Corne Sinkhole in 2012 was used to check the consistency of KKF results in this research. In 2012, the subsidence near Bayou Corne accelerated during the sinkhole year and further expanded as an accelerating subsidence area since 2012. The subsidence rate near Bayou Corne was stabilized at nearly 10 mm per year during and after the sinkhole incident (2012–2013). This stabilized subsidence rate maintains a basic consistency with the measured subsidence rate at approximately 0.4 inches/year near the Bayou Corne Sinkhole from the Itasca-Subsidence Report, which checks this study by KKF consistently (Itasca 2013; Jones and Blom 2014; Jones and Blom 2015). Thus, the KKF results are valid and outperformed the traditionally used spatial interpolation method that disregards the continuity of data in time.

Chapter 4 Spatial Pattern Modeling of Subsidence by Regression and Kriging

4.1. Regression-Kriging and its main steps

As illustrated in the research methods chapter, the fundamental model of Regression-Kriging can be formatted as follows (Hengl et al. 2004; Wang 2006):

$$\mathbf{y(s) = X\,\beta + \sum_{i=1}^{n} w_i(s) * e(s_i)}$$

In this formation, X is the vector for independent variables, y(s) is the value of dependent variable y at the location s, β is the vector for regression coefficient by OLS, and $\mathbf{w_i(s)}$ are the Kriging weights (Hengl et al. 2004; Wang 2006).

Thus, based on this formation, the main steps of Regression-Kriging can be summarized as follows:

Step 1: Data collection and rasterization for the dependent variable and the independent variables (Pebesma 2006; Hengl et al. 2004).

Step 2: Regression analysis by OLS.

Step 3: Interpolation of the OLS residuals.

Step 4: Generating the drift raster based on the OLS regression coefficients (Hengl et al. 2004).

Step 5: Generating the prediction raster for the dependent variable by summing the drift raster and the interpolation raster of the OLS residuals (Hengl et al. 2004).

Step 6: Accuracy evaluation of the prediction by Regression-Kriging.

4.2. Data collection and rasterization of the contributing factors to subsidence

In this dissertation, subsidence data have been collected via GPS observations for modeling. For the subsidence prediction work of points-to-area by Regression-Kriging, the study site should have many GPS stations recording subsidence in the coastal area of Louisiana; thus, this study site may be mapped as follows:

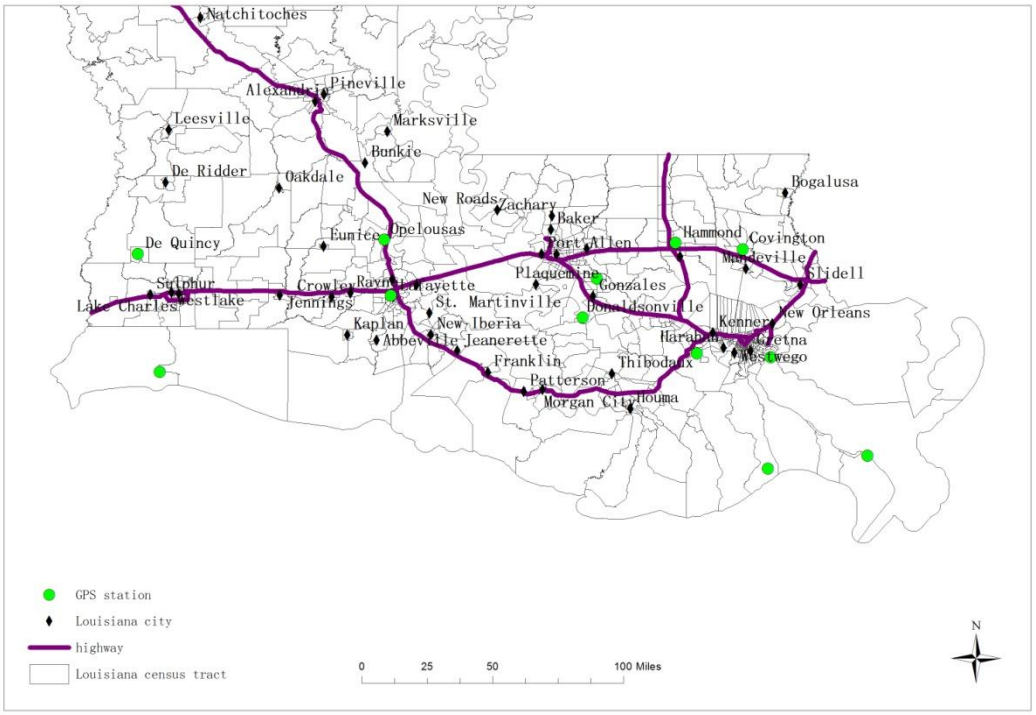

Figure 18. Study site with 12 GPS stations (Some map data were extracted from: http:// atlas.lsu.edu)

This study site for Regression-Kriging has 12 GPS stations, and 736 Louisiana census tracts. Subsidence data should be collected and calculated from these GPS station as the dependent variable in OLS and Regression-Kriging, and in this dissertation, the subsidence rates at GPS stations have been calculated based on the OLS regression in Chapter 3. For these 12 stations in the study site, the calculated subsidence rates in 2013 should be used for Regression-Kriging as follows:

Table 2. Subsidence rates in 2013 for 12 GPS stations in the study site (Unit: m/year)

GPS station	Subsidence rate in 2013
GVMS	-0.000730
AWES	-0.010950
DQCY	-0.007300
CAMR	-0.001460
GRIS	0.007300
TONY	0.003285
ENG6	-0.003650
BVHS	-0.000730
LWES	0.003650
THHR	0.000073
COVG	0.001095
HAMM	0.000730

For the Regression-Kriging model, the contributing factors to subsidence, such as groundwater, oil/gas, sediment, faulting, and the loading of buildings, should be collected and rasterized as the independent variables, in addition to the subsidence data collection for the dependent variable (Abdollahzadeh et al. 2013). Thus, this collection and rasterization work has been done as follows:

Groundwater level change

Former research showed that the groundwater change should be a main factor of subsidence, so for 2013, many wells of groundwater-level changes in the study site have been collected from the USGS website (http://groundwaterwatch.usgs.gov/) (Shang et al. 2011; Abdollahzadeh et al. 2013). Then, based on these changes, an interpolation process using the Inverse Distance Weighting (IDW) method has been used to generate a raster showing the spatial pattern of groundwater changes in the study site (Shang et al. 2011; Shepard and Donald 1968).This interpolated raster has

been mapped as follows:

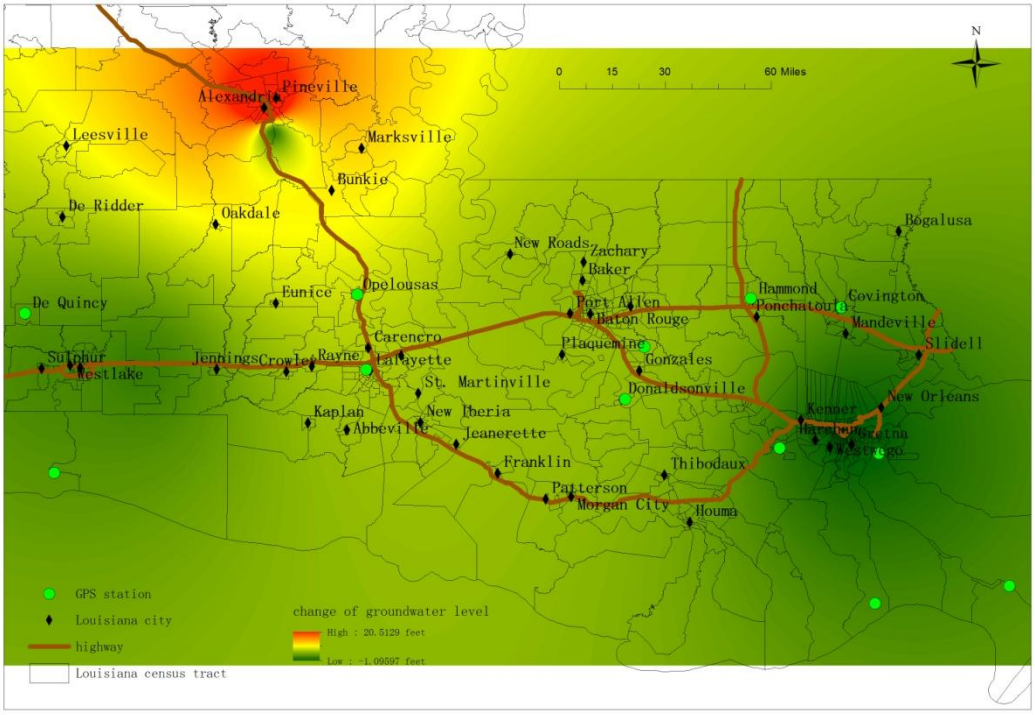

Figure 19. Interpolated groundwater level changes in the study site (Some map data were extracted from: http://atlas.lsu.edu)

Further, for the OLS work in Regression-Kriging, the interpolated groundwater level change at each GPS station should be recorded from the raster as follows:

Table 3. Interpolated groundwater level change at each GPS station (Unit: feet)

GPS station	Groundwater level change
GVMS	3.409013
AWES	3.365736
DQCY	1.590018
CAMR	1.564772
GRIS	0.994465
TONY	4.057013
ENG6	-0.952839
BVHS	1.175898
LWES	0.291490
THHR	4.939754
COVG	1.315575
HAMM	2.723452

Oil and gas pumping

The SONRIS website provides the distribution data of oil and gas pumping wells in Louisiana, and based on this distribution, the point density of wells may be calculated in the study site (http://sonris.com and http://sonris-www.dnr.state.la.us/gis/agsweb/IE/JSViewer/index.html?TemplateID=181).For Regression-Kriging, the calculated point densities have been rasterized in the following image:

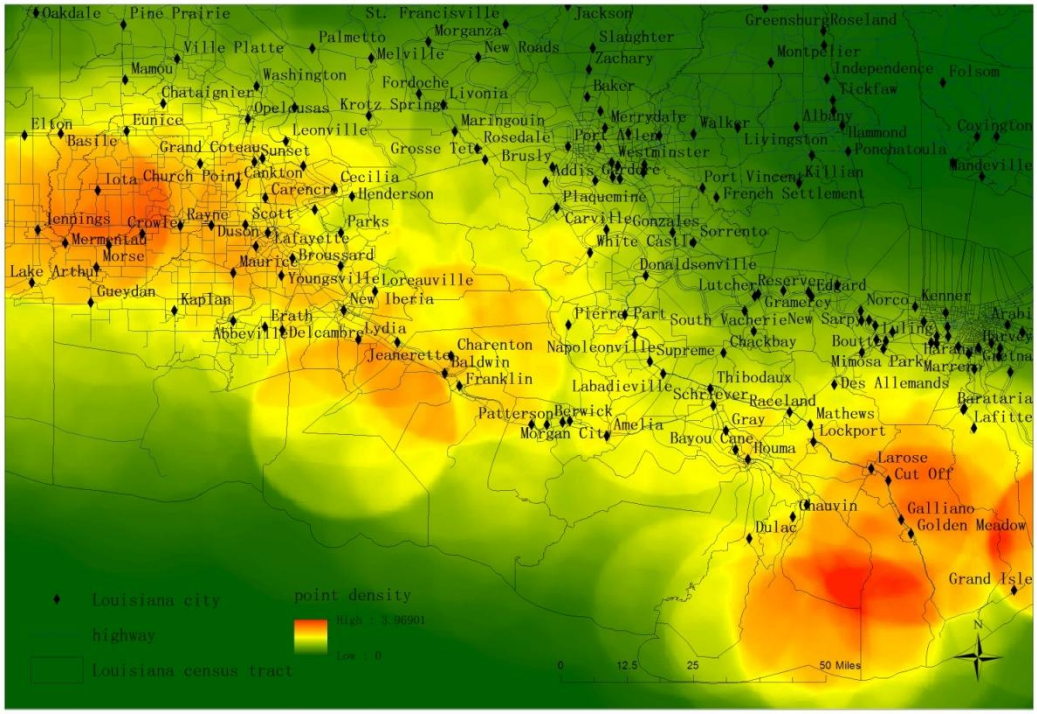

Figure 20. Distribution of the point densities for oil and gas pumping wells in the study site (Some map data were extracted from: http://atlas.lsu.edu)

In addition, for the OLS work in Regression-Kriging, the oil and gas pumping data at one GPS station may be quantified by the point density value for the coordinate where this GPS station is located; thus, the wells' density data at each GPS station may be quantified and recorded as follows:

Table 4. Quantified point density of the wells at each GPS station

GPS station	Density
GVMS	0.81189209223
AWES	1.36438834667
DQCY	1.60287892818
CAMR	1.45654213428
GRIS	2.29616570473
TONY	2.24582242966
ENG6	0.57809448242
BVHS	2.49753880501
LWES	1.25303578377
THHR	1.45142245293
COVG	0.02431836538
HAMM	0.06698216498

Sediment

The former research shows that sediment attributes may be spatially correlated, and the thickness of sediment may be a main factor to subsidence, due to the sediment compaction process of the coastal area of Louisiana (Lima et al. 2003; Abdollahzadeh et al. 2013); the SONRIS website also provides the attribute data for the sediment thickness

(http://sonris-

www.dnr.state.la.us/gis/agsweb/IE/JSViewer/index.html?TemplateID=181).

Based on the collected thicknesses, empirical Bayesian kriging interpolated the sediment thickness in any area in the study site and accordingly, the interpolated raster has been mapped as shown in Figure 21.

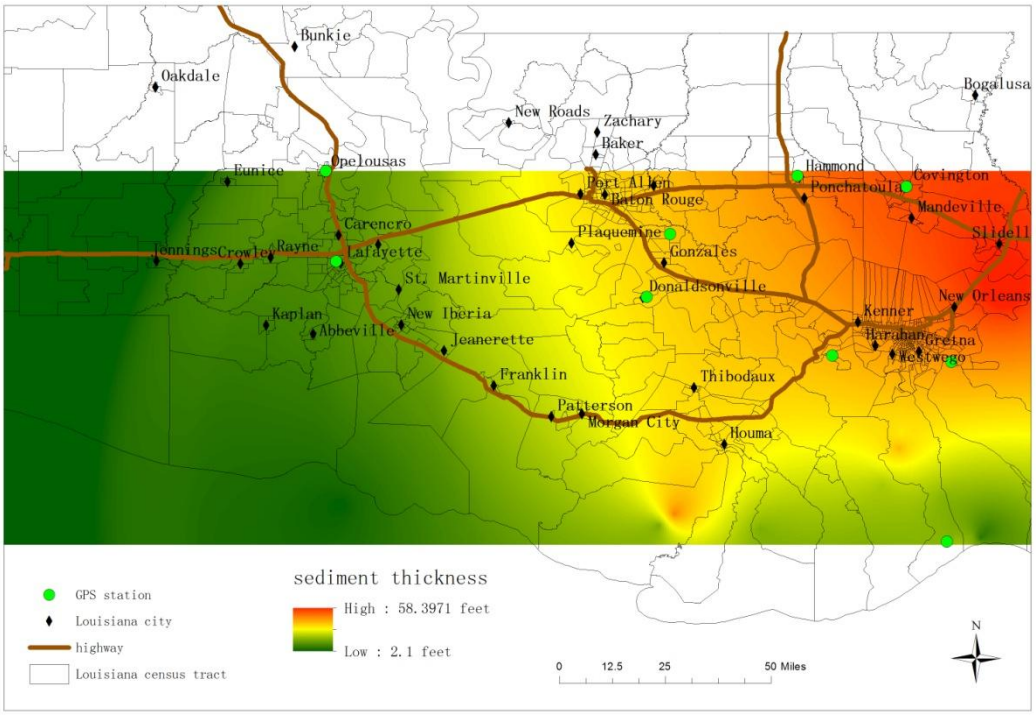

Figure 21. Interpolated sediment thickness in the study site (The map data were extracted from: http://atlas.lsu.edu)

In Regression-Kriging, the interpolated sediment thickness at each GPS station was recorded from the raster for the OLS work as follows:

Table 5. Interpolated sediment thickness at each GPS station (Unit: feet)

GPS station	Thickness
GVMS	36.75794601440
AWES	34.20343780520
DQCY	2.09999990463
CAMR	2.09999990463
GRIS	18.06450653080
TONY	12.52227115630
ENG6	42.41160202030
BVHS	19.37388038640
LWES	39.00268173220
THHR	14.75399875640
COVG	50.97607040410
HAMM	46.10993576050

Faulting

The USGS website provides the faulting data in Louisiana, while the important attributes of faulting data from this website are nearly the same (http://earthquake.usgs.gov/hazards/qfaults/). Thus, if used, the faulting data reflect no clear variation for the faulting variable in the OLS model; therefore, these types of data will not be considered for OLS and Regression-Kriging in this chapter.

Mass loading

Mass loading, such as the loading of buildings, may cause subsidence. This contributing factor may be collected and quantified from the National Land Cover Database (NLCD). The NLCD website provides a classified image in the study site, which shows designated classes for mass loading constructed areas with low, medium, and high intensity, and this classified image was converted into a GIS map (Extracted from: http://www.mrlc.gov/nlcd2011.php). For the GIS map, the percentage of mass loading area in each census tract may be calculated by the ratio of the total constructed area and the total census tract area, as well as rasterized, into an image, as shown in Figure 22.

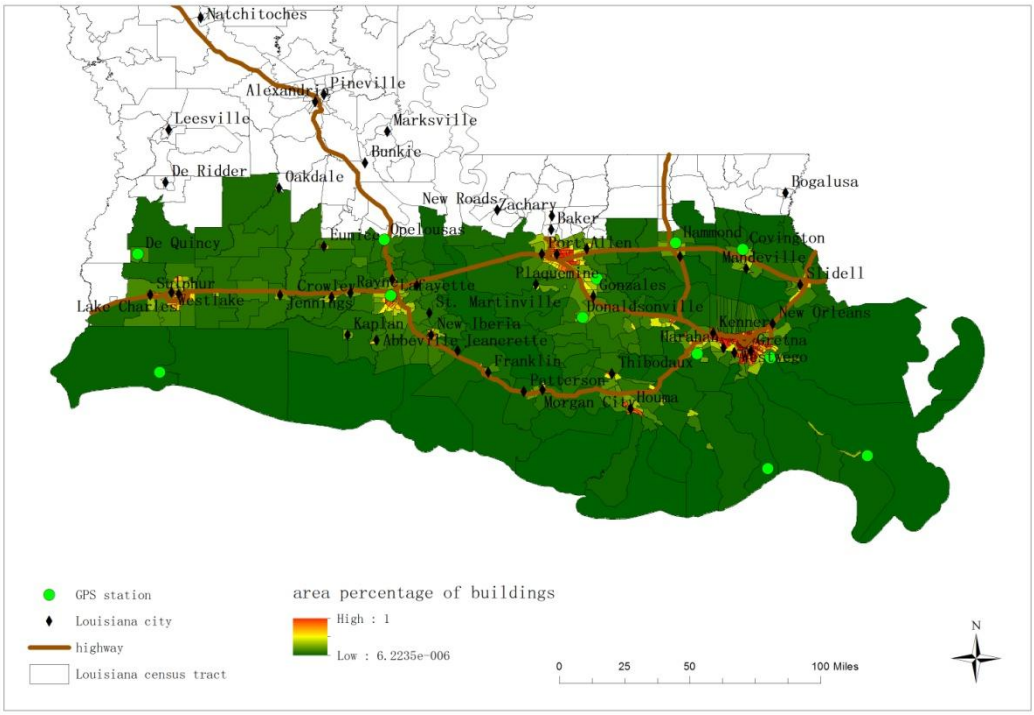

Figure 22. Percentage of the mass loading area in each census tract in the study site (Some map data were extracted from: http://atlas.lsu.edu&http://www.mrlc.gov/nlcd2011.php)

Further, for the OLS work in Regression-Kriging, the mass loading data at one GPS station may be quantified by a percentage of mass loading that covers the area for the census tract in which this GPS station is located, as nearly all the census tracts in the study site have small areas; as a result, each pair of GPS stations is not necessarily located in the same census tract. Thus, the mass loading data at each GPS station may be quantified and recorded as shown in Table 6.

Table 6. Quantified percentage of the mass loading area at each GPS station

GPS station	Percentage of mass loading area
GVMS	0.08964340000
AWES	0.20841900000
DQCY	0.12412500000
CAMR	0.01025500000
GRIS	0.00963580000
TONY	0.88093900000
ENG6	0.29752800000
BVHS	0.00742552000
LWES	0.20472900000
THHR	0.65296100000
COVG	0.37777900000
HAMM	0.71174000000

Distance to the sinkhole

Prior research shows that disasters initiated by humans, such as mining disasters or sinkholes, can cause an accelerating subsidence, which in turn badly impacts lives (Kim et al. 2006; Kim et al. 2009; Oh and Lee 2010; Oh et al. 2011; Cusanza and Kris 2013). As Chapter 3 shows, the Bayou Corne Sinkhole, having been formed by a carven collapse, caused adverse subsidence in the coastal area of Louisiana after 2012. These contributing factors to the sinkhole subsidence are similar to those for mining subsidence (Cusanza and Kris 2013; Jones and Blom 2014; Jones and Blom 2015). Thus, the distance to the sinkhole could represent a main contributing factor to the subsidence in the 2013 study site. The inverse distance from each GPS station to the sinkhole has been calculated in this dissertation (Kim et al. 2006; Kim et al. 2009; Oh and Lee 2010; Oh et al. 2011; Cusanza and Kris 2013). By IDW interpolation (Shepard and Donald 1968), these calculated inverse distances were used to rasterize into an image, as shown in Figure 23.

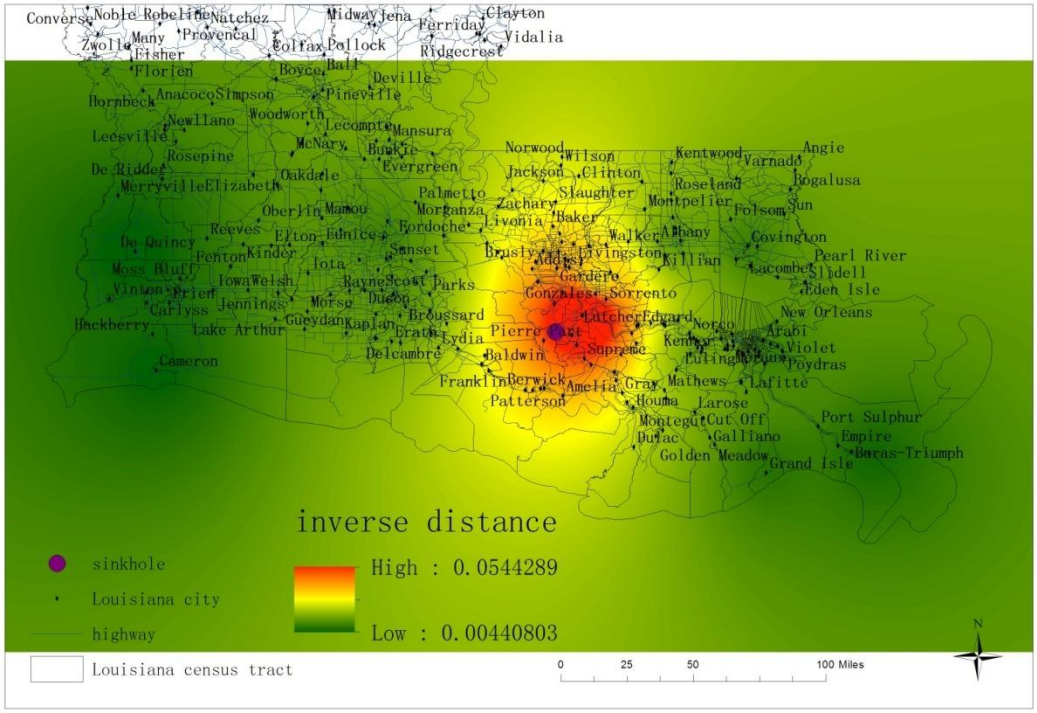

Figure 23. Interpolated inverse distance to the sinkhole in the study site (Some map data were extracted from: http://atlas.lsu.edu)

For the OLS work in Regression-Kriging, the data for the sinkhole at one GPS station can be quantified by the inverse distance from the sinkhole to the coordinate at which this GPS station is located. Thus, the data for the sinkhole at each GPS station may be quantified and recorded as shown in Table 7.

Table 7. Inverse distance to the sinkhole at each GPS station (Unit: 1/km)

GPS station	Inverse distance to the sinkhole
GVMS	0.024493
AWES	0.054434
DQCY	0.004408
CAMR	0.004718
GRIS	0.007068
TONY	0.011112
ENG6	0.008554
BVHS	0.005433
LWES	0.012885
THHR	0.009350
COVG	0.008826
HAMM	0.011679

4.3. Regression-Kriging

4.3.1. OLS regression results

The OLS regression of contributing factors to Louisiana subsidence, useful for analyzing the correlations of factors with subsidence, should be considered the first main step in the Regression-Kriging work. As Chapter 4.2 shows, five kinds of contributing factors involving a) groundwater, b) oil and gas, c) sediment, d) loading of buildings, and e) sinkholes were collected and quantified at all GPS stations in the study site. Additionally, the subsidence rates at these GPS stations were also calculated, based on a one-year observation (2013). Thus, for the OLS regression in this dissertation, quantifying contributing factors at GPS stations would be the independent variables, while subsidence rates at these GPS stations would be the dependent variables. The regression work would generate coefficients for contributing factors, with the P-values showing significance levels. As an important part of OLS regression results, coefficients and P-values may be generated, as shown in Table 8.

Table 8 The OLS results

	Coefficient value	P-value
Groundwater	0.001407	0.277470
Oil/gas	0.004534	0.088545
Sediment	0.000304	0.058838
Mass loading	-0.001813	0.764078
Sinkhole	-0.344435	**0.028043**
Intercept	-0.012359	0.086861
R-square	0.660775	-
Adjusted R-square	0.378087	-

This table shows the correlation of contributing factors with subsidence modeling by OLS. It also illustrates that the sinkhole (distance to the sinkhole) constitutes a significant factor for the study site in 2013 that is negatively correlated with subsidence. This significant correlation of sinkhole with subsidence may match a real subsidence situation at the same study site, as near Bayou Corne, Louisiana, an adverse sinkhole had emerged in 2012.While monitoring this disaster, an increasing subsidence area could be observed near Bayou Corne in 2013 (Cusanza and Kris 2013; Jones and Blom 2014; Jones and Blom 2015; Itasca 2013).

4.3.2. Prediction raster of Louisiana subsidence patterns using Regression-Kriging

Other than the OLS coefficients, the residuals at all the GPS stations were also generated. Based on the fundamental Regression-Kriging model, the residuals at these GPS stations should be collected for interpolation. Thus, in this dissertation, Empirical Bayesian Kriging was used to interpolate the OLS residuals, and the prediction of a spatial pattern for Louisiana subsidence may be generated based on the OLS coefficients and the interpolation raster of residuals. Based on the fundamental

Regression-Kriging model, the prediction of a Louisiana subsidence pattern can be generated by the equation as follows (Pebesma 2006; Hengl et al. 2004):

$$\text{Prediction raster for subsidence rates} = \sum \text{the OLS coefficient} * \text{quantified raster for independent variables} + \text{interpolation raster of OLS residuals}$$

For this equation, the quantified raster for one contributing factor in Chapter 4.2 should be used to multiply with the OLS coefficient to generate the drift, and the final prediction raster for subsidence rates can generate as follows, by summing the drift and interpolation of residuals (Hengl et al. 2004):

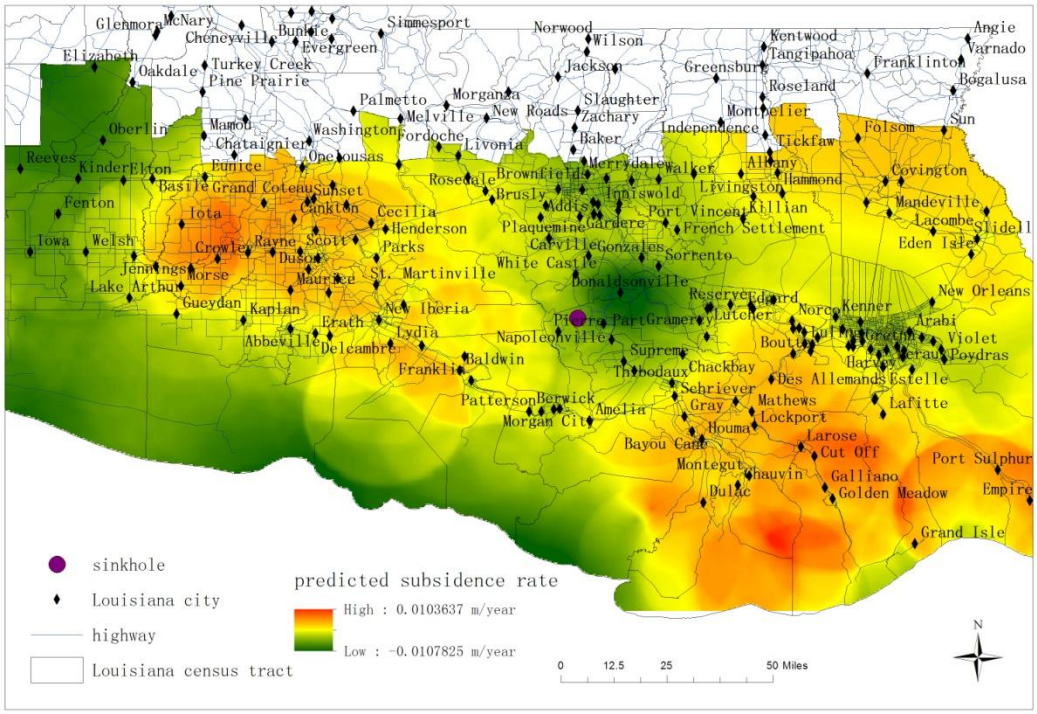

Figure 24. Predicted subsidence rates in the study site using Regression-Kriging (Some map data were extracted from: http://atlas.lsu.edu)

From this prediction raster, the spatial pattern for subsidence rates in the study site is similar to the 2013 KKF result in Chapter 3, based on comparisons. Like the 2013 KKF raster (Figure 11), an area with a high speed of subsidence emerged near

Bayou Corne in 2013, and the highest speed for subsidence may be predicted at nearly 10.8mm/year in some small areas around Bayou Corne. In accordance with Regression-Kriging, a high-speed subsidence area emerged near Lake Charles at nearly 10mm/year; yet in accordance with KKF, the subsidence speed near Lake Charles may be considered at nearly 20mm/year.

Based on OLS regression, the Regression-Kriging prediction may be viewed as a consistent alignment with KKF results, due to an emergent area near Bayou Corne with a high-speed subsidence. This predicted high speed (nearly 10.8mm/year) closely matches the formal observation (10–20mm/year) (Itasca 2013).

Further, other than generating the prediction raster, the prediction accuracy should also be calculated and analyzed (Hengl et al. 2004). Thus, the accuracy should be evaluated. Section 4.4 will show the accuracy evaluation results.

4.4. Prediction accuracy using Regression-Kriging

The work in Section 4.3 predicted a spatial pattern for the subsidence rates in Louisiana. The Regression-Kriging results were checked for consistency with the monitoring observation near Bayou Corne. The question remains as to the accuracy of the subsidence prediction work by Regression-Kriging. Thus, additional work should be implemented to quantify the prediction results. In this dissertation, important quantities for accuracy evaluation, such as the RMSE, served to calculate the prediction accuracy (Hung et al. 2011; Hengl et al. 2004).

In regard to the prediction raster using Regression-Kriging, the subsidence rates at all coordinates in the study site may be predicted, and these subsidence rates may

be collected and recorded as predicted values. On the other hand, based on a research method used by Hengl et al. in 2004 for calculating prediction accuracy, six other GPS stations in the study site may be collected as the standard points in the following:

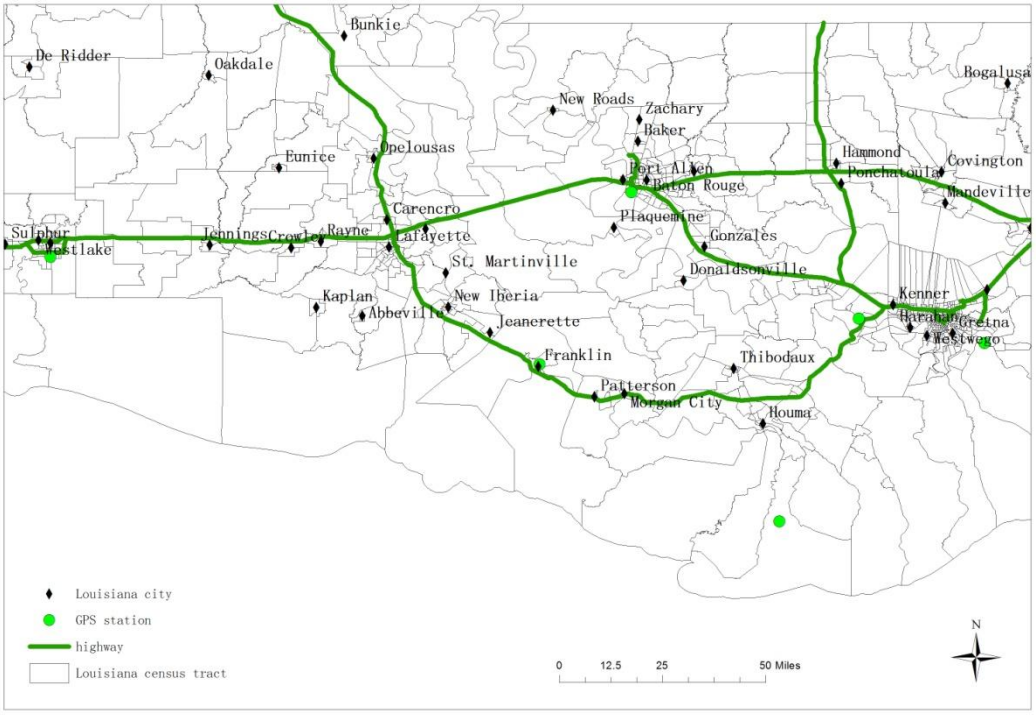

Figure 25. Distribution of six GPS stations as the standard points in the study site (Some map data were extracted from: http://atlas.lsu.edu)

In this map, similar to the work in Chapter 4.2, the subsidence rates for these six standard points may also be calculated, based on a one-year observation, and recorded as the standard values for accuracy evaluation (Hengl et al. 2004; Hung et al. 2011). The difference may be calculated as follows to show the accuracy at these standard points (Hung et al. 2011):

Difference = Absolute value of (predicted value – standard value)

Thus, in this dissertation, based on the research method used by Hung et al. in 2011, the difference between the predicted value and the standard one at each GPS station was calculated and mapped, as shown in Figure 26.

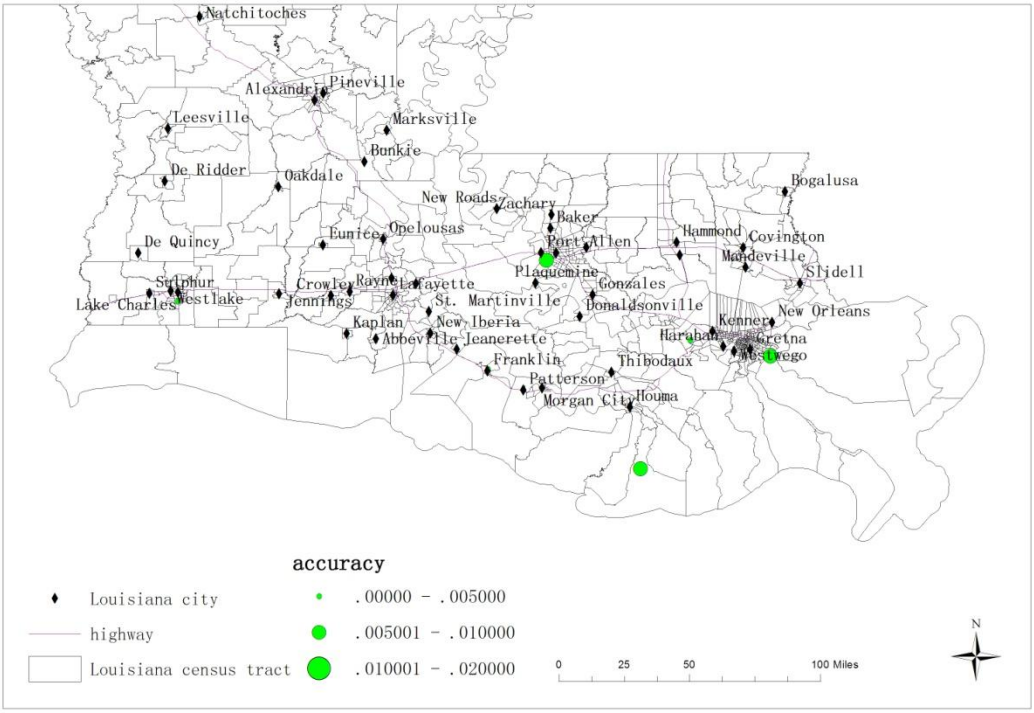

Figure 26. Accuracy of the subsidence rates using Regression-Kriging predictions for each standard point in the study site (Unit: m/year) (Some map data were extracted from: http://atlas.lsu.edu)

As the research by Hengl et al. indicates for accuracy comparisons, the interpolation of subsidence rates at standard points by Kriging (Empirical Bayesian Kriging) was displayed in Figure 14. The differences at these standard points were calculated and mapped as follows (Hengl et al. 2004; Kent and Dokka 2012):

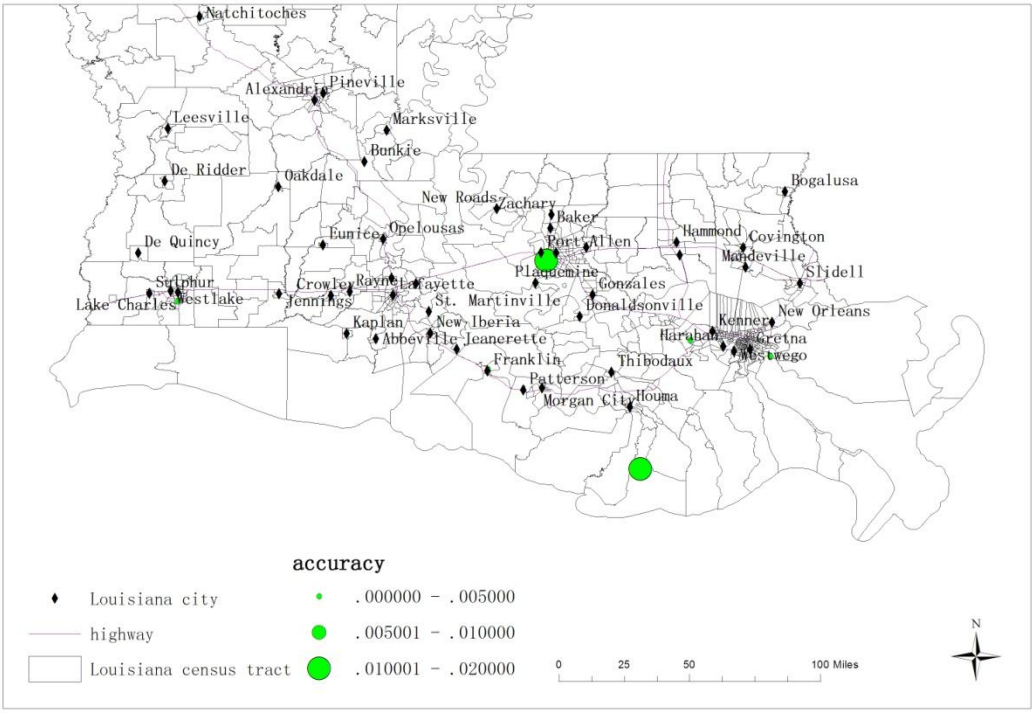

Figure 27. Accuracy of the subsidence rates using Empirical Bayesian Kriging for each standard point in the study site (Unit: m/year) (Some map data were extracted from: http://atlas.lsu.edu)

Further, Hengl et al.'s findings from 2004 showed that RSME may be used to calculate the prediction accuracy by Regression-Kriging. RSME may be formatted as follows (Hengl et al. 2004):

$$\text{RMSE}=\sqrt{\frac{1}{\text{number of points}}*\sum(\text{predicted value}-\text{standard value})^2}$$

Thus, based on the difference (predicted value-standard value) for each standard point, the RSME value obtained via Regression-Kriging equals 5.95mm/year. Likewise, the RSME value obtained from Empirical Bayesian Kriging equals 8.00mm/year.

Prior research shows that for the accuracy evaluation of a soil variables prediction by Regression Kriging, the accuracy by Empirical Bayesian Kriging, or Kriging, was applied for comparisons, similar to the comparisons of this dissertation

(Hengl et al. 2004). The distribution maps of difference at standard points using Regression-Kriging (Figures 26 and 27) also show that the subsidence rates may not be accurately predicted for the GPS stations “1LSU and “LMCN.” Nevertheless, these predictions, with differences at nearly—or less than—2 mm/year, may prove to be more accurate than the ones obtained via Empirical Bayesian Kriging for most of the GPS stations, such as “DSTR” and “FSHS.” Further, for total prediction accuracy, the RSME value obtained through Regression-Kriging at 5.95 mm/year may be slightly smaller than the one at 8.00 mm/year from Empirical Bayesian Kriging. This smaller RMSE value also indicates that the subsidence prediction work by Regression-Kriging can be acceptable.

Thus, this dissertation introduced Regression-Kriging to make a subsidence prediction for the spatial pattern generated from the data of contributing factors, an unprecedented selection not applied in former subsidence research. By means of Regression-Kriging, a spatial pattern of subsidence may be predicted accurately from contributing factors. This dissertation therefore provides a spatial points-to-area subsidence prediction based on Regression-Kriging.

4.5. Summary and discussion

In previous research, the spatial pattern of subsidence may be modeled by a common interpolation, such as Kriging (Kent and Dokka 2012). Such a model may generate a subsidence spatial pattern only from points of observed subsidence data, as well as from multiple other contributing factors. Yet the model may not be considered as sufficient auxiliary information necessary to generate an accurate spatial pattern

(Hengl et al. 2004). Thus, in this chapter, multiple kinds of factors contributing to subsidence, such as groundwater, oil/gas, sediment, loading of buildings, and sinkholes, were collected and quantified for Regression-Kriging. The Regression-Kriging work was based on the OLS regression between points of observed subsidence and contributing factors, together with an interpolation of residuals. The prediction raster known as the Regression-Kriging result may be checked consistently with the formal organizational observation, due to the predicted high subsidence rate at nearly 10.8mm/year near Bayou Corne, Louisiana (Itasca 2013). Additionally, the higher prediction accuracy of Regression-Kriging than that of Empirical Bayesian Kriging shows that this dissertation provides an acceptable, spatial points-area prediction work of subsidence a) using the data of contributing factors, and b) by the common subsidence research found with Regression-Kriging. As a research method based on OLS regression, the model was introduced to spatially predict subsidence.

The Regression-Kriging prediction is acceptable, yet future improvement is possible. One clear area for improvement lies in the minimal amount of six standard points for accuracy evaluation, which caused the prediction results to be less statistically accurate. Thus, an increase in standard GPS stations of data collection is recommended for accuracy evaluation in the future.

Chapter 5 Regionalization of Contributing Subsidence Factors by GWR

5.1. GWR and its application in land subsidence modeling

As demonstrated in the research methodology chapter, the equations for GWR (Fotheringham et al. 2002; Shang et al. 2011) are as follows:

$$y(g) = \beta_0(g)+\beta_1(g)\ x_1+\beta_2(g)x_2+\ldots+\beta_n(g)x_n+\varepsilon$$

$$\beta = (X^T W(g) X)^{-1}(X^T W(g) Y)$$

y is the dependent variable, x_1, x_2,…x_n are predictor variables, g is the known coordinates for observation points (Fotheringham et al. 2002; Shang et al. 2011), β are the varied coefficients as the GWR results (Fotheringham et al. 2002; Shang et al. 2011), and *W(g)* is usually defined by a Gaussian function (Fotheringham et al. 2002; Shang et al. 2011).

To show the spatial heterogeneity of Louisiana subsidence in this dissertation, GWR will be based on multiple contributing factors to subsidence. These contributing factors were collected and quantified as predictor variables, while data for a subsidence rate were used as the dependent variable (Shang et al. 2011). The spatial heterogeneity feature for Louisiana land subsidence, when reflected clearly by GWR, enables the formation of location-based, hazard mitigation policies in land subsidence for the Louisiana state government.

5.2. Data collection and factor quantification

Prior research findings showed that the ordinary factors for subsidence rates should be a) groundwater level variations, b) oil and gas pumping, c) sediment, and d) faulting and mass loading (Shang et al. 2011; Abdollahzadeh et al. 2013). The 2012 disaster of the Bayou Corne Sinkhole caused an accelerated subsidence at the study site. Therefore, the distance to the sinkhole is considered a contributing factor, especially for the nearby areas. The census tracts of the coastal Louisiana are used as the basic geographic unit for the spatial statistics, as shown in the following map:

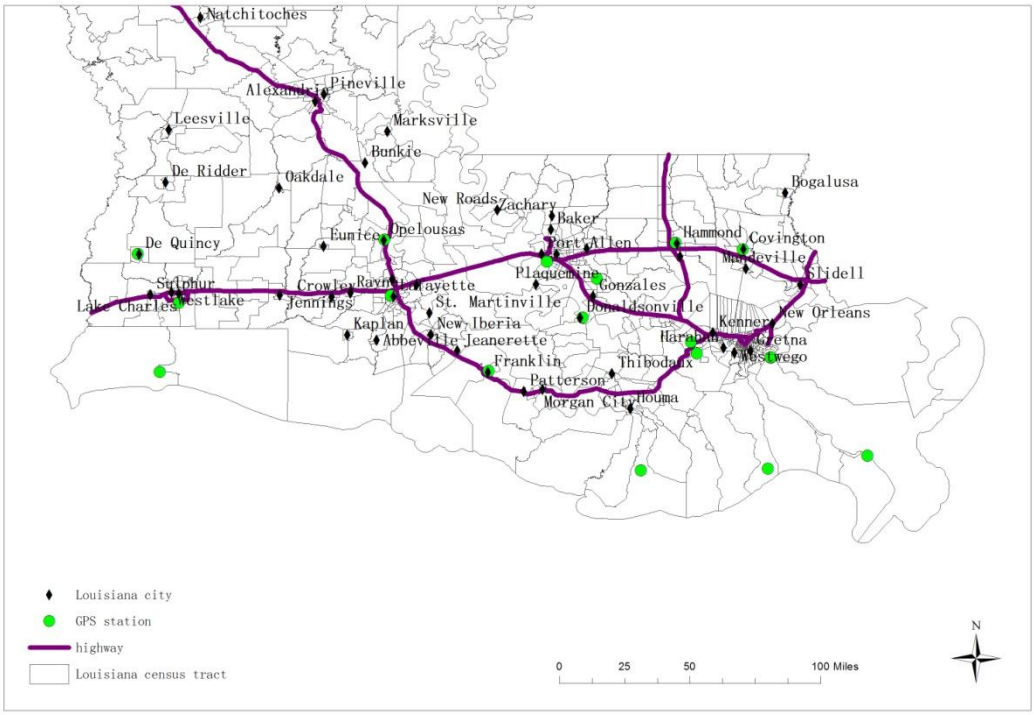

Figure 28. Study site with 736 census tracts, green points: GPS stations (Some map data were extracted from: http://atlas.lsu.edu)

The factor data were collected and mapped to these 736 census tracts. The following paragraphs describe how the data were collected.

Groundwater level change

Groundwater withdrawn by human activity has not been measured directly. However, former research by Shang et al. in 2011 shows that many areas of subsidence strongly relate to the groundwater level variations, based on their GWR modeling results (Shang et al. 2011; Abdollahzadeh et al. 2013). Thus, groundwater level change data were collected from the USGS website for groundwater level data in the study site: (http://groundwaterwatch.usgs.gov/). Changes in the groundwater levels for all available wells in 2013 were recorded. Based on these wells, an interpolation process employing the IDW method was used (Shang et al. 2011; Shepard and Donald 1968). This interpolation raster result shows the predicted distribution for average changes in the groundwater level at the study site. The average raster values enclosed by each census tract were calculated for each tract, as shown in the following map (Figure 29).

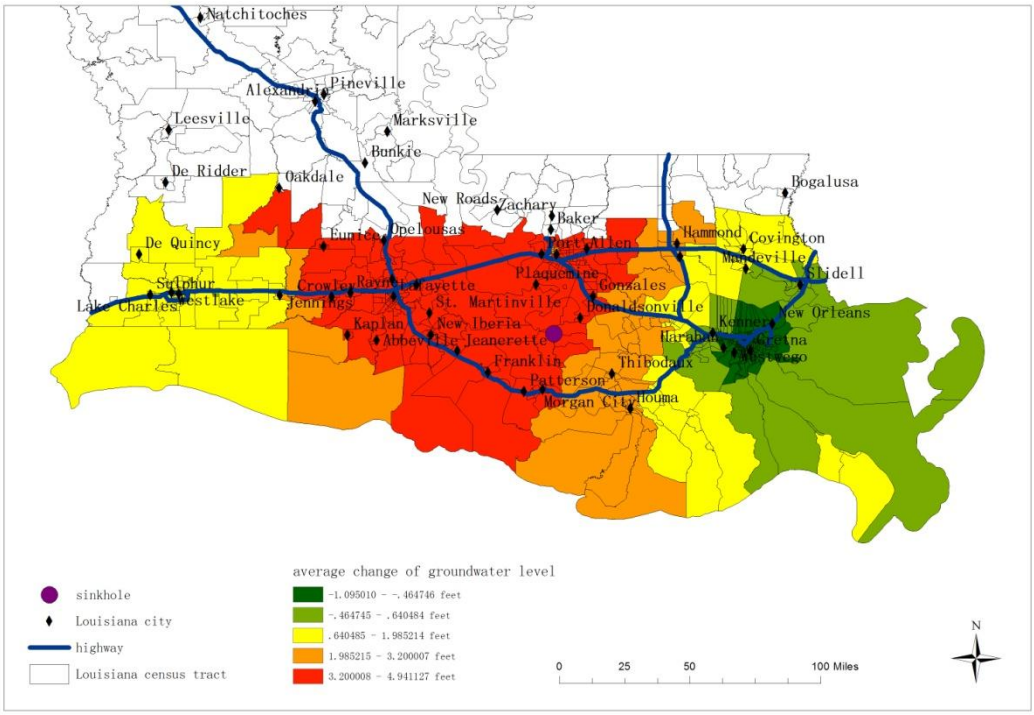

Figure 29. Average change in the groundwater level for census tracts in 2013 (unit: feet, natural break classification into 5 intervals) (Some map data were extracted from: http://atlas.lsu.edu)

Oil and gas pumping

Oil and gas data were obtained from the SONRIS website (Extracted from: http://sonris.com&http://sonris-www.dnr.state.la.us/gis/agsweb/IE/JSViewer/index.html?TemplateID=181).

Based on data from the SONRIS website, the density of pumping wells for each census tract at the study site was calculated, as shown in the following map (Figure 30). It must be noted that the productivity of the wells is not known from the data, although that information could be helpful to interpret the oil and gas pumping data.

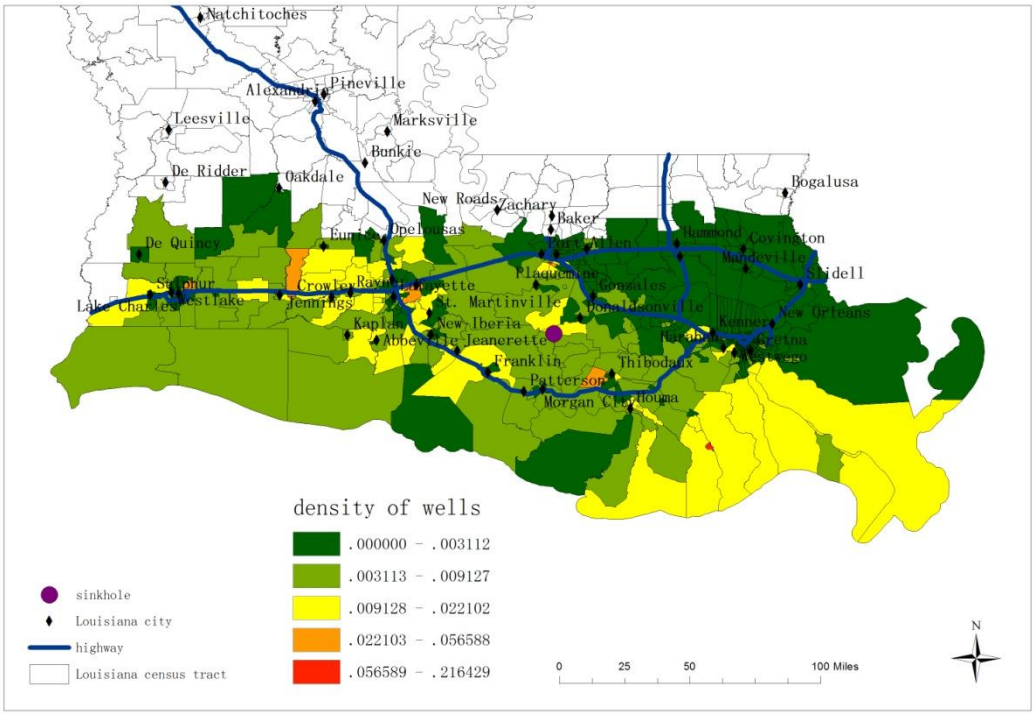

Figure 30. Density of oil and gas pumping wells for census tracts in 2013 (natural break classification into five intervals) (Some map data were extracted from: http://sonris.com&http://sonris-www.dnr.state.la.us/gis/agsweb/IE/JSViewer/index.html?TemplateID=181&http://atlas.lsu.edu)

Sediment:

The SONRIS website (http://sonris-www.dnr.state.la.us/gis/agsweb/IE/JSViewer/index.html?TemplateID=181) provides sediment sampling data to download. Lima et al. (2003) illustrated the application of sediment interpolation by GIS, and the authors also showed that attributes of sediment, such as chemical elements and sample thicknesses, may be spatially correlated in a small area (Lima et al. 2003). All sampling sites of data were interpolated using Empirical Bayesian Kriging (Olea 1999).

The thickness of the sediment samples reflects the sediment compaction feature that can be correlated with the subsidence in the coastal area of Louisiana (Sclater and Christie 1980; Abdollahzadeh et al. 2013). The average thickness of the sediment was

applied at the census tracts as the sediment factor for land subsidence analysis (The sediment data were extracted from: http://sonris.com&http://sonris-www.dnr.state.la.us/gis/agsweb/IE/JSViewer/index.html?TemplateID=181) (Figure 18).

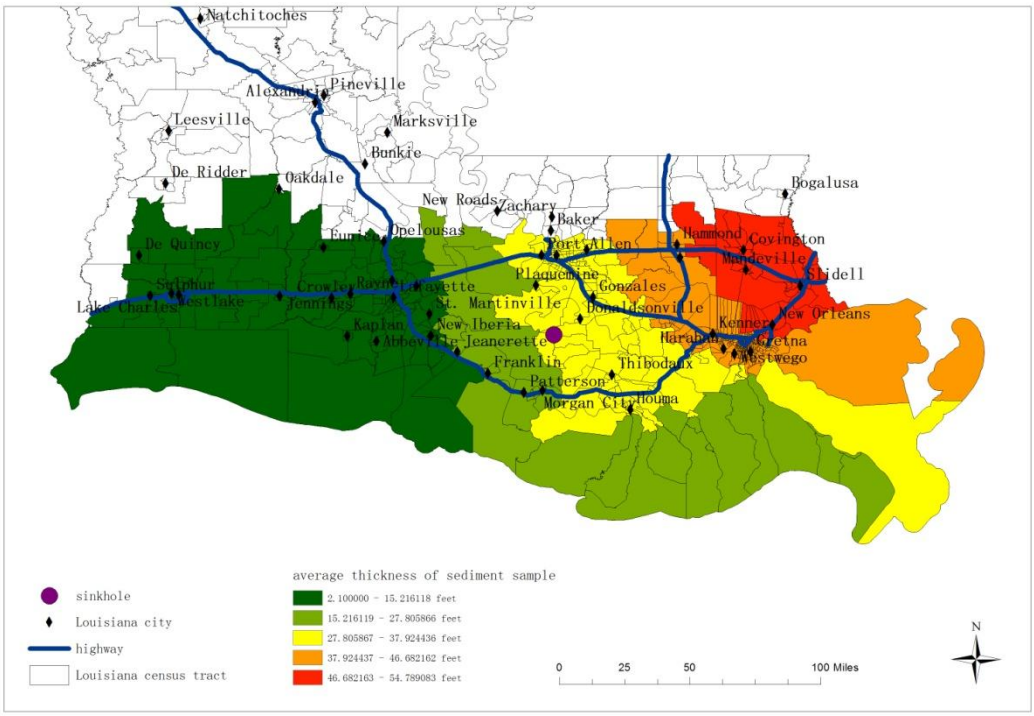

Figure 31. Average thickness of clay-sand mixture samples for census tracts (unit: feet, natural break classification into five intervals) (The map data for sediment were extracted from: http://sonris.com&http://sonris-www.dnr.state.la.us/gis/agsweb/IE/JSViewer/index.html?TemplateID=181; Some map data were extracted from: http://atlas.lsu.edu)

Faulting

Faulting data were downloaded from the USGS earthquake data website (http://earthquake.usgs.gov/hazards/qfaults/). The faulting data contain attributes of rates, years, and moving directions of faulting in Louisiana. However, due to the scale of the faulting phenomenon, all census tracts in the coastal Louisiana have almost the

same values in the attributes. This variable worked as the intercept. Therefore, the faulting data were not included in the regression formulas.

Mass loading

The excessive weight of buildings expedites the downward motion of land. The mass loading from buildings in the study area is considered one of the factors leading to subsidence (Abdollahzadeh et al. 2013)., The image classification produced by the USGS Land Cover Institute (LCI) in the study site was extracted from the National Land Cover Database (NLCD) website (Extracted from: http://www.mrlc.gov/nlcd2011.php).

In regard to classified thematic data collected from the NLCD website, the classes for human constructions of low, medium, and high intensity were extracted and then converted into a GIS map for the census tracts (Extracted from: http://atlas.lsu.edu/&http://www.mrlc.gov/nlcd2011.php). Based on this GIS map, the ratio of the total constructed land and the total area of each census tract was calculated as the mass loading factor, as shown in the following map (Figure 32).

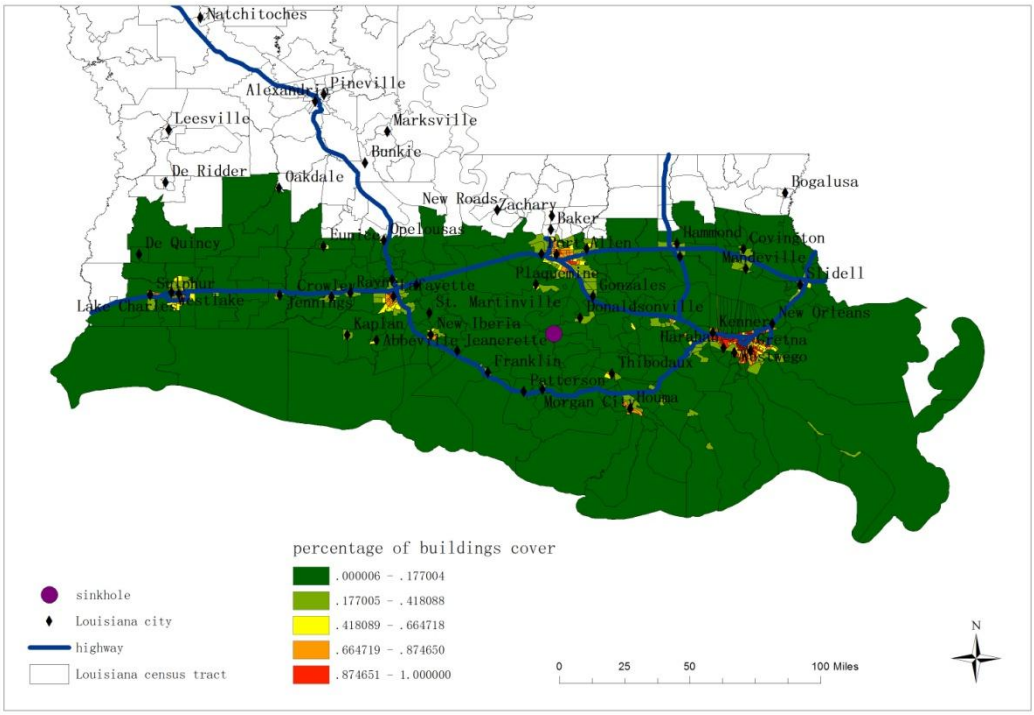

Figure 32. Percentage of mass loading area for each census tract (natural break classification into 5 intervals) (Some map data were extracted from: http://atlas.lsu.edu/&http://www.mrlc.gov/nlcd2011.php)

Distance to the sinkhole

The literature shows that certain human activities, such as mining accidents, can cause adverse subsidence in our living area (Kim et al. 2006; Kim et al. 2009; Oh and Lee 2010; Oh et al. 2011). In addition, former research revealed that a) the depth and distance from drift, b) DEM and slope gradient, c) groundwater permeability, and d) geology and land use are the main factors for mining subsidence (Kim et al. 2006; Kim et al. 2009; Oh and Lee 2010; Oh et al. 2011; Coal Industry Promotion Board 1997; Coal Industry Promotion Board 1999).

The Bayou Corne Sinkhole, formed by a cavern collapse, also caused an accelerated subsidence at the study site for a period of time after the sinkhole year 2012 (Cusanza 2013; Jones and Blom 2014; Jones and Blom 2015). The factors for

sinkhole subsidence should be very similar to those for mining subsidence. Prior research also shows that many factors, such as the distance to the sinkhole and sinkhole depth, can contribute to an accelerating subsidence (Kim et al. 2006; Kim et al. 2009; Oh and Lee 2010; Oh et al. 2011; Cusanza 2013; Jones and Blom 2014; Jones and Blom 2015;). Thus, besides the common factors, the inverse of the distance to the sinkhole was also calculated as a factor (Figure 21).

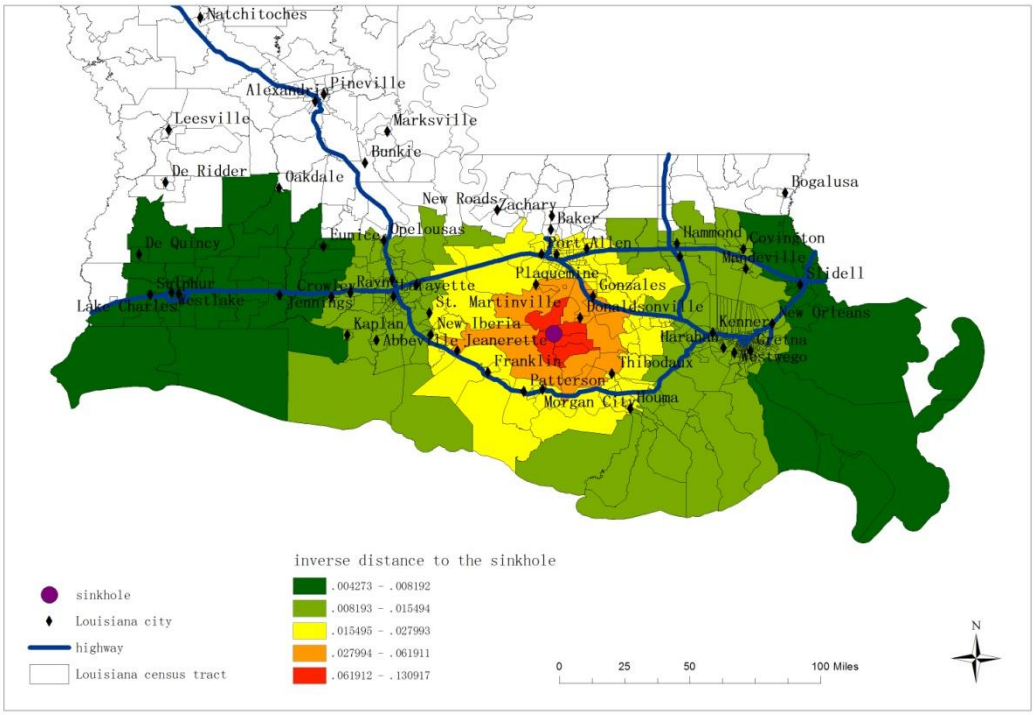

Figure 33. Inverse distances from the Bayou Corne Sinkhole location to the geographic center of each census tract in the study site (unit: 1/km, natural break classification into five intervals) (Some map data were extracted from: http://atlas.lsu.edu)

5.3. GWR results

The GWR analysis was supported by the ArcGIS software. All the above factors were used as independent variables. The interpolated space-time elevation change data were used as the dependent variable (Figure 32).

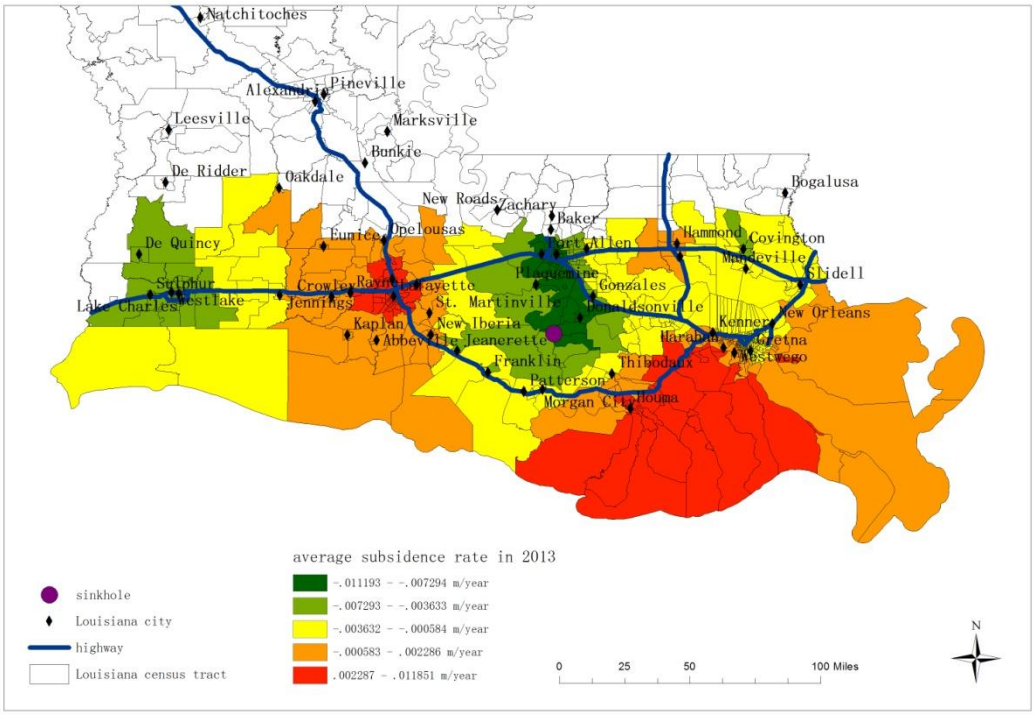

Figure 34. Average subsidence rate for each census tract in 2013 (unit: m per year, natural break classification into five intervals)(Some map data were extracted from: http://atlas.lsu.edu)

The local R-squared values and the coefficients for each census tract are shown in Figures 32–38, following the research example of Xu and Wang (2015)

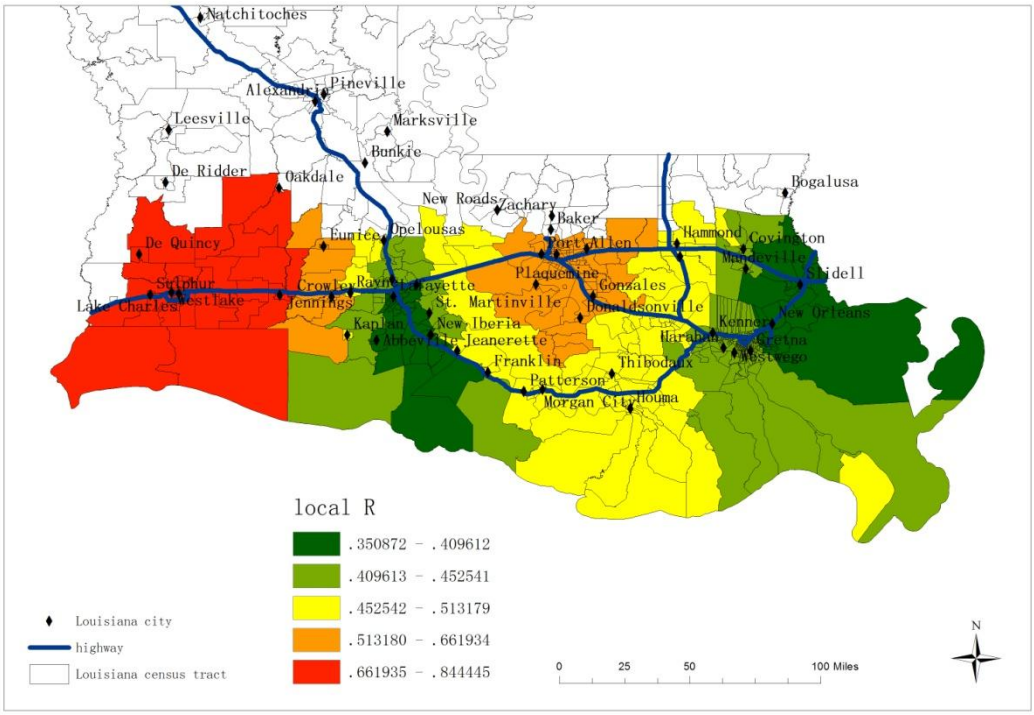

Figure 35. Local R square values for census tracts (Some map data were extracted from: http://atlas.lsu.edu)

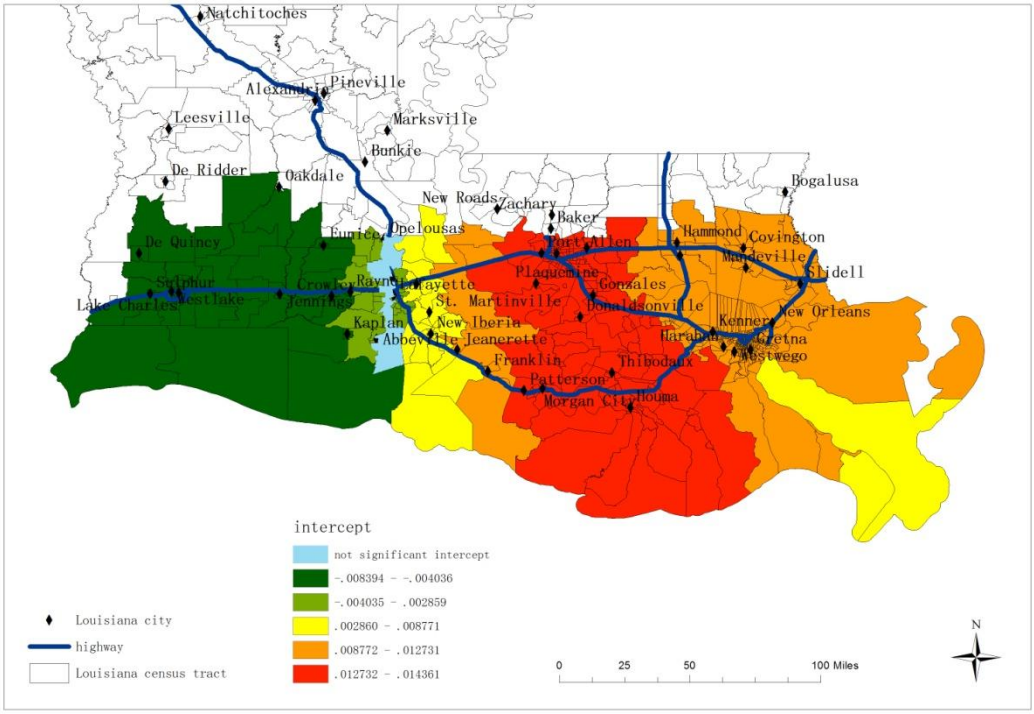

Figure 36. Intercept for census tracts (Some map data were extracted from: http://atlas.lsu.edu)

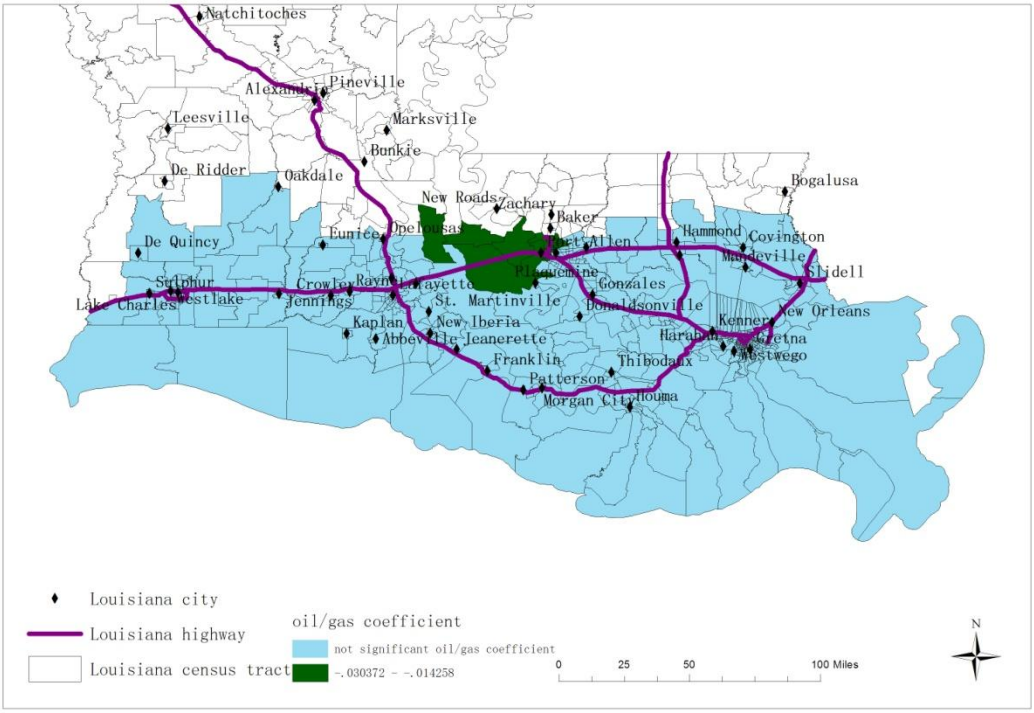

Figure 37. Oil/gas coefficients for census tracts (Some map data were extracted from: http://atlas.lsu.edu)

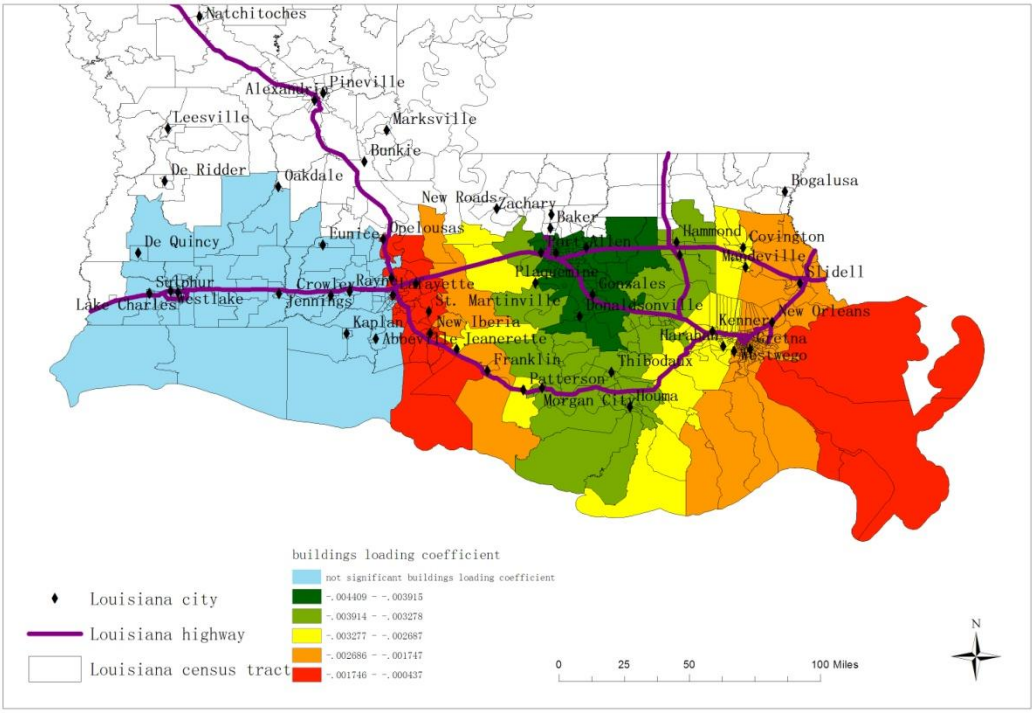

Figure 38. Mass loading (buildings) coefficients for census tracts (Some map data were extracted from: http://atlas.lsu.edu)

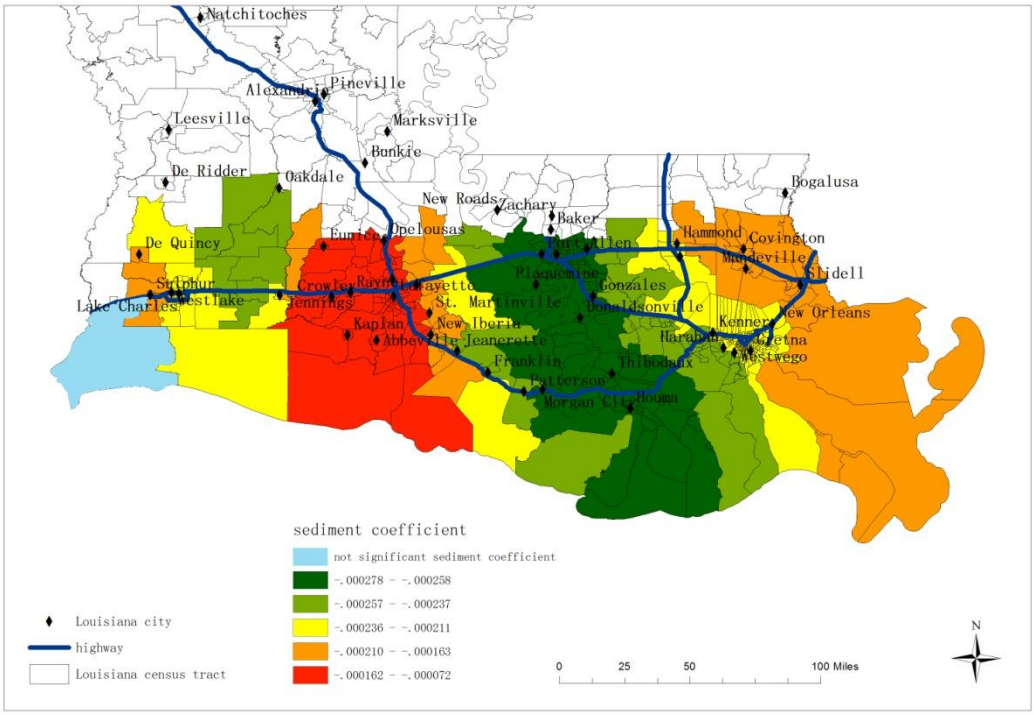

Figure 39. Sediment coefficients for census tracts (Some map data were extracted from: http://atlas.lsu.edu)

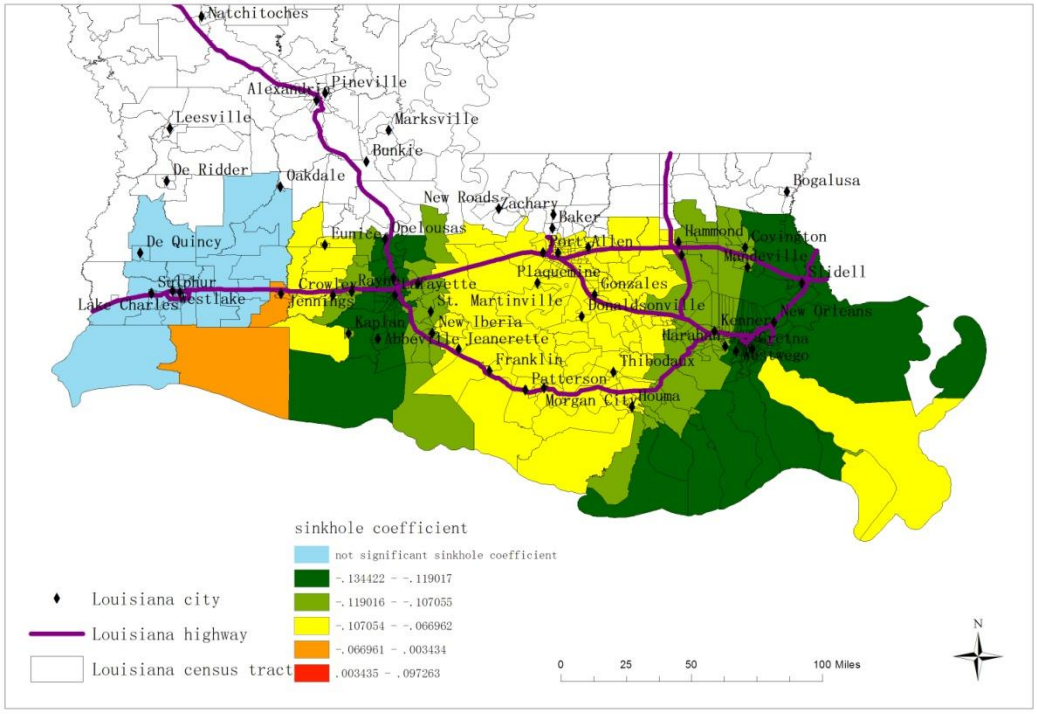

Figure 40. Sinkhole coefficients (inverse distances to sinkhole location) for census tracts (Some map data were extracted from: http://atlas.lsu.edu)

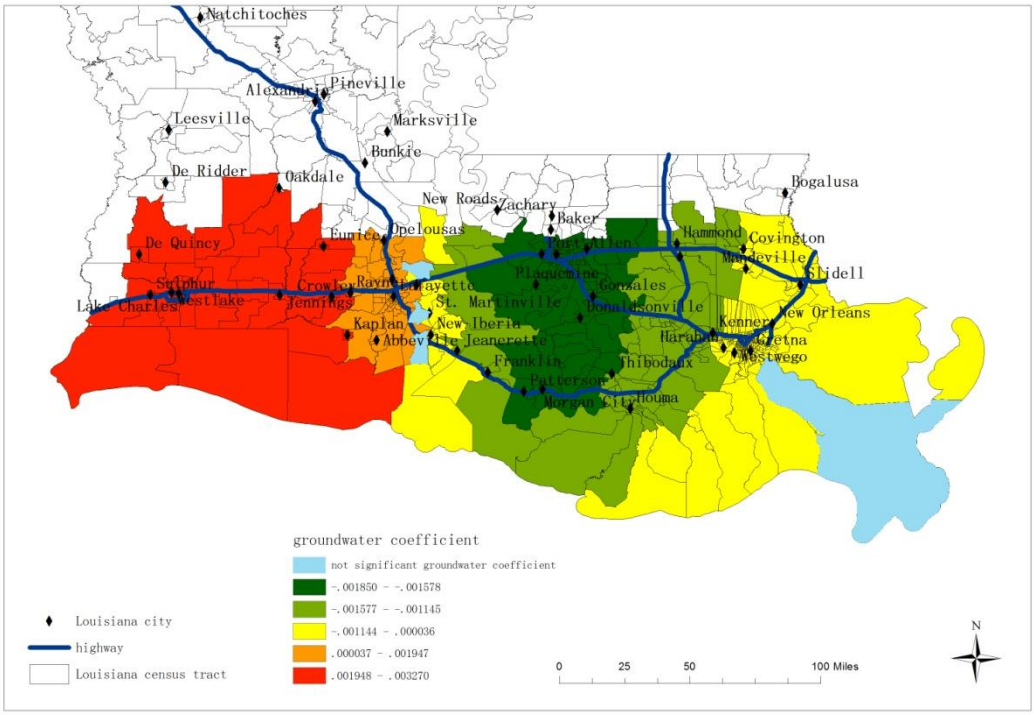

Figure 41. Groundwater coefficients for census tracts (Some map data were extracted from: http://atlas.lsu.edu)

5.4. Goodness of fit for the GWR model

From the GWR output report, the average R-squared value is approximately 0.6650 (60.50%), and the adjusted R-squared value is approximately 0.6583 (65.83%). The spatially varied coefficients for various factors are calculated in Table 2, following the previous research examples (Shang et al. 2011; Xu and Wang 2015).

Table 9. Modeling results using GWR

	25% quartile	50% quartile	75% quartile
Intercept	0.010387	0.011762	0.012591
Oil/gas	-0.010249	0.011426	0.012289
Mass loading	-0.003346	-0.002593	-0.002250
Sediment	-0.000247	-0.000232	-0.000220
Sinkhole	-0.123039	-0.118171	-0.100977
Groundwater	-0.001400	-0.000982	-0.000830

Based on the same set of data in the GWR model, modeling results were generated using OLS. By comparing the GWR results to the OLS results, the total R-squared value obtained by GWR (about 0.6650) is much greater than that of the OLS (0.1681). This indicates that the GWR model explained more variability in the land subsidence. This is consistent with previous research (Shang et al. 2011; Xu and Wang 2015). Additionally, the GWR results (Figure 35) also show that the local R-squared values for census tracts vary spatially. The R-squared values in the study site range from 0.350872 (about 35.09%) to 0.844445 (about 84.44%), showing clear spatial heterogeneity in the study area (Fotheringham et al. 2002; Shang et al. 2011; Xu and Wang 2015).

For each factor contributing to the subsidence, such as groundwater, oil/gas, sediment, building loading, and inverse distance from the sinkhole location, Table 9 shows that all the coefficients for census tracts considerably vary spatially, with clear

spatial heterogeneity for the contributing factor weights. The maps for GWR results also depict clear spatial clusters for each coefficient, indicating that there may be a spatial dependency of the land subsidence phenomenon in this research area (Shang et al. 2011; Xu and Wang 2015; Knegt et al. 2010).

Figure 37 illustrates that the oil/gas coefficients for nearly all the census tracts at the study site are insignificant. This result is inconsistent with the previous research by Abdollahzadeh et al. (2013). It may be that in the process of collecting oil/gas data, the important production data and the capacity data of wells were not collected for use in this research (Extracted from: http://sonris.com). This reflects the limitation of this research, due to data availability. Should the findings reflect production data, the modeling results may show improved significance levels.

Figure 38 shows that the buildings' loading coefficients are mostly significant, although some green-colored polygons in the figure represent census tracts with non-significant coefficients. The negative sign for the coefficients shows that a greater percentage of the building loading area may contribute to the downward motion of land (negative value) in the coastal area of Louisiana (Abdollahzadeh et al. 2013). In addition, the higher absolute values for this coefficient, found in the Baton Rouge area, reveal that the impact of buildings loading on the subsidence becomes clearly larger than for other areas in the study site. For the coastal areas, the smaller absolute value of the coefficient indicates a smaller impact on subsidence, due to much lessloading of buildings.

Figure 39 shows that for nearly all the census tracts in the study site, the

sediment coefficient is significant. This finding is in agreement with previous research (Abdollahzadeh et al. 2013). Further, the negative value for the sediment compaction coefficient shows that the subsidence rate and the sediment factor are negatively correlated. This negative correlation can be explained: In the process of sediment formation, a greater thickness for the sediment sample indicates a more significant compaction process, which in turn causes obvious subsidence (Sclater and Christie 1980) Further, the higher absolute value for this coefficient in Figure 36 shows a clearly larger impact of sediment on subsidence from north to south for the central area in the study site, while for other areas, such an impact on subsidence would be less important.

Figure 40 shows that the sinkhole coefficient is significant for nearly all the census tracts in the study site, except for those located far from the Bayou Corne sinkhole (Cusanza 2013). The negative sign of the coefficients suggests that when the distance was closer, the land subsidence rate became higher. This correlation is consistent with the continually expanding situation of the Bayou Corne Sinkhole, as reported by monitoring reports since August of 2012 (Cusanza 2013; Jones and Blom 2014; Jones and Blom 2015). Additionally, the coastal census tracts near the Assumption Parish sinkhole location display evidence of higher absolute values for this coefficient. In turn, the evidence for these census tracts reveals a much larger impact of sinkholes on subsidence (Cusanza 2013).

Finally, Figure 41 shows that the groundwater coefficients for nearly all the census tracts are significant with several exceptions (green-colored polygons). The

correlation between the subsidence rate and the groundwater factors is positive for many census tracts, although this correlation remains negative for other census tracts in the study site. Shang et al. indicated that either the positive correlation or the negative correlation can be explained, as different layers of groundwater aquifers may cause different correlations (Shang et al. 2011). Their findings show that the correlation can be positive in some areas, as the decreasing groundwater level will cause an increasing internal pressure for the unconfined aquifer in these areas; as a result, the internal pressure can make the aquifer compress and the ground move downward. The correlation can also be negative in other areas, as the confined aquifer in these areas may uplift due to a decreased loading of the unconfined aquifer (Shang et al. 2011; Dokka 2006; Kent and Dokka 2012). Thus, in Figure 41, the positive values for this coefficient in the census tracts around Lake Charles demonstrate a large impact of unconfined aquifers on subsidence. Yet in census tracts around Baton Rouge, this coefficient becomes negative, due to data showing that the impact on subsidence could clearly be larger for confined aquifers than unconfined aquifers.

Thus, findings indicate that the modeling results from GWR show spatially varying R-squared values and factor coefficients for the census tracts in the study site. The spatial heterogeneity of the factors may be used to form location-based, land subsidence, hazard mitigation policies. For example, those areas shown with high, negative coefficients of the building mass loading factor (red-colored polygons) in Figure 38 would aid in the avoidance of excessive construction.

5.5. Regionalization of GWR results

As Chapter 5.4 shows, the GWR results clearly reflect a spatial heterogeneity feature for most kinds of contributing subsidence factors, underscored with significant levels of GWR coefficients. The coefficient for each contributing factor is significantly space-related, which could aid in location-based land subsidence policies if regionalized by GIS to mitigate the disasters caused by land subsidence. Thus, in the regionalization process that follows, the work for regionalization of GWR results should be accomplished when combined into region-related classes with multiple contributing factors (Xu and Wang 2015).

Chapter 5.4 also shows space-related significance levels for each kind of contributing subsidence factor in the study site, such as groundwater, sediment, the loading of buildings (mass loading), and sinkholes. Based on the research findings of Xu and Wang in 2015, these four kinds of contributing factors for subsidence were combined into six region-related classes as follows: Each class by combination can represent one sub-region in the study site, and the entire study site can be covered by these six sub-regions (Xu and Wang 2015).

Table 10. Six region-related classes by the combination of four kinds of contributing subsidence factors

Class name	Buildings loading	Sediment	Sinkhole	Groundwater
Class 1	Not significant	Not significant	Not significant	Positive
Class 2	Not significant	Negative	Negative	Positive
Class 3	Not significant	Negative	Not significant	Positive
Class 4	Negative	Negative	Negative	Positive
Class 5	Negative	Negative	Negative	Negative
Class 6	Negative	Negative	Negative	Not significant

In this table, “positive” means the positive and significant correlation with subsidence for one contributing factor; likewise, “negative” means the negative and significant correlation, while “not significant” means no significant correlation with subsidence for this factor.

Thus, based on the research method used by Xu and Wang in 2015, these six combinations (classes) for four kinds of contributing subsidence factors—groundwater, sediment, the loading of buildings, and sinkholes—the regionalization results for all six sub-regions can be mapped in the study site as follows:

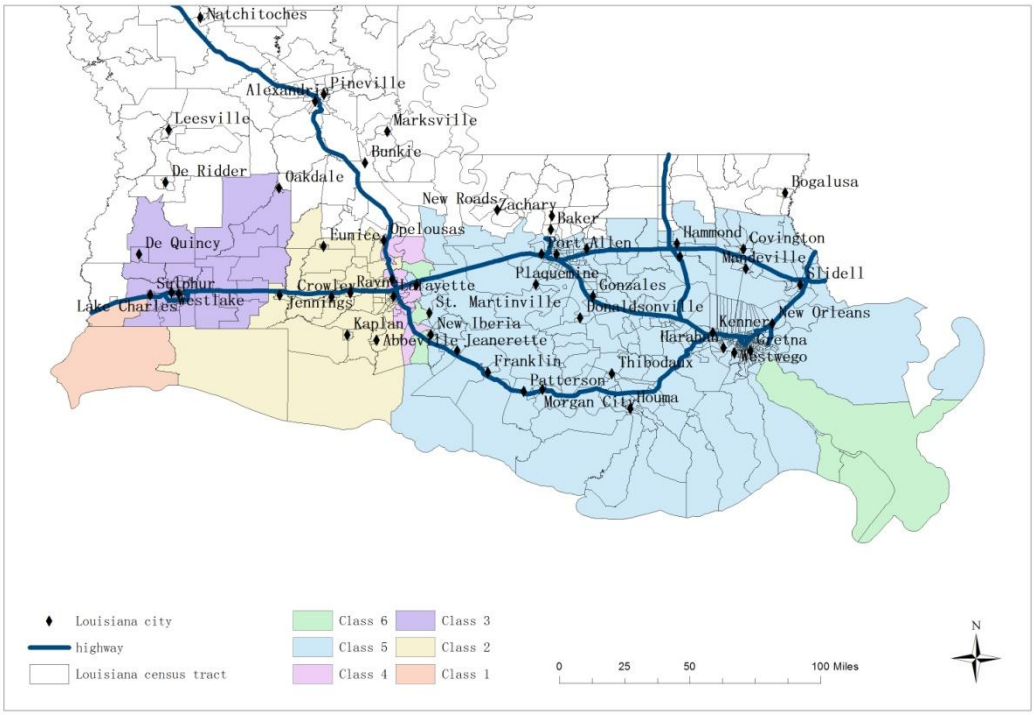

Figure 42. Regionalization of contributing subsidence factors in the study site (Some map data were extracted from: http://atlas.lsu.edu)

In this map showing the regionalization results, six sub-regions represent “Class 1,” “Class 2”…“Class 6;” these are colored and named “Region 1,” “Region 2”…“Region 6,” for discussion.

Region 1, representing Class 1 and colored orange in the left-hand side of Figure 42, shows the City of Lake Charles in this region. As Table 10 shows, all subsidence factors were insignificant, except for groundwater. The positive correlation for the groundwater factor shows that the decreasing groundwater levels at the unconfined aquifers could easily cause a main subsidence for Region 1, due to increasing internal pressure for these aquifers (Shang et al. 2011).

Region 2 (yellow-colored) is located near Region 1, and Table 10 shows that sediment, sinkholes, and groundwater are significant factors for the main subsidence in this region. The negative correlation for sediment and sinkholes, and the positive correlation for groundwater in Table 10 demonstrate that the main subsidence in Region 2 could be caused by sediment compaction, the Bayou Corne Sinkhole, and decreasing groundwater levels in the unconfined aquifers (Sclater and Christie 1980; Cusanza and Kris 2013; Shang et al. 2011).

Region 3, colored purple, is near Regions 1 and 2. For this region, the GWR results show that two factors, sediment and groundwater, are significant. A negative correlation for sediment, coupled with a positive correlation for groundwater, reveals that we should control not only an adverse sediment compaction, but also decreasing levels existing at unconfined groundwater aquifers, to deal with subsidence problems in this region.

Region 4, colored pink, is the smallest sub-region in the study site. This area represents Class 4 in Table 10. The main subsidence in this region was caused by all four factors—mass loading (loading of buildings), sediment, sinkholes, and

groundwater. Similar to Region 2, sediment compaction, the Bayou Corne Sinkhole, together with decrease of water in unconfined groundwater aquifers could be the main contributing factors to adverse subsidence (Shang et al. 2011). Yet, unlike Region 2, the loadings of buildings in Region 4 might also be related to adverse subsidence, in addition to the same contributing factors.

The largest sub-region in the study site, blue-colored Region 5, also has four significant contributing subsidence factors, similar to Region 4. Baton Rouge and New Orleans, two large Louisiana cities, are located in this region. Similar to Region 4, Region 5 has the same correlations for the loading of buildings, sediment, and sinkhole. The opposite and negative correlations for groundwater in Region 5 mean that main subsidence in this region might also be caused by increasing levels in confined groundwater aquifers, rather than decreasing ones in unconfined groundwater aquifers for Region 4 (Shang et al. 2011).

Region 6, depicted in green, represents Class 6 and is mainly located in the coastal area near New Orleans. Unlike the other five sub-regions in the study site, the groundwater factor for Region 5 was insignificant. In addition, the negative correlations for the other three contributing factors indicate that the loading of buildings, sediment compaction, and the Bayou Corne Sinkhole could cause main subsidence in this region.

Thus, based on the GWR results, the entire study site, classified as six sub-regions, is based on different combinations of contributing subsidence factors. This regionalization work seeks to form location-based policies to mitigate the

adverse subsidence in the coastal area of Louisiana. The Louisiana state government can apply these policies to control subsidence-related problems. The regionalization work in this dissertation shows that governmental location-based policies are possible. Each combination of all contributing factors serves to represent a unique policy for a singular sub-region in the study site. Thus, for these six sub-regions (Regions 1–6), six different policies could be formed to control subsidence concerns. For example, to deal with adverse subsidence in Region 1, meaningful policies would control the impact of decreasing levels in unconfined groundwater aquifers. For Region 2, different polices could address adverse subsidence. Such a policy ought to control not only the groundwater impact in the unconfined aquifers, but also the strong impacts of both sediment compaction and the Bayou Corne Sinkhole.

5.6. Summary and discussion

The GWR model modeled the factors that contributed to subsidence in the study site. The modeling results demonstrated that the GWR model can be advantageous to map the spatial heterogeneity of the regression models by producing spatially varied local R-squared values and coefficients of the factors (Xu and Wang 2015; Shang et al. 2011).Based on the GWR results, regionalization work was done to create location-based subsidence mitigation policies for the study site. The study site was classified into six sub-regions by regionalization. Each sub-region presented a unique combination of contributing subsidence factors. As a result, the policy for each sub-region can uniquely address the adverse subsidence, thereby making location-based subsidence policies for government possible.

The regionalization results in this dissertation show that the GWR model can be useful for developing location-based subsidence policies, yet flaws in the GWR modeling process for factors were identified. One flaw was that in the quantification of oil and gas data, researchers collected only the well data related to the well distribution, not the production data for each well. The well production data contribute directly to subsidence; thus, for oil/gas wells, well density—rather than production—is considered an independent variable in the factor modeling process. The modeling results not only show that the oil/gas coefficient is insignificant, but these results do not match prior research (Abdollahzadeh et al. 2013; Wang et al. 2014).

Chapter 6 Conclusions and Summary

6.1. Research conclusions

This research consisted of two main stages. First, GPS data were processed by a spatial temporal interpolation model to map land surface motion. In the second stage, spatial statistical models related the direction and magnitude of land surface motion to five selected factors.

6.1.1. Conclusions on the spatial temporal data model

GPS data were obtained from Louisiana stations by the public domain data server. The data were then processed to create point maps and time series of elevation data on those particular stations. Finally, the KKF was applied to interpolate the point data.

The first conclusion involves the line regression fitting on the time series data, which produced the land elevation change rate (mm/year), proven to be both effective and valid. In a further validation by Bayou Corne Sinkhole knowledge, the final KKF results shown in Chapter 3 rest on the yearly distribution of subsidence rates.

The second conclusion of the GPS data process applies the KKF to the GPS data. The KKF results show a significantly accelerating subsidence area near Bayou Corne. These results were validated by the Bayou Corne Sinkhole knowledge, as well.

The third conclusion is that the KKF can be useful for detecting and monitoring ground movement in related disasters near bayou areas, such as sinkholes. The integrated spatial and temporal interpolation from KKF captured the subtle surface elevation change when measured by a high-precision GPS.

6.1.2. Conclusions from the factor modeling results

Regression-Kriging, a model based on OLS regression and Kriging interpolation, was used to predict the spatial pattern for subsidence rates in 2013. The first conclusion is that Regression-Kriging is effective in modeling the land subsidence rate. The data are inclusive of such factors as groundwater, oil/gas, sediment, the loading of buildings, and sinkholes.

This spatial pattern is similar to the 2013 KKF results in Chapter 3 and is drawn from the predicted high subsidence rate near Bayou Corne—one which approaches10.8mm/year. Furthermore, in regard to accuracy, the Regression-Kriging prediction is more accurate than that of Empirical Bayesian Kriging. Thus, an acceptable subsidence prediction is provided by this dissertation based on OLS regression.

A second conclusion is that in modeling contributing factors to subsidence, the GWR model is more advantageous than a global OLS regression model. The modeling results indicate that there is clear, spatial heterogeneity for subsidence data in the study site. Not only are the local R-squared values for the census tracts spatially varied, but the coefficients for each type of contributing factor are spatially varied as well. Furthermore, the GWR results differ substantially from the OLS results, which further indicates clear spatial heterogeneity in the subsidence models. In viewing the results, GWR may be considered the more advantageous model.

The third conclusion is that the regionalization work in this dissertation can be helpful in forming location-based policies for the government to mitigate subsidence

problems. Based on the GWR results, the regionalization work classified the entire study site into six sub-regions, which in turn represent six different combinations for contributing subsidence factors. Thus, the regionalization results show that although the combination of contributing factors for each sub-region may be unique, a policy can also become unique to deal with an adverse subsidence for each sub-region. This process would permit location-based policies.

6.2. Final summary and future work

The land subsidence problem has received much attention in Louisiana. For this research, GPS data mapped the adverse situation of land subsidence, particularly in coastal Louisiana. Based on the data analyses estimation, this study suggests that in the near future, the State of Louisiana will experience substantial land loss caused by land subsidence. Thus, the people of Louisiana should focus keenly on this subsidence study, taking positive actions to prevent serious subsidence in the coastal area.

After the subsidence problem was presented, the literature review revealed the recent research progress on subsidence done by researchers. A major section of the literature review involves subsidence observation and prediction. This section presents three kinds of common observation techniques. These techniques consisting of leveling, GPS, and InSAR were previously discussed with respect to the different advantages and flaws (Lu, C. et al. 2012). Additionally, combinations of these techniques focused on improving the observation levels for subsidence. The KKF model has also been introduced as a new method to process subsidence data (Mardia et al. 1998).

Another section of the literature review involved modeling the factors contributing to subsidence. The findings indicated that the contributing factors presented by prior research were the groundwater level, oil and gas pumping, sediment compaction, faulting, and mass loading (Abdollahzadeh et al. 2013). Previous modeling methods on subsidence factors were discussed; most of the modeling processes either lacked local views or drew a conclusion for spatial heterogeneity (Fotheringham et al. 2002; Shang et al. 2011).

Based on the literature review, research questions and a research workflow were proposed. The main research workflow involves two important research techniques of KKF processing and factor modeling, such as Regression-Kriging and GWR. Thus, in the following chapters, these two techniques and their subsequent applications on subsidence data were discussed, together with instructions on how to use these techniques to process Louisiana's subsidence data.

Chapter 3 shows that KKF can be a valid method to interpolate subsidence rates in coastal Louisiana by means of incorporating time series GPS data in a Kriging interpolation (Mardia et al. 1998; Kalman 1960).

Regression-Kriging, used in Chapter 4, was based on OLS regression to predict the spatial pattern for subsidence rates in 2013. This study modeled contributing factors, thus providing a subsidence prediction work and thereby achieving acceptable prediction results.

In Chapter 5, the modeling results showed that GWR can be advantageous for factor modeling. As a result, the regionalization work based on these GWR results

could be instrumental in forming location-based policies toward mitigating adverse subsidence.

Although this study has produced new progress on subsidence research in coastal Louisiana, there are also flaws or defects in the data and models that could be improved in future research. The first instance is found in the collection of oil and gas data for factor modeling, as only the well data on the distribution online could be collected. In the future, should the production data for each well be collected, the modeling results may then reflect an explainable coefficient for the oil and gas pumping factor, showing a more significant level.

The second instance is that the faulting data were not considered in the factor modeling process due to the fact that spatial heterogeneity for faulting data could not be found in the study site; thus, future work may focus on how to quantify the faulting data with other knowledge. This improvement could produce more contributing factors for the factor modeling process.

The third instance is that the building mass loading data were approximated using the land cover data from the National Land Cover Database. However, the land cover data only indicate whether the land is highly constructed and the accuracy is questionable. Thus, future work may choose to focus on how to more accurately quantify the loading, based on better sources of remote sensing images.

The fourth instance is that the KKF results were only checked by the Bayou Corne Sinkhole knowledge for a consistency to validate these results. The consistency was checked in a small area around Bayou Corne, while the KKF results were not

validated in the whole study site due to the lack of available subsidence data from the other kinds of observations. Thus, for future work, the InSAR data in the same study site can be collected to show the subsidence pattern, and the validation of the whole study site can be made if this subsidence pattern by InSAR is available.

The fifth instance is that only six GPS stations as the standard points were used to calculate the prediction accuracy using Regression-Kriging. Thus, more GPS stations as standard points can be used to calculate the prediction accuracy in future work, and this work may show higher accuracy.

References

Abdollahzadeh, M.; Dixon, T. H.; Malservisi, R. Geodetic subsidence rate in coastal Louisiana. American Geophysical Union, Fall Meeting 2013. December 2013.

Addison Paul S. The Illustrated Wavelet Transform Handbook, Institute of Physics, 2002.

Anselin, L., A. K. Bera, R. Florax, and M. J. Yoon. GeoDa: An Introduction to Spatial Data Analysis. Geographical Analysis 38 (1): 5-22.

Baller, R. D., L. U. C. Anselin, S. F. Messner, G. Deane, and D. F. Hawkins. 2001. Structural Covariates of U. S. County Homicide Rates: Incorporating Spatial Effects. Criminology 39 (3): 561-588.

Blom, R. G., Chapman, B. D., Dokka, R. K., Fielding, E. J., Hensley, S., Ivins, E. R., Lohman, R. B. Hazards of gulf coast subsidence: crustal loading, geodesy, InSAR and UAVSAR observations. American Geophysical Union, Fall Meeting 2009. December 2009.

Brodie, Kate, Fettes, Douglas, Harte, Ben, Schmid, Rolf (29 January 2007). Structural terms including fault rock terms. International Union of Geological Sciences.

Burgmann, R., Rosen, P.A., Fielding, E. J. (2000), "Synthetic aperture radar interferometry to measure earth's surface topography and its deformation", Annual Review of Earth and Planetary Sciences 28, pp. 169-209.

Carolina Pagli, Freysteinn Sigmundsson, Thora Arnadottira, Pall Einarsson, Erik Sturkell. Deflation of the Askja volcanic system: Constraints on the deformation source from combined inversion of satellite radar interferograms and GPS measurements. Journal of Volcanology and Geothermal Research, 2006. 152, 97–108.

CHEN Beibei, GONG Huili, LI Xiaojuan, LEI Kunchao, ZHANG Youquan, LI Jiwei, GU Zhaoqin, DANG Yanan. Spatial-temporal characteristics of land subsidencecorresponding to dynamic groundwater funnel inBeijing municipality, China. Chin. Geogra. Sci., 2011. 21(6), 753–764.

Coal Industry Promotion Board, CIPB (1997). A study on the mechanism of subsidence over abandoned mine area and the construction method of subsidence prevention. Coal Industry Promotion Board, Seoul, 97-06, pp 1-67.

Coal Industry Promotion Board, CIPB (1999). Fundamental investigation report of the stability test for Gosari. Coal Industry Promotion Board, Seoul, 99-06, pp 7-22.

Cusanza, Kris. “Bayou Corne evacuation could last for years” NBC 33. Retrieved 24 July 2013.

Daniel R. Roman, Yan Ming Wang, William Henning, and John Hamilton. Assessment of the New National Geoid Height Model, GEOID03. 2004 ACSM/TAPS Conference and Technology Exhibition. Nashville, Tennessee, April 16-21, 2004.

Dempster, A.P.;Laird, N.M.;Rubin, D.B.. Maximum Likelihood from Incomplete Data via the EM Algorithm. Journal of the Royal Statistical Society.1977. Series B 39 (1): 1–38.

Dokka, R. K.Modern-day tectonic subsidence in coastal Louisiana. Geol, 2006. 34(4), 281–284.

DOLEŽALOVÁ Hana, KAJZAR Vlastimil, SOUÈEK Kamil, STAŠ Lubomir. Evaluation of mining subsidence using GPS data. Acta Geodyn. Geomater., 2009. Vol. 6, No. 3 (155), 359–367.

Forsberg, R., Skourup, H. Arctic Ocean gravity, geoid and sea-ice freeboard heights from ICESat and GRACE. Geophysical Research Letters, 2005, 32(21), L21502.

Fotheringham A. S., C. Brunsdon C, Charlton M. Geographically Weighted Regression: The analysis of spatially varying relationships. Wiley, 2002.

Freedman David A. (2009). Statistical Models: Theory and Practice. Cambridge University Press.

Gabriele Bitelli, Flavio Bonsignore, Marco Unguendoli. Levelling and GPS networks to monitor ground subsidence in the Southern Po Valley. Journal of Geodynamics,2000. 30, 355-369.

Ge L. Development and testing of augmentations of continuously-operating GPS networks to improve their spatial and temporal resolution, PhD Thesis, School of Surveying and Spatial Information Systems, The University of New South Wales, Sydney NSW 2052, AUSTRALIA, UNISURV S-63, xvi+230pp.

Ge Linlin, Cheng Eric, Li Xiaojing, and Rizos Chris. Quantitative subsidence monitoring the integrated InSAR, GPS and GIS approach. The 6th International Symposium on Satellite Navigation Technology Including Mobile Positioning & Location Serivces Melbourne, Australia, 22–25 July 2003.

Geisser, Seymour (1993). Predictive Inference. New York, NY: Chapman and Hall. ISBN 0-412-03471-9.

Hasanuddin Z. Abidin, H. Andreas, Rochman Djaja,Dudy Darmawan, M. Gamal. Land subsidence characteristics of Jakarta between 1997and 2005, as estimated using GPS surveys. GPS Solut, 2008, 12, 23–32.

Hayashi, Fumio (2000). Econometrics. Princeton University Press.

Hengl, T., Heuvelink, G., Stein, A. A generic framework for spatial prediction of soil variables based on Regression Kriging. Geoderma, 120 (2004), 75-93.

Hung Wei-Chia, Hwang Cheinway, Chen Yi-An, Chang Chung-Pai, Yen Jiun-Yee, Hooper Andrew, Yang Chin-Yi. Surface deformation from persistent scatterers SAR interferometry and fusion with leveling data: A case study over the

Choushui River Alluvial Fan, Taiwan. Remote Sensing of Environment, 2011. 115, 957–967.

Jones, C. and Blom, R., “Pre-event and post-formation ground movement associated with the Bayou Corne Sinkhole” (2015).

Jones, C. and Blom, R., Bayou Corne, Louisiana, sinkhole: Precursory deformation measured by radar interferometry. Geology, February 2014, v. 42, no. 2, p. 111-114.

Kalman, R. E. A new approach to linear filtering and prediction problems. Journal of Basic Engineering, 1960. 82 (1), 35–45.

Kanti V. Mardia, Colin Goodall, Edwin J. Redfern, Francisco J. Alonso. The Kriged Kalman filter. Test, 1998. Vol. 7, No.2, 217-285.

Kent, J., Dokka, R. Potential impacts of long-term subsidence on the wetlands and evacuation routes in coastal Louisiana. GeoJournal, 2012. 4, 641-655.

Kim Ki-Dong, Lee Saro, Oh Hyun-Joo, Choi Jong-Kuk, Won Joong-Sun. Assessment of ground subsidence hazard near an abandoned underground coal mine using GIS. Environ Geol, 2006. 50, 1183–1191.

Kim Ki-Dong, Lee Saro, Oh Hyun-Joo. Prediction of ground subsidence in Samcheok City, Korea, using artificial neural networks and GIS. Environ Geol, 2009. 58, 61–70.

Knegt, De, Coughenour, M. B., Skidmore, A. K., Heitkonig, I. M. A., Knox, N. M., Slotow, R., Prins, H. H. T. (2010). Spatial autocorrelation and the scaling of species-environment relationships. Ecology 91: 2455-2465.

Li Kenan. Temporal changes of coastal community resilience in the gulf of Mexico region. A LSU thesis, 2011.

Li Xiaolu, Wang Lei and Liu Shan. Geographical Analysis of Community Resilience to Seismic Hazard in Southwest China. International Journal of Disaster Risk Science (2016). pp 1-20. doi:10.1007/s13753-016-0091-8.

Lima, A., Vivo, B. De, Cicchella, D., Cortini, M., Albanese, S., Multifractal IDW interpolation and fractal filtering method in environmental studies: an application on regional stream sediment of (Italy), Campania region. Applied Geochemistry. Volume 18, Issue 12, December 2003, Pages 1853-1865.

Louisiana Department of Natural Resources, 2013b, Blue Ribbon Commission initial technical briefing: http://dnr.louisiana.gov/assets/OC/BC_All_Updates/Plans_Reports/BlueRibb.04.05.13.pdf (May 2013).

Louisiana Department of Natural Resources, Fenstermaker Area Survey: http://dnr.louisiana.gov/assets/OC/BC_All_Updates/Plans_Reports/Fenstermaker.Jan.2014.areasurvey.pdf (January 2014).

Louisiana Department of Natural Resources, Itasca-Subsidence Report: http://dnr.louisiana.gov/assets/OC/BC_All_Updates/Itasca.results.1152013.pdf (October 2013).

Lu Chih-Heng, Ni Chuen-Fa, Chang Chung-Pai, Yen Jiun-Yee, Hung Wei-Chia: Integrations of multiple observations and inversion of subsidence parameters in Choushui River Fluvial Plain of central Taiwan. AGU Fall Meeting, San Francisco, 3-7 December 2012.

McLachlan, G. J. (2004). Discriminant Analysis and Statistical Pattern Recognition. Wiley Interscience.

Oh Hyun-Joo, Ahn Seung-Chan, Choi Jong-Kuk, Lee Saro. Sensitivity analysis for the GIS-based mapping of the ground subsidence hazard near abandoned underground coal mines. Environ Earth Sci, 2011. 64, 347–358.

Oh Hyun-Joo, Lee Saro. Assessment of ground subsidence using GIS and the weights-of-evidence model. Engineering Geology, 2010. 115, 36–48.

Oh Hyun-Joo, Lee Saro. Integration of ground subsidence hazard maps of abandoned coal mines in Samcheok, Korea. International Journal of Coal Geology, 2011. 86, 58–72.

Olea, R.A. (1999). Geostatistics for engineers and earth scientists. Kluwer Academic Publisher.

Olea, Ricardo (1991) A. Geostatistical Glossary and Multilingual Dictionary. Oxford University Press. pp. 47, 67, 81.

Pebesma, Edzer J (1 July 2006). The role of external variables and GIS databases in geostatistical analysis. Transaction in GIS. 10 (4): 615-632.

Poland Michael, Burgmann Roland, Dzurisin Daniel, Lisowski Michael, Masterlark Timothy, Owen Susan, Fink Jonathan. Constraints on the mechanism of long-term, steady subsidence at Medicine Lake volcano, northern California, from GPS, leveling, and InSAR. Journal of Volcanology and Geothermal Research, 2006. 150, 55– 78.

Psimoulis P., Ghilardi M., Fouache E., Stiros S. Subsidence and evolution of the Thessaloniki plain, Greece, based on historical leveling and GPS data. Engineering Geology, 2007. 90, 55–70.

Robbins, Herbert (1956). “An Empirical Bayes Approach to Statistics”. Proceedings of the Third Berkeley Symposium and Mathematical Statistics and Probability, Volume 1. Contributions to Theory of Statistics: 157-163.

Samsonov Sergey, Tiampo Kristy, Rundle John, and Li Zhenhong. Application of DInSAR-GPS Optimization for derivation of fine-scale surface motion maps of southern California. Transactions on Geoscience and Remote Sensing, IEEE, 2007. Vol.45, No.2, February 2007.

Sclater, J. G. and Christie, P. A. F. 1980. Continental stretching: an explanation of the post-mid-Cretaceous subsidence of the Central North Sea Basin. Journal of Geophysical Research, 85, 3711-3739.

Shang Rong-Kang, Shiu Yi-Shiang, Ma Kuo-Chen. Using geographically weighted regression to explore the spatially varying relationship between land subsidence and groundwater level variations: A case study in the Choshuichi alluvial fan, Taiwan. International Conference on Spatial Data Mining and Geographical Knowledge Services, ICSDM 2011, Fuzhou, China, June 29 - July 1, 2011.

Shepard and Donald (1968). “A two-dimensional interpolation function for irregularly-spaced data". Proceedings of the 1968 ACM National Conference. pp. 517-524.

Shinkle, K., & Dokka, R. Rates of vertical displacement at benchmarks in the lower Mississippi Valley and the northern Gulf Coast. NOAA Technical Report 50, 2004.

Shumway, R.H. and D.J. Stoffer (1982). An approach to time series smoothing and forecasting using the EM algorithm, Journal time series analysis, 3, 253-264.

Strozzi Tazlo, Wegmiiller Urs, Tosl Luigl, Bitelli Gabrlele, Spreckels Volker. Land Subsidence Monitoring with differential SAR interferometry. Photogrammetric Engineering & Remote Sensing, 2011. Vol. 67, No. 11, November 2001, 1261-1270.

The Atlas website. Extracted from:http://atlas.lsu.edu/.

The CMU website. Weighting function. Extracted from:http://www.cs.cmu.edu/~schneide/tut5/node12.html.

The Esri website. Extracted from:http://www.esri.com/news/arcuser/1012/empirical-byesian-kriging.html.

The National Land Cover Database website. Extracted from:http://www.mrlc.gov/nlcd2011.php.

The NCSU Libraries website. DOQQs. Extracted from:http://www.lib.ncsu.edu/gis/doqq.html.

The SONRIS website. Extracted from: http://sonris.com.

The SONRIS website. SONRIS Interactive Maps. Extracted from:http://sonris-www.dnr.state.la.us/gis/agsweb/IE/JSViewer/index.html?TemplateID=181.

The USGS website. Extracted from:http://groundwaterwatch.usgs.gov/.

The USGS websites. Faults. Extracted from:http://earthquake.usgs.gov/hazards/qfaults/.

The website of Murphy Lab. Back-propagation neural network. Extracted from:http://murphylab.web.cmu.edu/publications/boland/boland_node17.html.

The website of OECD Glossary of Statistics Terms. Frequency ratio. Extracted from:http://stats.oecd.org/glossary/detail.asp?ID=1066.

The website of State University of Campinas. Weights of evidence method. Extracted from:http://www.ige.unicamp.br/wofe/documentation/wofeintr.htm.

The website of TRE. DInSAR. Extracted from: http://treuropa.com/technique/insar-evolution/.

TheArcGISresource website. Extracted from: http://resources.arcgis.com/en/help/main/10.1/index.html#//0031000000q9000000.

WANG Chong chang, LV You, SONG Ying. Researches on mining subsidence disaster management GIS `s system. 2012 International Conference on Systems and Informatics (ICSAI 2012), 19-20 May 2012.

Wang Fahui, Tang Quan and Wang Lei. Post Katrina population loss and uneven recovery in New Orleans, 2000-2010. Geographical Review. Volume 104, Issue 3, 310-327, July 2014.

Wang Fahui. Quantitative methods and Application in GIS [M]. CRC Press. 2006.

Wang Guoquan, ASCE M., Yu Jiangbo, Kearns Timothy, J., Ortega Jesse. Assessing the accuracy of long-term subsidence derived from borehole extensometer data using GPS observations: Case study in Houston, Texas. J. Surv. Eng. 2014. 140(3), 05014001.

Wegmuller Urs, Strozzi Tazio, and Bitelli Gabriele. Validation of ERS differential SAR interferometry for Land subsidence mapping: the Bologna case study. Geoscience and Remote Sensing Symposium, 1999. IGARSS '99 Proceedings. IEEE 1999 International (Volume:2).

Xu Yanqing and Wang Lei. GIS based analysis of obesity and the built environment in the US. Cartographic and Geographic Information Science, 2015. Vol 42, No. 1, 9-21.

Yuan Changfeng, Wang Xuchun, Wang Ning, Zhao Qianqian. Study on the effect of tunnel excavation on surface subsidence based on GIS data management. Procedia Environmental Sciences, 2012. 12, 1387 – 1392.

Zhang Fengshuang, Bo Wanju. Primary discussion about the application of GPS results to research of ground subsidence. Science of Surveying and Mapping, 2012. 4, 37-39.

Zhang J. X. Scale, Uncertainty and Fusion of Spatial Information [M] Wuhan: Wuhan University Press, 2008.

Zheng Minxue, Kaoru Fukuyama, Kazadi Sanga-Ngoie. Application of InSAR and GIS techniques to ground subsidence assessment in the Nobi Plain, central Japan. Sensors, 2014. 14, 492-509.

Zhou Guoyun, Esaki Tetsuro, Mori Jiro. GIS-based spatial and temporal prediction system development for regional land subsidence hazard mitigation. Environmental Geology, 2003. Volume 44, Issue 6, 665-678.

Zou Lei, Kent Joshua, Lam Nina S.-N., Cai Heng, Qiang Yi, Kenan Li. Evaluating land subsidence rates and their applications for land loss in the Lower Mississippi River Basin. Water 2016, 8(1), 10.

Vita

Hanyu Xiang, originally from Wuhan City in the Hubei Province of China, pursued his Ph.D. degree at Louisiana State University with a major in Geography. Before coming to the USA, Hanyu gained a Bachelor of Science degree in 2005 from the Wuhan University of Technology, as well as a Master of Engineering degree from Peking University. His research topic is Subsidence in Louisiana.